

ON-LINE HPLC / PHASE-MODULATION
FLUORESCENCE LIFETIME
DETERMINATIONS FOR
POLYCYCLIC AROMATIC
HYDROCARBONS

By

WILLIAM TYLER COBB

Bachelor of Science in Chemistry
Southeastern Oklahoma State University
Durant, Oklahoma

1984

Submitted to the Faculty of the
Oklahoma State University
in partial fulfillment of
the requirements for
the Degree of
DOCTOR OF PHILOSOPHY
December, 1989

Thesis
1989D
C653e
cop.2

DEDICATION

Dedicated to My Wife,

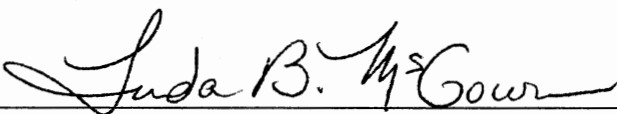
Irma

and Children,

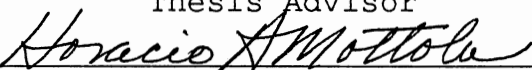
Carolina, Steven and Salvador

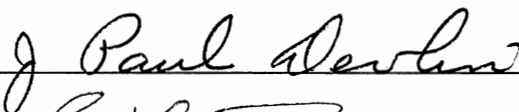
ON-LINE HPLC / PHASE-MODULATION
FLUORESCENCE LIFETIME
DETERMINATIONS FOR
POLYCYCLIC AROMATIC
HYDROCARBONS

Thesis approved:

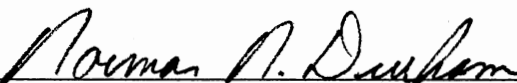


Thesis Advisor









Dean of the Graduate College

PREFACE

This dissertation describes efforts to incorporate on-line fluorescence lifetime selectivity into the detection and determination of polycyclic aromatic hydrocarbons separated by high performance liquid chromatography. This goal was approached through the use of multifrequency phase-modulation fluorescence spectroscopy and non-linear least squares fluorescence lifetime heterogeneity analysis. The technique yields phase and modulation fluorescence lifetimes at several points along each chromatographic peak; peak heterogeneity is indicated if present, and components in unresolved peaks can be quantitated without the need for chromatographic resolution.

The support of several agencies and institutions was critical to the eventual completion of this work and I wish to acknowledge and extend my sincere thanks to them. First I want to thank the United States Environmental Protection Agency which was gracious enough to fund this project through its entirety. Special thanks goes to the OSU Center for Water Research which supplied funding for the purchase of an HPLC, and also for a very nice and appreciated Presidential Fellowship while I was at OSU. My appreciation is extended to Oklahoma State University for providing support in the form of teaching assistantships

and scholarships. Lastly, I would like to thank Duke University and the people in the Duke chemistry department who very much helped make the transition from Oklahoma a much smoother and enjoyable experience than it otherwise would have been.

I would like to express my sincere gratitude to several individuals without whose help, encouragement, and understanding I would never have made it this far. My research advisor, Dr. Linda B. McGown, in addition to being an unending source of research-related ideas and encouragement, was equally supportive and understanding of issues outside of the laboratory. Without this understanding, attempting to simultaneously raise a family and pursue a Ph.D. in chemistry would surely have resulted in failure in either one or both of these areas. I would also like to thank the McGown research group for putting up with me through thick and thin and especially to Kasem Nithipatikom and Dave Millican for their support, friendship and extensive help during my graduate career.

A special note of appreciation goes to my parents and sisters whose expressions of joy and encouragement during each phase of my educational career have provided me with unequalled inspiration and hope to reach each subsequent step in the climb to where I am now.

Above all my deepest and most heartfelt thanks goes to my wife, Irma, who has been a source of undying support and inspiration in spite of all the hardships, both financial

and emotional, that pursuing a Ph.D. has placed on our marriage and on our family. She unfortunately was forced to delay her graduate studies in order to raise and support our children, and now it's her turn to finish up her Ed.D. in Adapted Physical Education. I would also like to thank my wife and children for being my critical link to the real world outside of graduate school, and it is to them that I dedicate this dissertation.

TABLE OF CONTENTS

Chapter	Page
I. INTRODUCTION.	1
II. DETERMINATION OF POLYCYCLIC AROMATIC HYDROCARBONS.	5
Separation Techniques.	5
Detection And Peak Purity Determination For HPLC	21
III. FLUORESCENCE LIFETIME THEORY AND APPLICATIONS .	49
Fluorescence: A General Description.	49
Fluorescence Lifetime Theory	52
Heterogeneity Analysis Based On Phase- Modulation Lifetimes	63
On-line Fluorescence Lifetime Detection For HPLC	77
IV. EXPERIMENTAL.	87
Chemicals.	87
Instrumentation.	88
V. RESULTS AND DISCUSSION.	104
Characterization Of Test Compounds	104
On-Line Fluorescence Lifetime Determinations	111
Application of Phase-Modulation Fluorescence Lifetime Determinations and Heterogeneity Analysis To Mixtures of B(k)F and B(b)F.	124
Fluorescence Lifetimes for PAHs On-line With HPLC Using A Multifrequency Phase- Modulation Fluorometer.	134
Fluorescence Lifetimes, Heterogeneity Detection, and Heterogeneity Analysis for Mixtures of PAHs Using HPLC and Multifrequency Phase-Modulation Fluorescence	162

Chapter	Page
Phase-Modulation Fluorescence Lifetime Chromatograms and Heterogeneity Analysis for the Sixteen EPA Priority Pollutant PAHs	169
Related Studies: On-Line HPLC/Phase- Resolved Fluorescence Intensity (PRFI) Detection of PAHs.	184
VI. CONCLUSION.	194
BIBLIOGRAPHY	197
APPENDICES	202
APPENDIX A - COMPUTER PROGRAM WRITTEN IN MICROSOFT QUICKBASIC TO CALCULATE INTENSITY-MATCHED LIFETIMES FOR CHROMATOGRAMS	203
APPENDIX B - COMPUTER PROGRAM WRITTEN IN MICROSOFT QUICKBASIC TO CALCULATE FRACTIONAL INTENSITIES FROM FRACTIONAL CONTRIBUTIONS OBTAINED FROM HETEROGENEITY ANALYSES.	209

LIST OF TABLES

Table	Page
1. EPA Priority Pollutant PAH	2
2. Identification of PAHs for Figures 1 and 2	13
3. Values of k' for PAHs Using LiChrosorb RP-18	18
4. Minimum Detectable Quantities Using UV Absorbance and Fluorescence Detection	34
5. Detection Limits Using a Diode-Array Absorbance Detector.	40
6. Fluorescence Lifetimes of Tryptophan at Different pH Values	66
7. Resolved Lifetimes for Data in Table 6 Using Weber's Algorithm	66
8. Resolved Lifetimes for 1:3 Mixture of Perylene and 9-Aminoacridine Using NLLS With 5, 10, 20, 40 and 80 MHz	71
9. Computer Program Routines.	74
10. Resolved Fluorescence Lifetimes of Pyrene and Carbazole.	75
11. Resolved Fluorescence Lifetime of POPOP in the Presence of Pyrene and Carbazole	76
12. Fluorescence Excitation and Emission Maxima.	106
13. Phase and Modulation Fluorescence Lifetimes.	108
14. Fluorescence Lifetimes for B(k)F	117
15. Fluorescence Lifetimes for B(k)F Along a Peak.	119
16. Results for Batch Heterogeneity Analysis for B(k)F and B(b)F.	128
17. Relative Errors for On-Line Heterogeneity Analysis	132

Table	Page
18. Mixtures of B(b)F and B(k)F for Heterogeneity Analysis	138
19. Fluorescence Lifetimes of Mixtures of B(b)F and B(k)F.	139
20. Results of Batch NLLS Heterogeneity Analysis . .	140
21. List of PAHs Used in Analysis in Order of HPLC Elution.	172
22. Peak Identification for Figures 78 and 79. . . .	189

LIST OF FIGURES

Figure	Page
1. Separation of PAHs Using Isocratic Elution With 80% Aqueous MeCN.	11
2. (a) Separation of PAHs Using Gradient Elution. (b) Solvent Program for (a) Using Aqueous MeCN	12
3. Separation of PAHs Using EPA Method 610.	16
4. Isothermal Separation of PAHs Using 80% Aqueous MeCN	19
5. Temperature Gradient Separation of PAHs Using 80% Aqueous MeCN	20
6. LC/MS Separation of Phenanthrene, 9-Methylanthracene, and Fluoranthene	25
7. Comparison of Direct Deposition and Spray Deposition of HPLC Eluent With Moving Belt Interface for LC/MS.	26
8. Comparison of UV and MS Detection for Normal Phase LC	27
9. Comparison of UV and MS Detection for Reversed- Phase LC	28
10. Simultaneous UV Diode-Array and MS Detection. Inserts Show UV Absorbance and Mass Spectra of Benzo(a)pyrene	30
11. UV Absorbance Detection Using 3 Detectors in Series	33
12. UV Absorbance and Fluorescence Detection. (A) PAH Standards, (B) Alkylated Naphthalenes, (C) Refinery Effluent After Enrichment	35
13. Effects of Baseline Drift and Offsets on Absorbance Ratios.	37

Figure	Page
14. Practical Effects of Peak Overlap and Peak Tailing on Absorbance Ratios	37
15. Separation of (1) Pyrene, (2) Fluoranthene, (3) Benzo(e)pyrene, (4) Biphenyl, (5) Fluorene, (6) Phenanthrene, (7) Naphthalene, (8) Acenaphthylene	45
16. Fluorescence Chromatogram of (a) Anthracene, (b) Chrysene, and (c) Benzo(a)pyrene	47
17. Constant Energy Synchronous Luminescence Spectra of the Three Peaks in Figure 16.	47
18. Exponential Fluorescence Decay After Pulsed Excitation	54
19. Least-Squares Reconvolution of a Two-Component Decay Using Single and Double Exponential Decay Laws for Fitting	55
20. Component Stripping for Two-Component Decay.	57
21. Excitation (E(t)) and Emission (F(t)) Functions for Harmonic Excitation Showing the Demodulation m and Phase Shift ϕ	59
22. Divergence of Calculated Lifetimes From an Arithmetic Mean of 4 ns in Heterogeneous Systems of Two Components of Equal Intensity	61
23. Divergence of Lifetimes in Two-Component Systems of 1 and 8 ns and Different Relative Intensity (weight)	62
24. Relative Fluorescence Intensity and Fluorescence Lifetimes as a Function of pH for Tryptophan	65
25. Distribution of Resolved Lifetimes Using Weber's Algorithm With More Than Two Frequencies for a Two-Component System of 3.1 and 8.7 ns	67
26. Phase and Modulation as a Function of Modulation Frequency for a Two-Component System of 3.1 and 8.7 ns	69
27. Errors in Resolved Lifetimes Using Weber's Algorithm as a Function of Frequency With One Frequency Fixed at 30 MHz.	70
28. Uncertainty in the Resolved Components of the 3.1 and 8.7 ns System Using NLLS	71

Figure	Page
29. Resolved Lifetimes for Anthracene (4 ns) and 9-CNA (12 ns) Using Global, Conventional, and Algebraic (Weber's) Heterogeneity Analyses . .	78
30. Resolved Lifetimes for System in Figure 29 With Dynamic Quencher Added to Yield Lifetimes of 3.9 and 7.2 ns for Anthracene and 9-CNA. . . .	79
31. Fluorescence Detection of Six PAHs Using Pulsed Excitation and Time Delays of (a) 0 ns, (b) 15 ns, and (c) 45 ns.	81
32. Fluorescence Detection of B(a)P and B(ghi)P Using Pulsed Excitation and Time Delays of (A) 0 ns and (B) 20 ns	81
33. Instrumental Setup to Obtain 10 ns Delay Between Oscilloscope Inputs.	83
34. Position of Oscilloscope Apertures for Ratio Measurement.	83
35. Illustration of the Two Channels of Raw Data (a,b) and Their Ratio (c) for Fluoranthene . .	84
36. Two-Component Peak Consisting of Perylene and Benzo(a)pyrene Showing How the Ratiogram Can Resolve Overlapping Peaks.	85
37. General Diagram of HPLC/UV/Spectrofluorometer Setup.	89
38. SLM 4800S Phase-Modulation Spectrofluorometer. .	92
39. Debye-Sears Modulation Tank for SLM 4800S. . . .	95
40. SLM 48000S Multifrequency Phase-Modulation Spectrofluorometer	96
41. Beam Path Through Modulation Compartment for Dynamic Measurements Showing Q-Switch Polarizer (Q) and Pockel's Cell (P).	98
42. Beam Path Through Modulation Compartment for Steady-State Measurements Showing Mirror (M) .	99
43. Chromatogram of 11 PAHs Using Gradient Elution and UV Absorbance Detection at 254 nm.	109
44. Fluorescence Lifetimes vs. HPLC Retention Time Time for PAHs From Figure 43	110

Figure	Page
45. Lifetime vs. Percent Aqueous Acetonitrile as Solvent.	113
46. Lifetimes vs. Time Using Scatter as the Reference.	122
47. Lifetimes vs. Time Using DimethylPOPOP as the Reference.	123
48. Chromatograms of B(k)F and B(b)F Using Different Mobile Phase Compositions With Isocratic Elution.	130
49. Fluorescence Lifetime Chromatogram for B(k)F at 0.5 mL/min and 100% MeCN	142
50. Fluorescence Lifetime Chromatograms of B(k)F Using 100% MeCN at (a) 0.2 and (b) 0.4 mL/min.	144
51. Fluorescence Lifetime Chromatograms of B(k)F Using 100% MeCN at (a) 0.6 and (b) 0.8 mL/min.	145
52. Fluorescence Lifetime Chromatograms at 0.5 mL/min and 80% MeCN for (a) B(k)F and (b) B(b)F.	147
53. Fluorescence Lifetime Chromatograms at 0.5 mL/min and 90% Aqueous MeCN for (a) B(k)F and (b) B(b)F.	148
54. Fluorescence Lifetime Chromatograms at 0.5 mL/min and 100% MeCN for (a) B(k)F and (b) B(b)F.	149
55. Batch Fluorescence Lifetime Chromatogram Simulations for B(k)F (a) Before and (b) After Reference Intensity Matching	150
56. Stopped-Flow Fluorescence Lifetime Chromatogram Simulations for B(k)F (a) Before and (b) After Reference Intensity Matching	152
57. Dynamic (a.c.) and Steady-State (d.c.) Intensities and Modulation (a.c./d.c.) vs. Time for B(k)F	154
58. Fluorescence Lifetime Chromatograms for Fluoranthene at 0.3 mL/min and 100% MeCN (a) Before and (b) After Reference Intensity Matching and a.c. Correction	156

Figure	Page
59. Fluorescence Lifetime Chromatograms for B(k)F With 100% MeCN at (a) 0.3, (b) 0.5, (c) 0.8, and (d) 1.0 mL/min	158
60. Fluorescence Lifetime Chromatograms for B(k)F at 0.5 mL/min With (a) 70%, (b) 80%, (c) 90%, and (d) 100% MeCN.	160
61. Fluorescence Lifetime Chromatogram Using 10 MHz Modulation Frequency, 100% MeCN, and 0.3 mL/min	164
62. NLLS Heterogeneity Analysis Results for Fractional Contributions Using 4, 10, 15, 25, and 35 MHz	166
63. NLLS Heterogeneity Analysis Results for Fractional Contributions With Lifetimes Fixed Using the Same Frequencies as in Figure 62	168
64. Intensity Output and Modulation of 450 Watt Xenon Arc Lamp vs. Wavelength.	171
65. Chromatograms of Compounds Listed in Table 21 Using 0.5 mL/min, 80% Aqueous MeCN and Fluorescence Detection With (a) Ex=330 nm, Em=345 nm LP + 600 nm SP Filters, (b) Ex=360 nm, Em=399 nm LP + 600 nm SP Filters.	173
66. Excitation and Emission Spectra of Black Quartz Fluorescence Flow Cell	175
67. Effect of Flow Cell Luminescence on Lifetime Chromatograms of B(k)F	177
68. Chromatogram of 11 Compounds Using 0.3 mL/min and 87% Aqueous MeCN	179
69. Lifetime Chromatogram for 11 Compounds at 10 MHz Modulation Frequency	180
70. Data From Figure 69 Expanded in Time	181
71. (a) Heterogeneity Analysis Results Using NLLS and Frequencies of 5, 10, 15, 25, and 40 MHz. (b) Same as in (a) but With Lifetimes Fixed.	183
72. PRFI Resulting From Setting the Detector Phase (a) Exactly in Phase With a.c. Curve, (b) Exactly Out of Phase With a.c., and (c) at an Arbitrary Location on the a.c. Curve	186

Figure	Page
73. PRFI Chromatograms vs. Frequency With Detector Phase Set to Null Out Scattered Light.	191
74. PRFI Chromatograms at 10 MHz With Detector Phase Set to Null Out (a) Scattered Light, (b) 7 ns Contribution, and (c) 25 ns Contribution	192





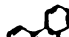


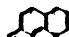

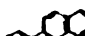


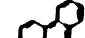

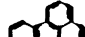

CHAPTER I

INTRODUCTION

One of the largest classes of environmental pollutants known today is the polycyclic aromatic hydrocarbons (PAHs), which are the homologs of benzene in which three or more aromatic rings are joined in various configurations. These compounds are important due to their carcinogenic, precarcinogenic, and/or mutagenic characteristics (1,2,3). The environmental concern about PAHs led the World Health Organization (WHO) to recommend that the total concentration of six specific PAHs not exceed 200 ng/L for domestic drinking water (4). The six specified PAHs are listed in Table 1 and designated by the asterisks. The Environmental Protection Agency (EPA) also designates sixteen EPA Priority Pollutant PAHs which are also shown in Table 1 along with their molecular weights, structures, and carcinogenic potentials (5).

Polycyclic aromatic hydrocarbons can be formed from both natural and anthropogenic sources; however, the latter have been by far the major contributors in the past several decades. Natural sources include volcanos, forest fires, biosynthesis, and long-term degradation followed by synthesis from biological material. Anthropogenic sources

TABLE 1
EPA PRIORITY POLLUTANT PAH^{a, c}

Compound	Abbreviation		Mol. Wt.	Carcinogenic Potential
1) NAPHTHALENE	Nph		128	-
2) ACENAPHTHENE	Ace		154	-
3) ACENAPHTHYLENE			152	
4) FLUORENE	Fl		166	-
5) PHENANTHRENE	Ph		178	-
6) ANTHRACENE	An		178	-
* 7) FLUORANTHENE	Fl		202	-
8) PYRENE	Py		202	-
9) BENZ[<i>a</i>]ANTHRACENE	B[<i>a</i>]A		228	+
10) CHRYSENE	Chy		228	+/-
* 11) BENZO[<i>b</i>]FLUORANTHENE	B[<i>b</i>]F		252	++
* 12) BENZO[<i>k</i>]FLUORANTHENE	B[<i>k</i>]F		252	-
* 13) BENZO[<i>a</i>]PYRENE	B[<i>a</i>]P		252	++++
14) DIBENZ[<i>a,h</i>]ANTHRACENE	diB[<i>a,h</i>]A		278	+++
* 15) BENZO[<i>ghi</i>]PERYLENE	B[<i>ghi</i>]P		276	-
* 16) INDENO[1,2,3- <i>cd</i>]PYRENE	I[1,2,3- <i>cd</i>]P		276	+

^aWorld Health Organization regulated PAHs indicated with *.
^bIndications are: - not carcinogenic; +/- weakly carcinogenic or uncertain; + carcinogenic; ++, +++, +++++ strongly carcinogenic.
 From ref. 3.

are extensive and include incomplete combustion of organic material in automobiles, industries, and domestic heating systems, as well as petroleum spills, sewage and industrial wastes (6). In previous years, the occurrence of PAHs in air has been given the majority of attention. However, due to their continuous accumulation in aqueous environments such as lakes, rivers, and groundwater, the focus has begun to shift to include this area of concern as well.

Due to the ubiquitous nature of PAHs and their obvious health risks to the general public, much effort has been applied to the analytical chemistry of PAHs. Selective and very sensitive detection techniques are needed to isolate, identify, and quantitate PAHs in sample matrices that are often very complex.

The research presented in this dissertation describes the use of phase-modulation fluorescence lifetime detection for PAHs on-line with HPLC. In the second chapter, a literature review describes several approaches to the determination of PAHs with emphasis on detection techniques for HPLC. The third chapter reviews the literature on the theory and applications of fluorescence lifetimes. The fourth chapter describes the results of my research, which represents the first use of multifrequency phase-modulation fluorescence lifetime measurements for on-the-fly detection in HPLC. The new technique is capable of determining the fluorescence lifetimes of PAHs separated by HPLC, flagging heterogeneous or unresolved peaks, and quantitating the

components present in the unresolved peaks through the incorporation of fluorescence lifetime selectivity.

CHAPTER II

DETERMINATION OF POLYCYCLIC AROMATIC HYDROCARBONS

Separation Techniques

In the period between 1970 and 1985 there were extensive advances in the analytical chemistry of PAHs. This surge in research seems to have come about due to two developing trends. One was the ever increasing public awareness and concern about the health risks associated with environmental pollutants, and the other was the advances in analytical instrumentation which occurred in this period. Some examples of the latter include the developments in HPLC, gas chromatography (GC), supercritical fluid chromatography (SFC), hyphenated systems such as GC-MS, LC-MS, SFC-MS, computerization of the analytical laboratory, as well as new methods for extraction, pre-concentration, and sampling. In the past few years these advances seem to have been reaching a plateau stage, not because concern or interest has declined but because further improvements in analytical instrumentation have come about at a much slower pace.

When one considers the number and complexity of PAHs present in environmental systems, it is clearly evident

that some form of separation is critical to the accurate determination of the individual PAHs present in such a system. Batch extractions are useful for isolating the PAHs from the environmental matrix such as water, soil, or air, and further separation into classes or groups of PAH compounds is possible. Beyond this point, a chromatographic separation is required. Three types of chromatography have been extensively explored for the separation of PAHs: gas chromatography (GC), supercritical fluid chromatography (SFC), and high performance liquid chromatography (HPLC).

Capillary Gas Chromatography

Probably the most widely used technique for the separation of PAHs is capillary gas chromatography. This is basically due to the high resolution and short analysis times, both of which are important for complex PAH samples. Much improvement in capillary GC separations for PAHs has resulted from the development of chemically bonded phases which allow a larger temperature range, and bonded liquid crystal phases which permit separations based on the shape of PAHs.

Separations of PAHs in the presence of additional compounds require a detector that is selective or can be made to be selective toward the PAHs. For this reason, flame ionization (FID) and photoionization (PID) detectors are not typically used for PAH separations due to their

very general response. By far the most frequently used gas chromatographic detector for PAHs is the mass spectrometer, which provides the molecular weight of compounds and structural information based on fragmentation patterns. Unfortunately, fragmentation patterns for PAH isomers are typically too similar to distinguish between them. When MS is the only type of detector used, and no selective ionization or derivitization techniques are used, misidentification of PAHs is common. Fourier transform infrared, UV absorption, and fluorescence detectors have been used for GC, but the need for matrix isolation, specialized flow cells, etc. has resulted in their limited use for PAH determinations with GC.

Advantages of GC separations include: (1) high resolution, (2) rapid analysis times, and (3) the capability of mass spectral detection. Some disadvantages include: (1) GC has only the stationary phase material, the thermal gradient range, and the rate of temperature increase as variable parameters for separation, (2) GC has difficulty in separating PAH isomers, and (3) only the more volatile (lower molecular weight) PAHs can be determined with GC.

Capillary Supercritical Fluid Chromatography

Capillary SFC has become a technique that helps fill the gap between HPLC and GC. The physical properties of

supercritical fluids provide the potential for significantly enhanced chromatographic efficiency per unit time compared to HPLC and for an extended molecular weight range compared to GC (7). Many of the same detectors used in HPLC and GC can be used in SFC. The FID detector is often used in SFC, however many supercritical fluids respond to the FID. Therefore, the FID detector is somewhat limited for determination of PAHs. Ultraviolet absorption detection can be used in packed-column SFC, but due to allowable UV absorption cell volume, high pressure requirements, and resulting lower sensitivities, UV absorption has not been used to a large degree for capillary SFC. Fluorescence is often used for detection in SFC and generally provides lower sensitivities than UV or FID, in addition to greater selectivity. The mass spectrometer is an ideal detector for SFC, allowing both electron impact and chemical ionization modes.

Advantages of capillary SFC include: (1) SFC can be used for higher molecular weight compounds than GC, (2) SFC provides greater separation efficiencies than HPLC, and (3) several detectors can be easily used for detection.

Disadvantages include: (1) pumping and injection are difficult due to very low flow rates and the need for a very small, reproducible injection amount, and (2) due to the small amount injected, typically a few nanoliters, the technique is not very useful for trace analysis.

High Performance Liquid Chromatography

High performance liquid chromatography is used extensively for the separation of PAHs due to its exceptional ability to separate PAH isomers, higher molecular weight non-volatile PAHs, and thermally unstable PAHs. The efficiency of HPLC separations is influenced by several factors such as column dimension, stationary phase dimension, sample volume, pressure, mobile phase flow rate, and the types of stationary and mobile phases used. Since the advent of chemically bonded stationary phases, reversed-phase HPLC (RPHPLC) has almost monopolized PAH separations. The RPHPLC technique utilizes a nonpolar stationary phase and a polar mobile phase. The mechanism of separation of PAHs in RPHPLC mainly involves the differential solubilities of the PAHs in the mobile phase, although interactions with the C-18 group of the support surface also affect the retention mechanism.

Although many researchers use isocratic elution for the reversed-phase separation of PAHs, gradient elution is typically the most common technique. Acetonitrile/water or methanol/water are the mobile phases that are most commonly used for RPHPLC of PAHs for both isocratic and gradient systems. For isocratic systems, a 70-95% organic system is typically used. For a gradient system, the initial composition is between 20% and 60% organic solvent and is increased to 100% organic solvent. A very important factor is the slope of the gradient program. Snyder et al. (8)

found that for a one minute dead time with acetonitrile, a 6.7% gradient slope is best for maximum resolution.

A comparison of isocratic and gradient separations of sixteen PAHs by Ogan et al. (9) is shown in Figures 1 and 2, and the peaks are identified in Table 2. The authors found that the retention times of several PAHs using gradient elution were strongly affected by the length of time the column has been equilibrated at initial conditions prior to injection of the sample. They state that a minimum equilibration time of 20 minutes is required under their experimental conditions, and this time must be constant from run to run in order to achieve reproducible retention times; precision within one day using their gradient elution program was 0.8% to 1.6% RSD for the first seven compounds listed in Table 2 and 0.5 to 0.7% for the rest. Day-to-day reproducibility was reported to be slightly less. Although it wasn't stressed in the paper, it is important to note that both the isocratic and gradient elution chromatograms took a little more than 40 minutes; in addition, the gradient elution required an additional 20 minutes for equilibration, which is not required for isocratic elution. Therefore, one must take these factors into consideration when designing a separation scheme.

Some advantages of gradient elution are: (1) regular band spacing throughout the entire chromatogram, (2) constant band widths in the chromatogram for all bands, and

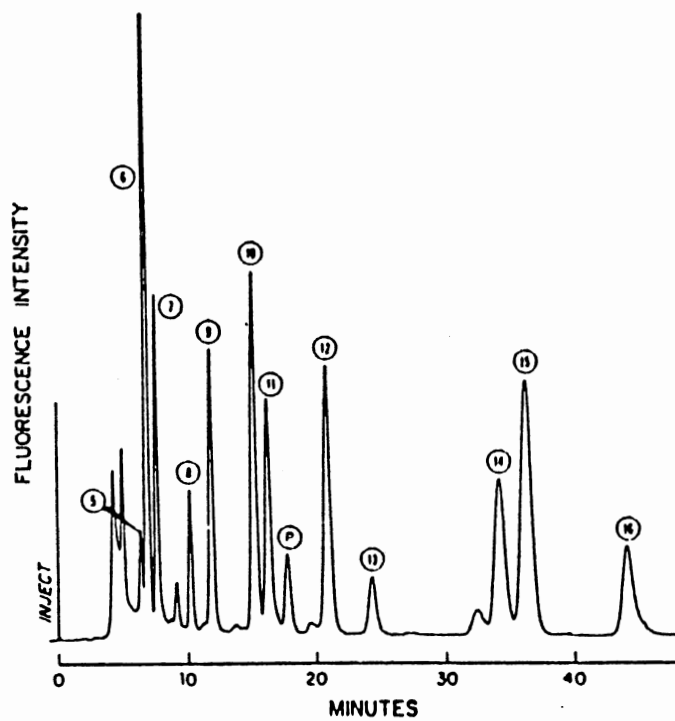


Figure 1. Separation of PAHs Using Isocratic Elution With 80% Aqueous MeCN. For Peak Identification See TABLE 2. From Ref. 9.

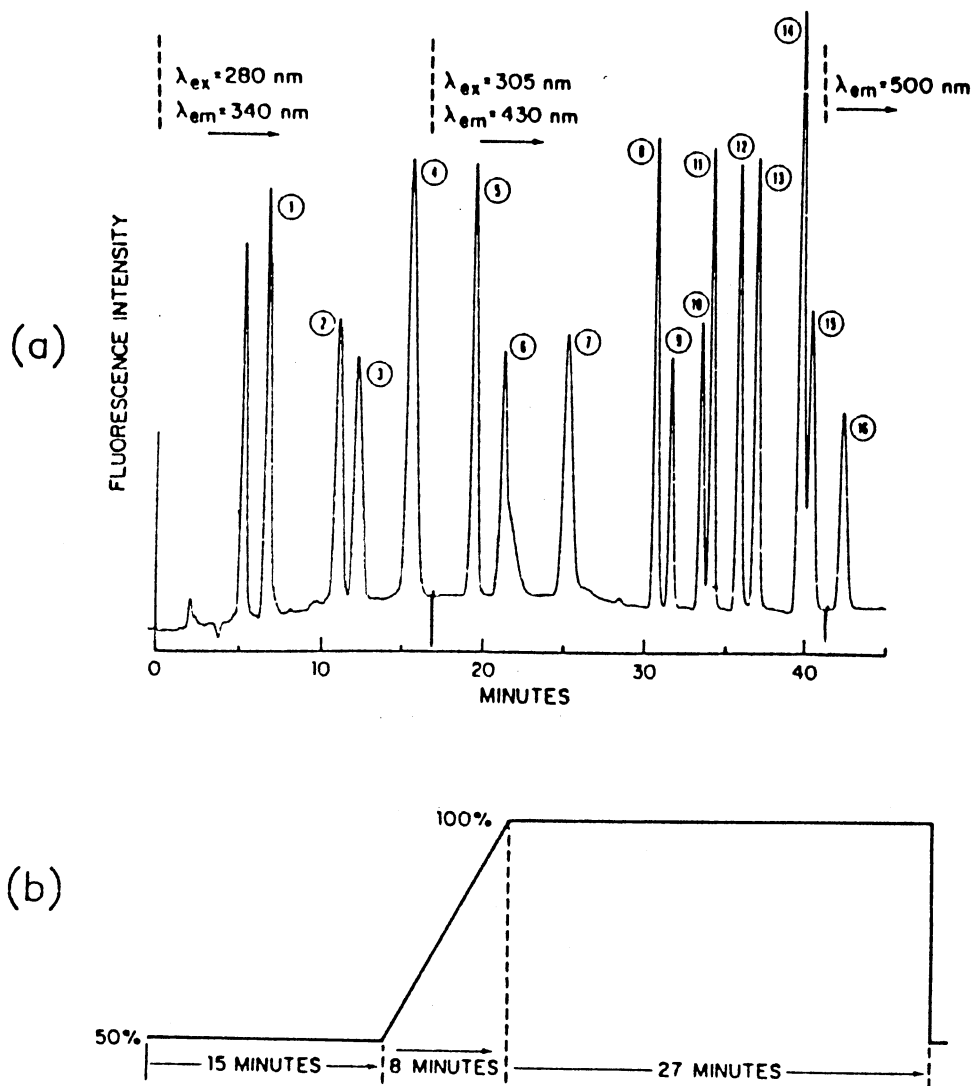


Figure 2. (a) Separation of PAHs Using Gradient Elution. (b) Solvent Program For (a) Using Aqueous MeCN. From Ref. 9..

TABLE 2
IDENTIFICATION OF PAHS
FOR FIGURES 1 AND 2

Peak Number	Compound
1.	Naphthalene
2.	Acenaphthene
3.	Fluorene
4.	Phenanthrene
5.	Anthracene
6.	Fluoranthene
7.	Pyrene
8.	Benz (a) anthracene
9.	Chrysene
10.	Benzo (e) pyrene
11.	Benzo (b) fluoranthene
12.	Benzo (k) fluoranthene
13.	Benzo (a) pyrene
14.	Dibenz (a, h) anthracene
15.	Benzo (ghi) perylene
16.	Indeno (1, 2, 3-cd) pyrene

From ref. 9.

(3) comparable resolution or effective plate number for early and late eluting bands. Some advantages of isocratic elution over gradient elution are: (1) increased reproducibility of retention times, (2) no need for column equilibration between runs, (3) no change in background signals due to changing solvent composition, and (4) the elimination of noise problems due to the solvent mixing during a gradient elution. Automated systems with programmable gradient controllers that are currently available have solved some of the problems of gradient elution but many difficulties still persist. When complete separation is required, the improved separations achievable with gradient elution usually outweigh any time constraints.

There are three groups of PAHs that are often poorly resolved, including: (1) benz(a)anthracene/chrysene; (2) benzo(e)pyrene/benzo(a)pyrene/benzo(b)fluoranthene/benzo(k)fluoranthene; and (3) benzo(ghi)perylene/indeno(123-cd)pyrene. Das and Thomas (10) used isocratic elution with 82% acetonitrile in water and a 250 X 2.1 mm Dupont Zorbax ODS column for PAH separation, but failed to separate B(k)F, B(e)P, and perylene. They were able to separate B(a)P from these, but were unable to separate B(a)A from chrysene. The poor separation is apparently due to a combination of isocratic elution and poor column selectivity. Sorrell and Reding (11) used isocratic elution with acetonitrile/water (70/30) at 1 mL/min and a

Waters μ Bondapak C-18 column to separate PAHs from a water sample. Several pairs of compounds were incompletely separated, including fluoranthene/pyrene, chrysene/benz(a)anthracene, and benzo(b)fluoranthene/benzo(k)fluoranthene. Consequently, the authors had to rely on absorbance ratio measurements and stopped-flow fluorescence spectra for complete identification and any quantitation at all. It is evident that these workers did not take full advantage of either column packing or mobile phase parameters.

The EPA method 610 (5) recommends using a reversed-phase HC-ODS Sil-X 250 X 2.6 mm Perkin-Elmer column and gradient elution for the separation of the sixteen PAHs that the EPA has defined as priority pollutant PAHs. The gradient program consists of 40% acetonitrile in water for 5 minutes, followed by a linear gradient to 100% acetonitrile over 25 minutes. UV-VIS detection at 254 nm is used for a general response, followed in series by a variable-wavelength fluorescence detector for the actual PAH determinations. The separation achieved for a standard sample is shown in Figure 3; this is an excellent example of the very good separation that can be obtained if full utilization of column packing type and mobile phase composition is employed. It is important to note that the above separation was of a synthetic sample and, more often than not, such good separation is not so easily achieved for "real samples". Symons and Crick (12) used isocratic

COLUMN: HC-ODS SIL-X
MOBILE PHASE: 40% TO 100% ACETONITRILE IN WATER
DETECTOR: FLUORESCENCE

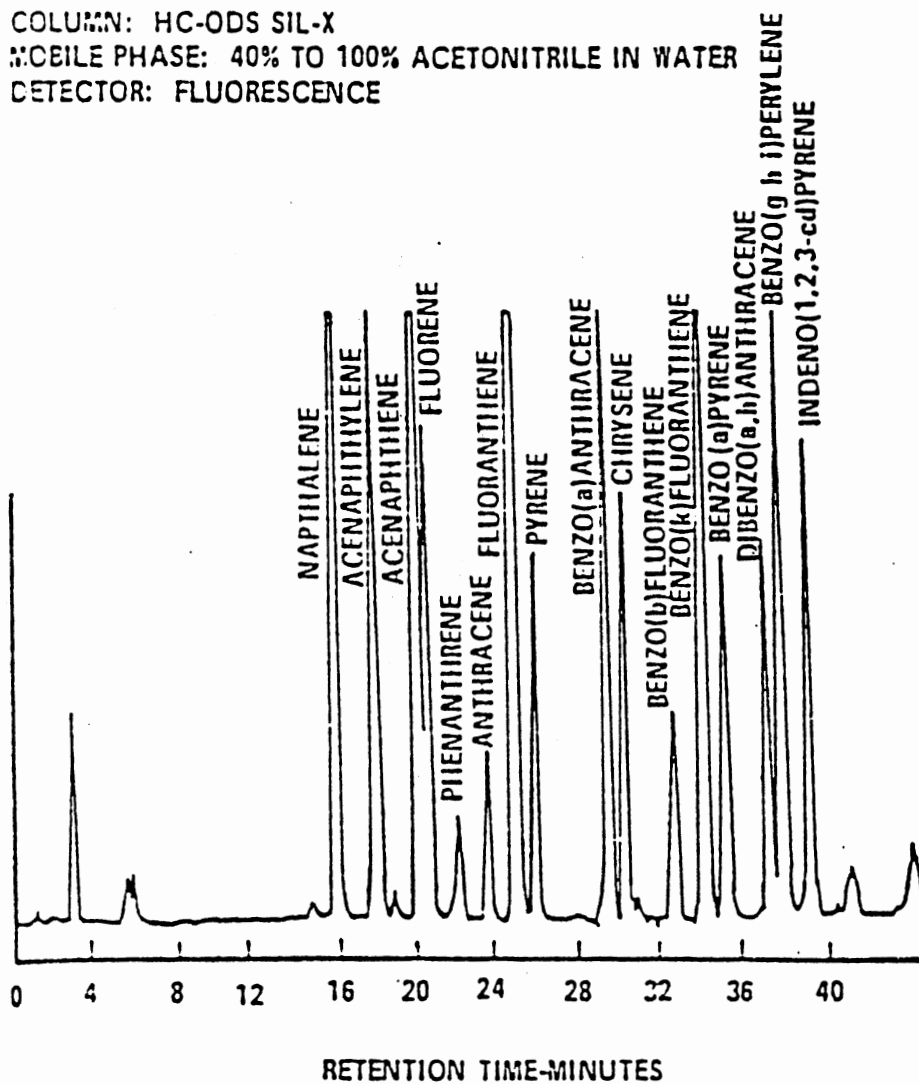


Figure 3. Separation of PAHs Using EPA Method 610. From Ref. 5.

elution with acetonitrile/water (75/25) and a 100 X 8 mm Rad-Pak C-18 column to separate a mixture of ten PAHs in both a synthetic and a real sample. The system did a good job of separating the PAHs in the synthetic mixture, but did not resolve most of the PAHs in the real sample.

Lankmayr and Muler (13) investigated the separation of 17 PAHs on a LICHrosorb RP-18, 150 X 3.2 mm column with an isocratic acetonitrile/water (85/15) mobile phase. The k' values (capacity factors), defined as the ratio of the amount of solute in the stationary phase to the amount of solute in the mobile phase and calculated as

$$k' = (t_r - t_0)/t_0$$

are shown in Table 3. Benz(a)anthracene and chrysene were not resolved, nor were perylene/ benzo(k)fluoranthene.

Chmielowiec and Sawatzky (14) investigated the use of temperature as a separation parameter. They used a Chromegabond C-18 314 X 4.6 mm column with 80% acetonitrile in water as the mobile phase. For temperature control they used a water bath circulated through a column jacket. Gradient temperature control was reported to be within 0.2° C. Figures 4 and 5 show the isothermal and temperature gradient chromatograms. The temperature gradient resulted in narrowing of the peaks as well as shortening of the separation time. Also noted is the fact that compounds 13 and 14 were unresolved isothermally but were separated with the gradient. Although temperature gradients may not be

TABLE 3
VALUES OF k' FOR PAHS USING
LICHROSORB RP-18

Compound	k'
Fluoranthene	2.09
Pyrene	2.71
Triphenylene	2.82
11 H-Benzi(a) fluorene	2.88
Benz(a) anthracene	3.29
Chrysene	3.35
Benzo(b) fluoranthene	4.89
Perylene	4.99
Benzo(e) pyrene	5.05
Benzo(k) fluoranthene	5.33
Dibenz(a,c) anthracene	5.84
Benzo(a) pyrene	6.17
Dibenz(a,h) anthracene	7.01
3-Methylcholanthrene	9.21
Indeno(1,2,3-cd) pyrene	9.29
Benzo(ghi) perylene	9.55
Coronene	18.96

From ref. 13.

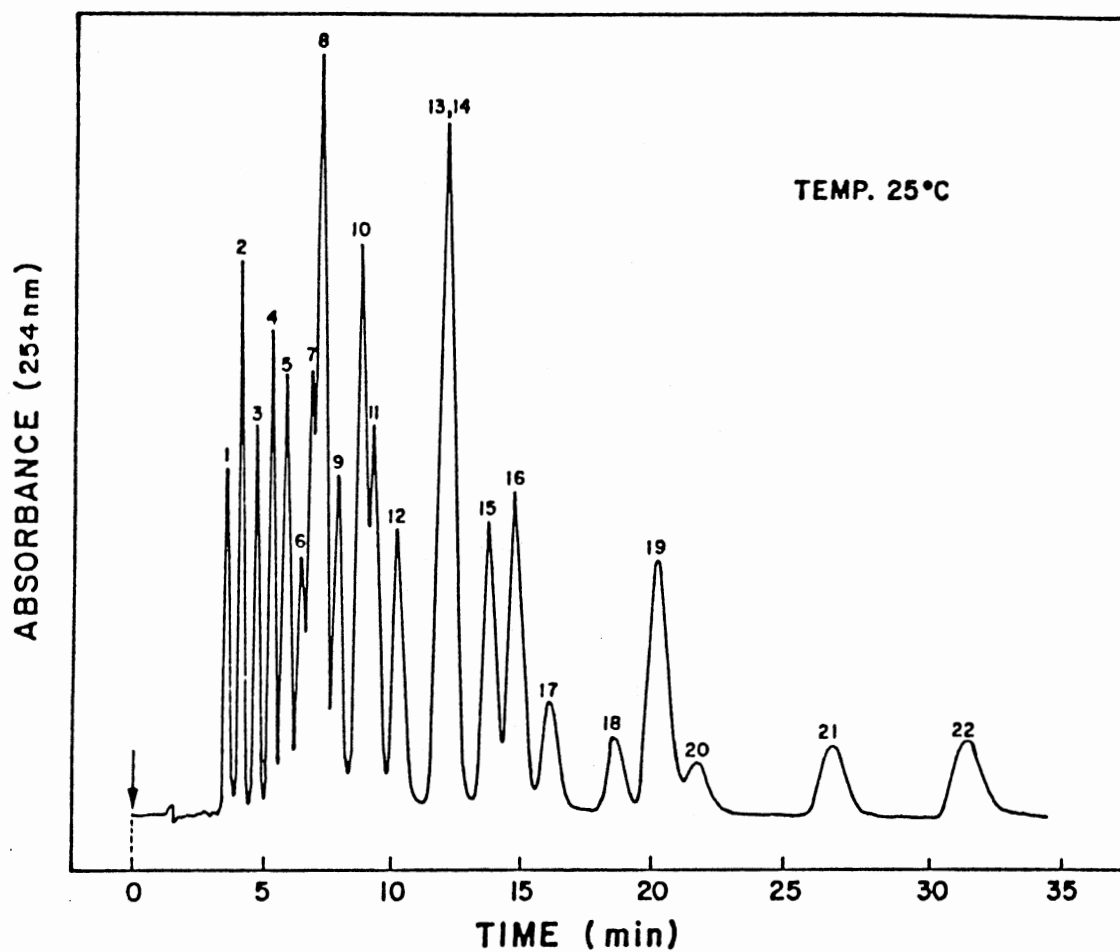


Figure 4. Isothermal Separation of PAHs Using 80% Aqueous MeCN. From Ref. 14.

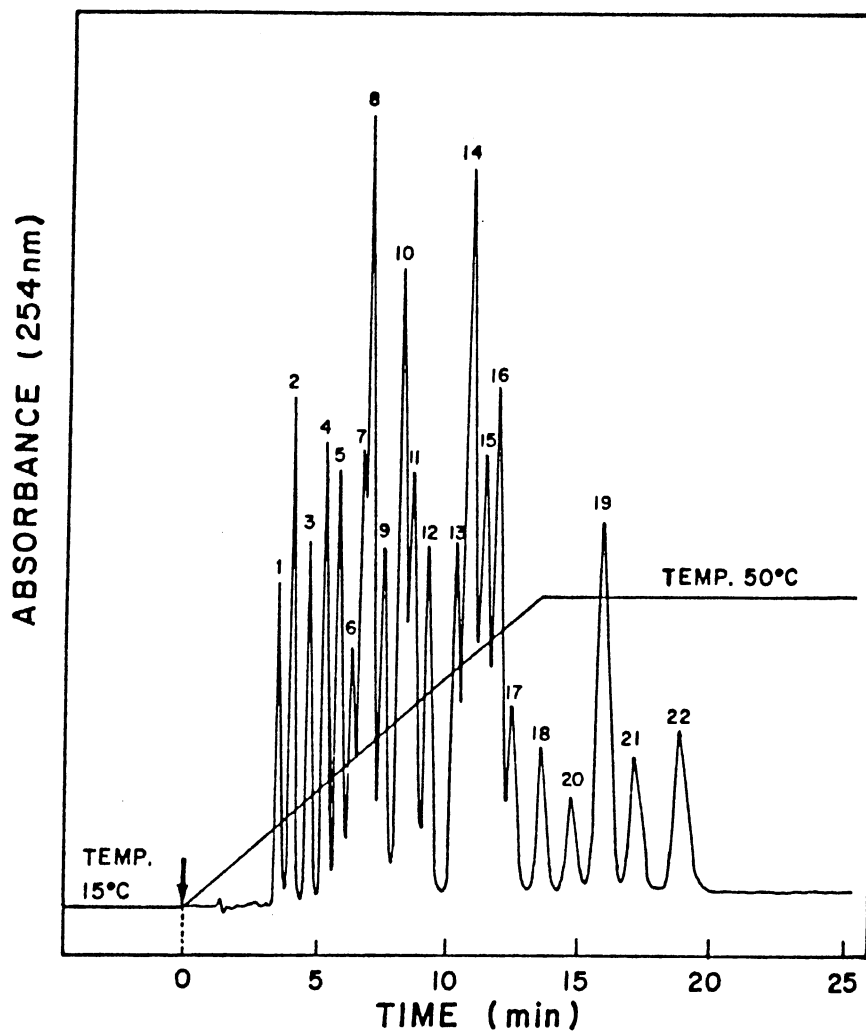


Figure 5. Temperature Gradient Separation of PAHs Using 80% Aqueous MeCN. From Ref. 14.

helpful in all cases, it is evident that they can be used as a separation parameter to improve resolution in some cases.

Detection And Peak Purity Determination For HPLC

A major advantage of HPLC for the separation of PAHs is the availability of very sensitive and selective detectors for their determinations, such as mass spectral, UV absorption, and fluorescence detectors. The first priority is for the detector to identify the components present in a particular sample. Once the identification is accomplished, it is often necessary to quantitate the individual components. However, any attempt at quantitation is meaningless unless one is confident that the peak to be quantitated is homogeneous, consisting of only one component.

Giddings states, based on probability theory, that chromatograms of real samples generally will contain no more than 37% of their potential peaks, and even worse, only about 18% of their potential single-component peaks. (15) He used theoretical examples and plots to illustrate that a chromatogram must be approximately 95% vacant in order to provide a 90% probability that a given component of interest will appear as an isolated peak. Given this prediction and the fact, as stated by Ebel and Mueck (16), "checking peak homogeneity is one of the first

and most important steps in chromatographic data evaluations in order to guarantee reliable qualitative or quantitative results", peak purity determination has and always will be of utmost importance in chromatographic separations. In this section, the capabilities of mass spectrometry, UV absorbance, and fluorescence detection are discussed in relation to peak identification, quantitation, and peak purity determination.

Mass Spectrometry

A mass spectrometer (MS) interfaced to an HPLC can provide, in addition to sensitivity, strong evidence for the identity of a compound by giving specific structural information. Most applications of HPLC-MS involve the use of microbore columns with very low mobile phase flow rates. Analytical scale HPLC-MS has been utilized for some PAH analyses, but it suffers from inherent problems because the vacuum system of the spectrometer cannot easily be coupled to the exit of the HPLC. Two types of analytical-scale HPLC-MS interfaces are commercially available and this is where the bulk of the research in recent years has been conducted.

The simplest approach to HPLC-MS consists of feeding a portion of the eluent from the HPLC directly into the ion source of the mass spectrometer that is configured for chemical ionization (CI) mass spectrometry. This arrangement is known as direct liquid introduction (DLI),

and produces solvent mediated CI mass spectra. If conventional HPLC columns are used, this system as such has limited sensitivity due to the splitting off of the major portion of the HPLC eluent. Also, since the amount of liquid entering the MS increases the source pressure to a level that precludes the use of other ionization techniques such as electron impact ionization (EI), only limited structural information can generally be obtained (17).

A second approach involves the removal of solvent by means of a continuously moving belt. The HPLC eluent is fed onto the belt and solvent is removed by an infrared heater and two vacuum locks. The residual solute is flash-vaporized into the ion source of a mass spectrometer where conventional EI and CI mass spectra can be obtained (18). The following two papers represent attempts to solve several of the problems inherent to DLI and the moving-belt interface.

Christensen and co-workers (19) developed a system that could preconcentrate the liquid stream and introduce the concentrate by DLI, thereby combining some of the advantages of both ordinary DLI and the moving belt technique. The eluent from the HPLC at 1 mL/min was concentrated by evaporation of the solvent, by allowing it to flow down an electrically heated wire. The concentrated eluent flowed through a very small needle valve which was constructed such that the eluent was sprayed into the ion source of a conventional, differentially pumped, quadrupole

mass spectrometer. Figure 6 shows the UV absorbance detection at 254 nm and single ion monitoring of compounds with and without preconcentration. With the UV detection, phenanthrene and 9-methylanthracene coelute and show up as a single peak. The mass ($m/z = 192$) chromatogram shows 9-methylanthracene without interference from the phenanthrene.

Hayes (20) developed a system that utilized spray deposition of the HPLC eluent onto a moving belt interface to help incorporate such things as high water contents in reversed-phase HPLC, increased chromatographic efficiency, the use of normal-bore columns, and applicability to quantitative analysis. The advantage of spray deposition is evident in Figure 7 when compared to the conventional method of flowing the eluent onto the belt in a continuous stream. Figure 8 is an example of the good comparison between UV and the MS total ion chromatograms for a normal-phase separation, and also of the additional power of the MS over fixed wavelength UV in its ability to pick out overlapping peaks with different MS fragmentation characteristics. Figure 9 provides further proof that a reversed-phase gradient starting with a high water content caused no major problems with the HPLC-MS profile. It is important to note that all of the above HPLC-MS work was done with normal-bore columns, i.e., 150 or 200 X 4.6 mm.

Peak Purity Determination. The availability of a mass spectrum for each peak in a chromatogram is extremely

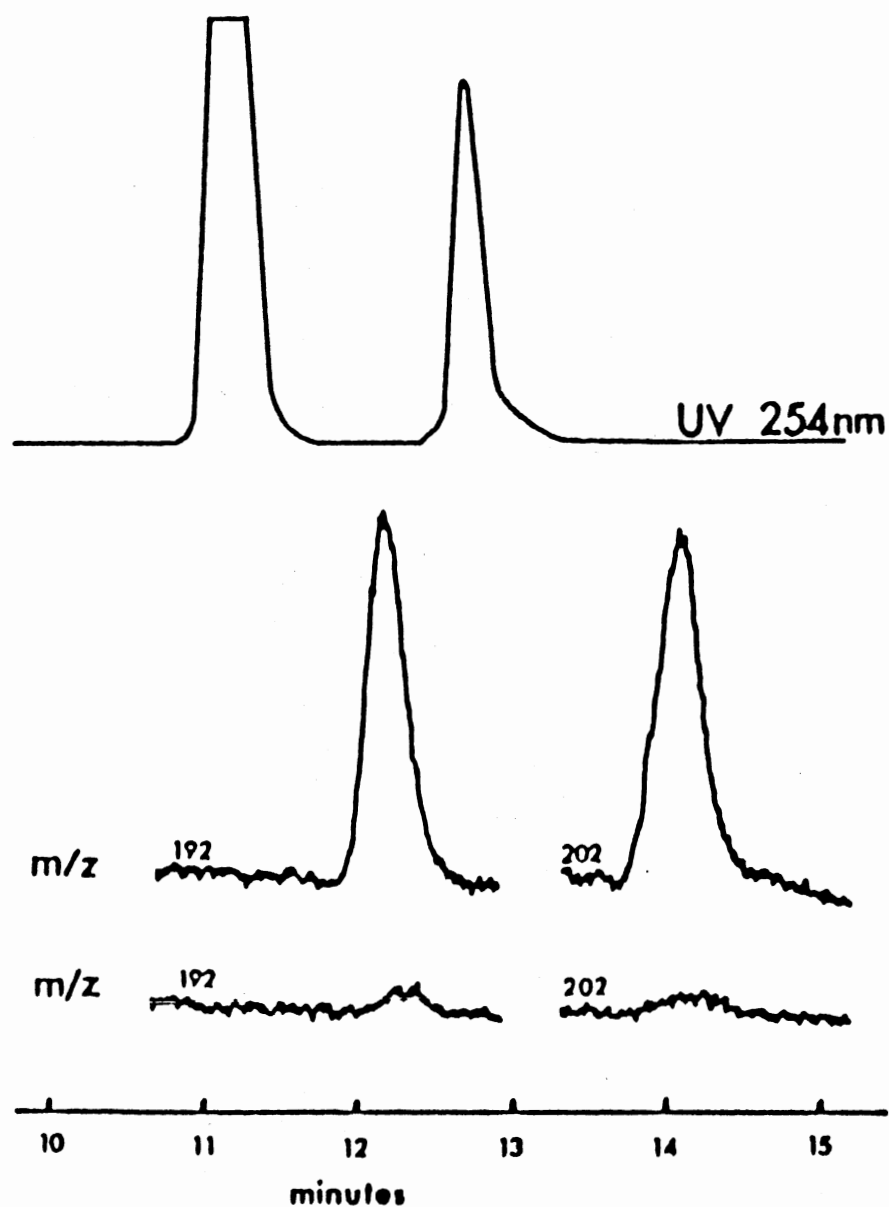


Figure 6. LC/MS Separation of Phenanthrene, 9-Methylanthracene, and Fluoranthene. Upper Single Ion Records are With Concentration Using Heated Wire. Lower Trace Is Without Wire. From Ref. 19.

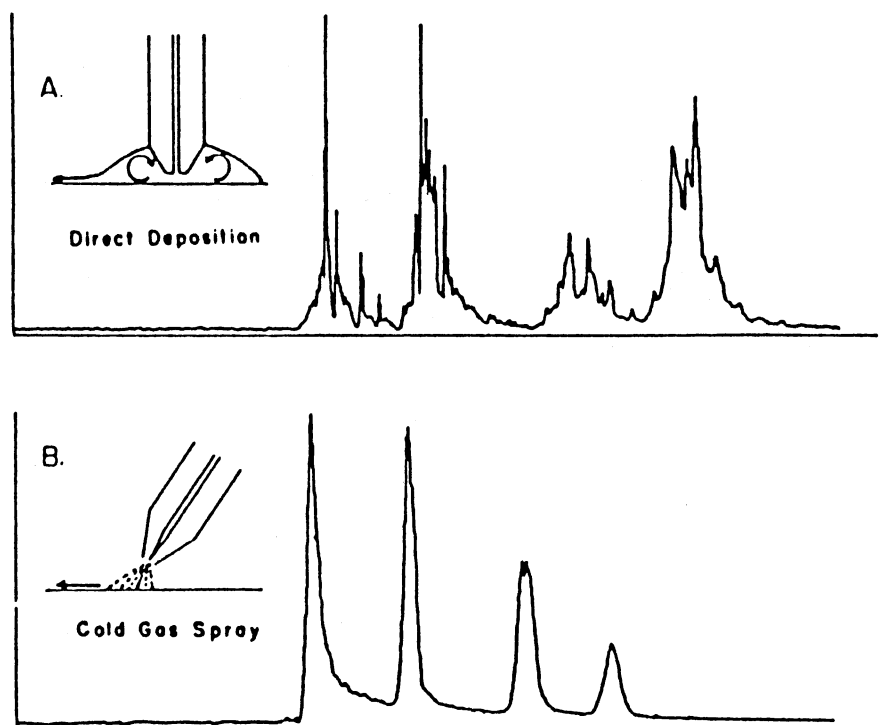


Figure 7. Comparison of Direct Deposition and Spray Deposition of HPLC Eluent With Moving Belt Interface For LC/MS. From Ref. 20.

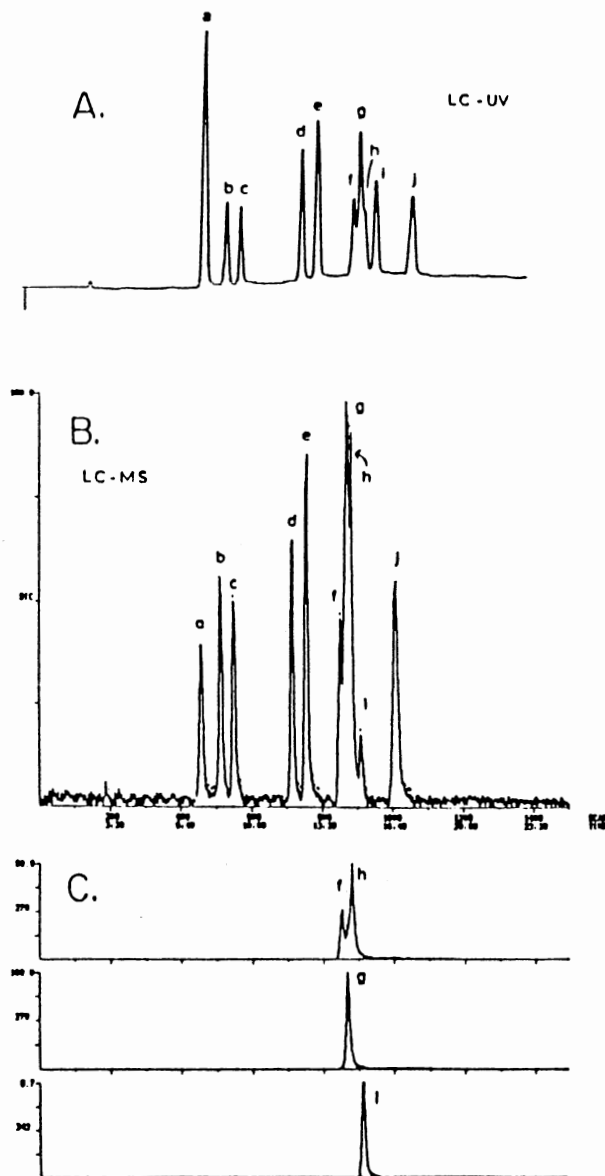


Figure 8. Comparison of UV and MS Detection For Normal Phase LC. From Ref. 20.

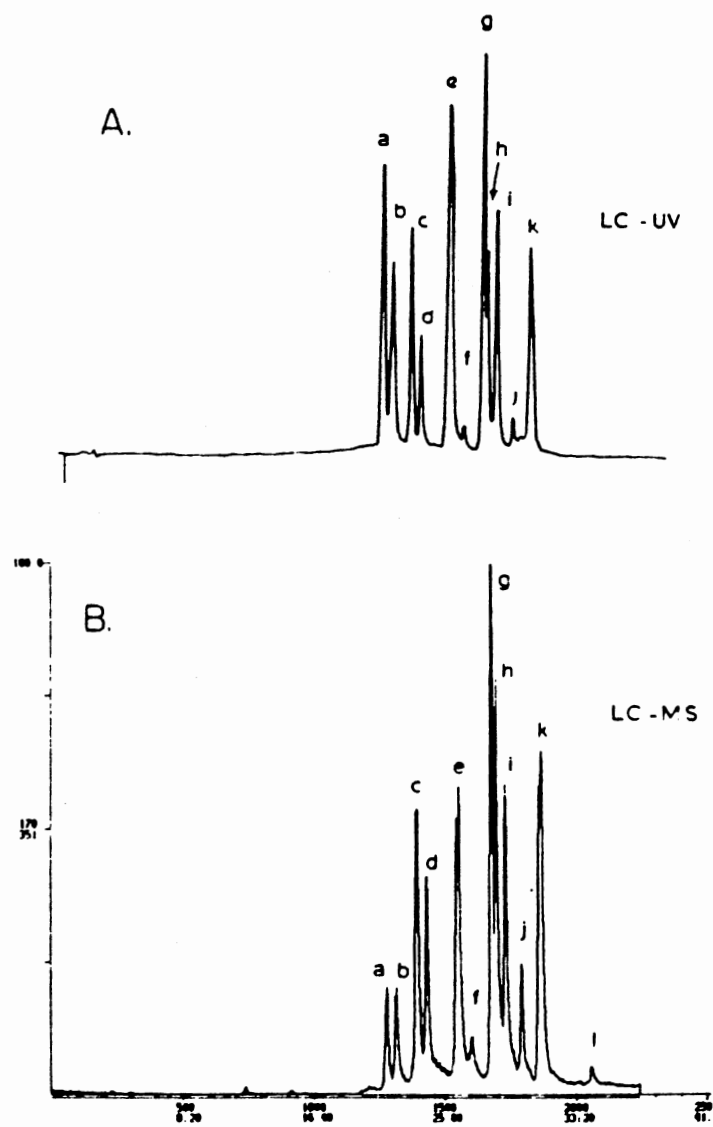


Figure 9. Comparison of UV and MS Detection For Reversed-Phase LC. From Ref. 20.

helpful for identification through structure elucidation. The mass spectrometer can also be very useful for determining peak homogeneity, since unresolved peaks can be resolved based on the difference in their molecular weights. However, the most problematic compounds in the PAH class are the isomers, which cannot be differentiated by MS since they have the same molecular weight. Even electron impact (EI) ionization does not help much because the fragmentation patterns for PAH isomers are typically indistinguishable.

Quillian et al. (21) used HPLC/MS and, while observing the isomers of mass 252, noted that "the mass spectra of these different isomers are very similar and are not useful for differentiating isomers". Therefore, while HPLC/MS can be very helpful, some other detection technique that can differentiate between PAH isomers is often additionally needed. For this reason, Quillian and Sim (22) investigated the use of simultaneous mass spectrometry and UV diode array detection (DAD). Figure 10 shows a separation of PAHs with the UV absorbance chromatogram at 254 nm, the mass spectrometer chromatogram for selected masses, the UV absorption spectrum for B(a)P, and the mass spectrum for B(a)P.

Ultraviolet Absorption Detection

Since PAHs strongly absorb in the ultraviolet region (250-280 nm), the UV detector can be considered a universal

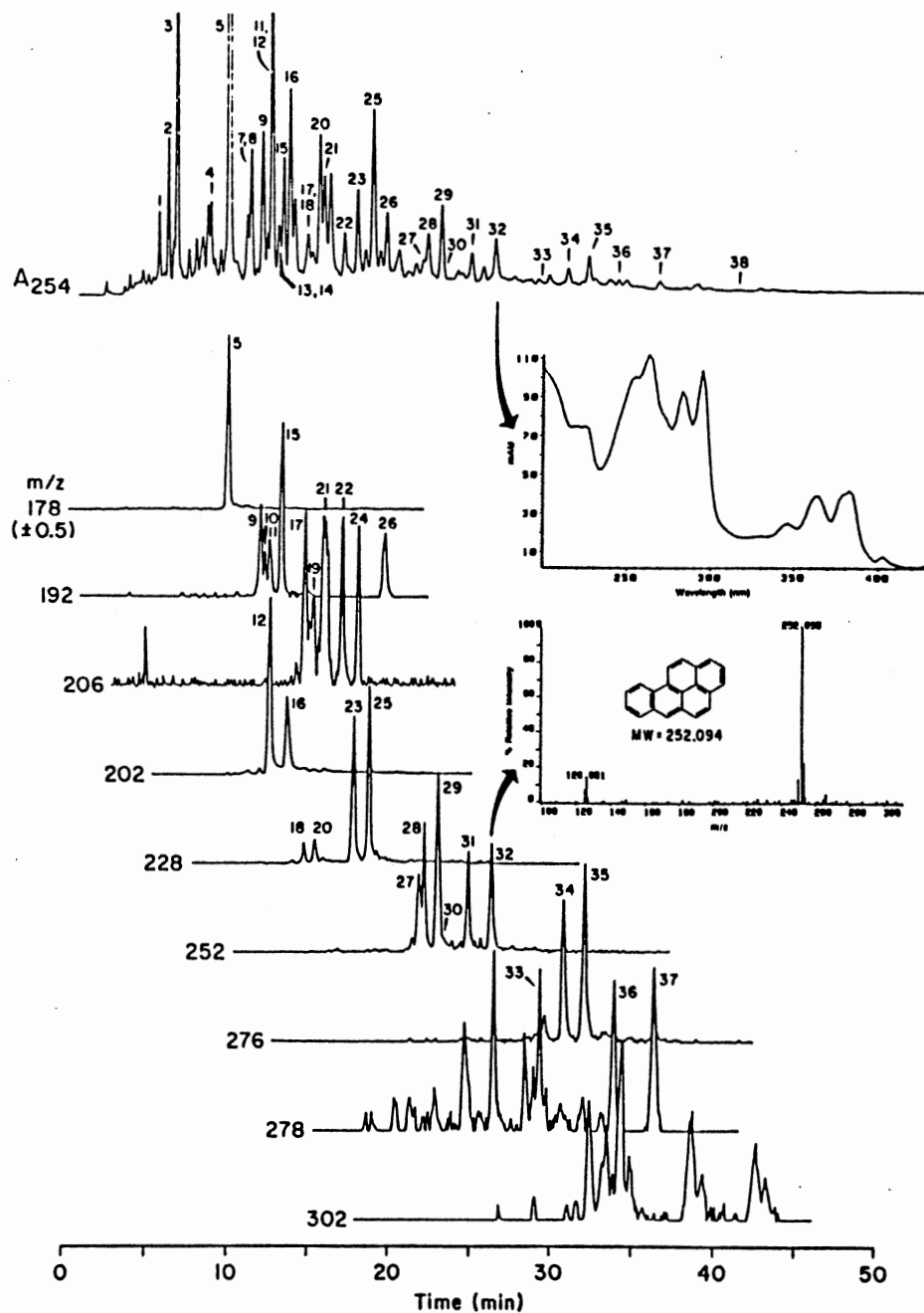


Figure 10. Simultaneous UV Diode-Array and MS Detection. Inserts Show UV Absorbance and Mass Spectra of Benzo(a)pyrene. From Ref. 22.

detector for this class of compounds. Because the absorption of UV light by PAHs generally follows the Beer-Lambert law, the calibration plots are linear over a broad concentration range.

The most common detector for PAHs separated by HPLC is a fixed-wavelength detector at 254 nm. These detectors are rugged and simple in design and therefore are very dependable for routine analysis (23,24). The source is usually a low pressure mercury lamp, which has strong emission at 254 nm.

Minimum detectable quantities for fixed UV at 254 nm were reported by Christensen and May (25) for phenanthrene (25 pg), pyrene (85 pg), chrysene (46 pg), and benzo(a)pyrene (21 pg). Sorrell and Reding (11) used three UV absorbance detectors in series, with the first at 254 nm, the second at 280 nm, and the third at 267, 308, or 340 nm. These optimal wavelengths were used to identify PAHs in three different sample clean-up fractions by minimizing interferences near a relative absorption maximum of the different PAHs. All but two of 17 PAHs could be sufficiently resolved from co-eluting PAHs and other interfering compounds by using the two fixed (254 and 280 nm) detectors and the one variable wavelength detector. They not only used this technique for suppression of impurities but also to lower the detection limits. For example, the response of chrysene is twice that of B(a)A at 267 nm and one-fifth that of B(a)A at 280 nm, therefore it

was possible to determine the concentrations of both of these compounds under optimal conditions, as seen in Figure 11. Dibenzo(a,h)anthracene was quantified from the 280 nm response since it was five times greater than at 254 nm. Using optimal wavelengths, 15 PAHs could be quantitated at concentrations of 1-3 ng/L.

Simons and Crick (12) used UV detection at 254 nm and 280 nm, and fluorescence detection in their determinations of PAHs in refinery effluent. Table 4 shows the minimum detectable quantities at each of the two UV wavelengths and also for fluorescence detection. Figure 12 shows the different selectivities obtained by each of the detector schemes. It is important to note the varied response of the detectors for the several PAH standards: Compounds 7 and 11 do not give any response at 280 nm, whereas they are sufficiently strong absorbers at 254 nm and fluoresce when excited at 360 nm.

The main advantage of UV detectors is that they are simple and easy to operate. They are often used in series with fluorescence detectors as a means of providing a general response before the fluorescence detector provides a more selective and sensitive response.

Peak Purity Determination. Since UV-VIS absorbance detection has been one of the most relied upon techniques for routine detection of PAHs, it seems only natural that this is the area which has historically been most concerned with identification of peak heterogeneity. If only single

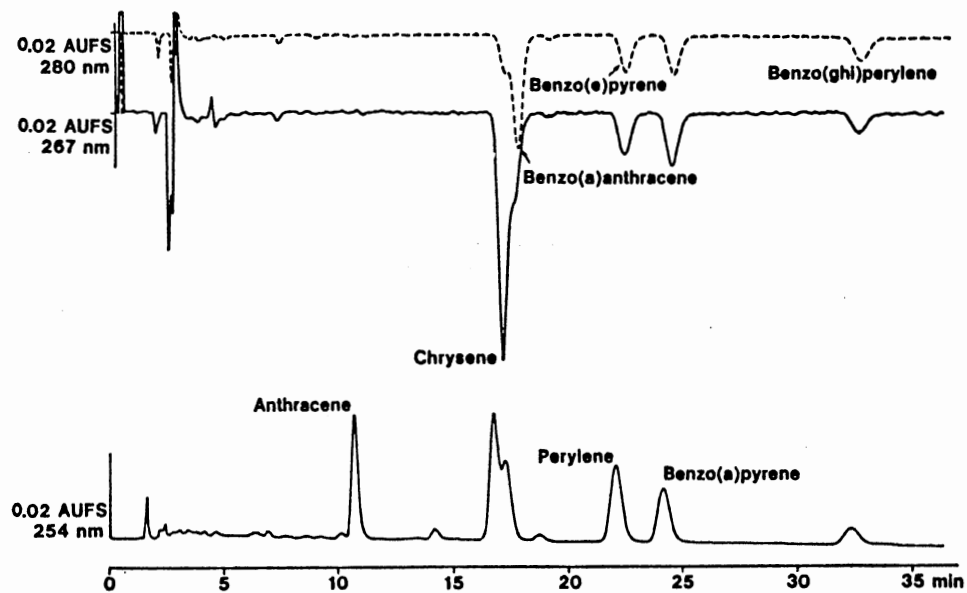


Figure 11. UV Absorbance Detection Using 3 Detectors In Series. From Ref. 11.

TABLE 4
 MINIMUM DETECTABLE QUANTITIES USING UV ABSORBANCE
 AND FLUORESCENCE DETECTION

Compound number	Compound	Detection limit (ng) ^a			k ^{1c}
		254 nm	280 nm	Fluor. ^b	
1	Naphthalene	6	4	—	2.56
2	1-Methylnaphthalene	10	2	—	3.48
3	2-Methylnaphthalene	8	4	—	3.61
4	Fluorene	1	2	—	3.97
5	Phenanthrene	0.8	3	—	4.64
6	2,3-Dimethyl-naphthalene	12	8	—	4.83
7	Anthracene	0.4	—	0.2	5.10
8	Fluoranthene	3	2	0.1	6.32
9	Pyrene	2	4	—	7.17
10	Benz(a)anthracene	1.5	0.9	0.9	9.63
11	Perylene	0.05	—	0.005	14.04
12	Benz(a)pyrene	1	1	0.05	15.93
13	Dibenz(a,h)-anthracene	25	5	5	19.55

^aSignal-to-noise ratio = 2. A dash indicates that no significant signal was observed. ^bFluorescence with excitation at 360 nm and measurement at 418–700 nm. ^cCapacity factors were calculated in the usual way.

From ref. 12.

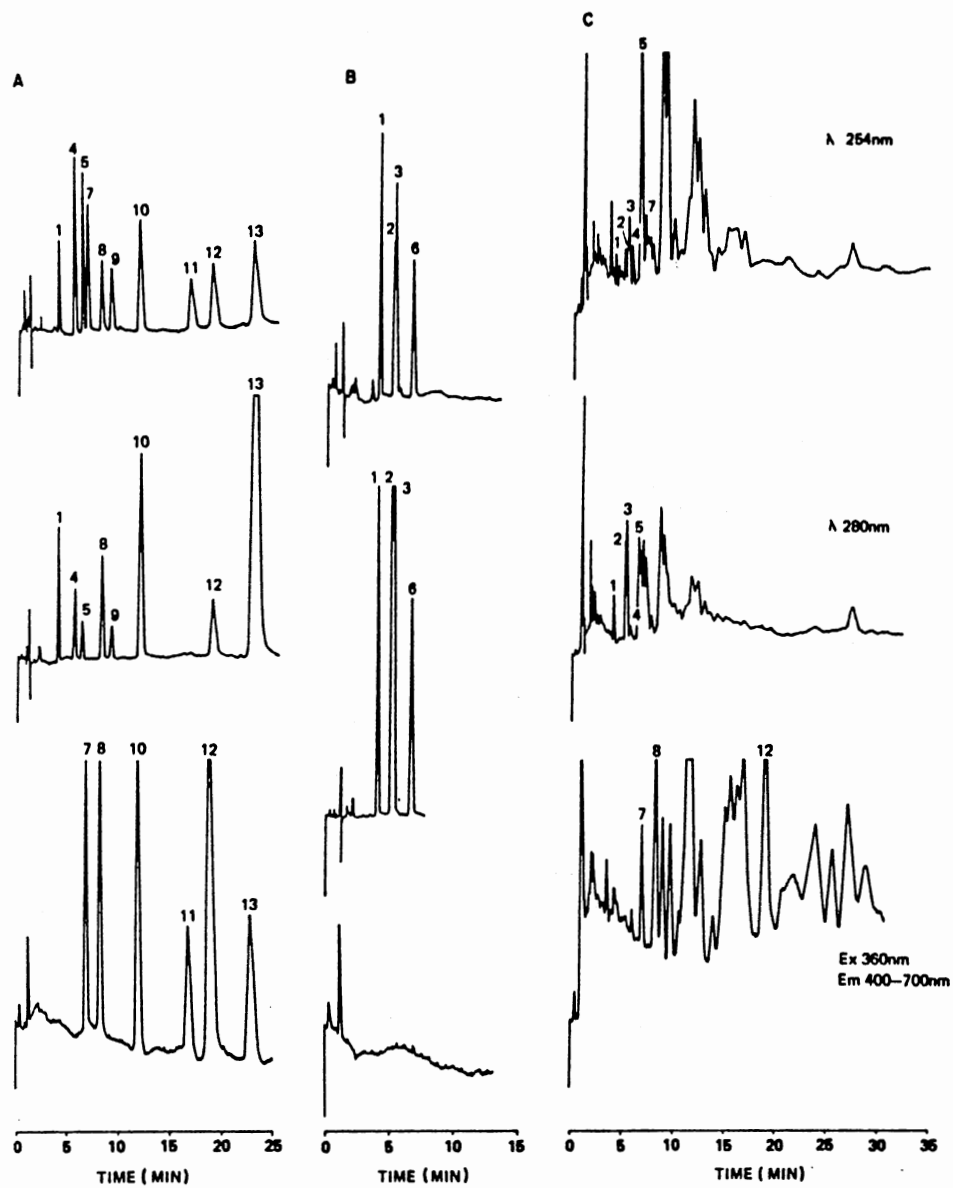


Figure 12. UV Absorbance and Fluorescence Detection. (A) PAH Standards, (B) Alkylated Naphthalenes, (C) Refinery Effluent After Enrichment. For Peak Identification See TABLE 4. From Ref. 12.

channel UV-VIS detection is available, only careful evaluations of peak shapes enables discriminations between pure and partially resolved peaks, usually based on peak moment analysis (26) or signal slope analysis using derivative chromatograms (27).

The introduction of dual-wavelength detection instrumentation brought about the development of the absorbance ratio (28,29,30) and various peak suppression techniques, based either on difference chromatography (31,32,33) or derivative chromatography (34,35). Both of the above approaches rely upon carefully chosen wavelengths (36,37) which are easily known for synthetic samples but difficult or impossible to know for unknown mixtures. The capabilities of the widely used absorbance ratio procedure are controversial (38).

Drouen and co-workers (39) used the absorbance ratio technique for solute recognition in liquid chromatography and noted that, "In principle, the ratio of the absorbances measured at two different wavelengths is characteristic for a given solute and provides the means to recognize unknown components in successive chromatograms. In practice, the applicability of the absorbance ratio is restricted by chromatographic and instrumental limitations, such as unresolved peaks, base line drift and offset, finite sampling rate, and peak tailing". Figure 13 shows the effects of baseline drift and offsets on the absorbance ratios. Figure 14 shows a practical example of the effects

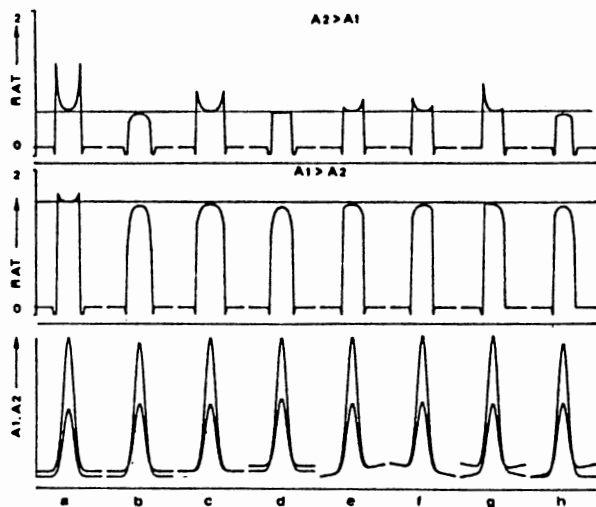


Figure 13. Effects of Baseline Drift and Offsets on Absorbance Ratios. From Ref. 39.

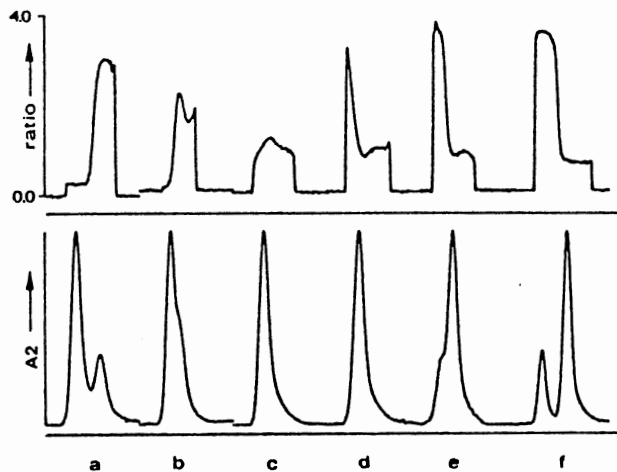


Figure 14. Practical Effects of Peak Overlap and Peak Tailing on Absorbance Ratios. From Ref. 39.

of peak overlap and peak tailing on the ratiogram. For this example, during a gradient run from 95% THF/water to 80% THF/water, a mixture of two solutes was repeatedly injected. As the solvent composition changes, one can observe the changes in the ratiogram, even for this relatively small change (15%) in solvent composition. The characteristics of the ratiograms shown in this example clearly illustrate the difficulty in interpreting ratiograms of tailing and overlapping peaks.

Since the advent of the commercially-available, optical multi-channel detectors, such as the photodiode array (PDA) and the charge-coupled device (CCD) (40,41,42), it is relatively easy to obtain full UV-VIS absorption spectra at several points along a chromatographic peak. This data can then be viewed or analyzed by the ratio and difference methods, spectral overlays (43), library searches, and many different types of multivariate data evaluation techniques (44,45,46,47,48,49,50), as well as principal component analysis.

Rossi and co-workers (51) conducted investigations of multiwavelength absorption spectroscopy for quantification and identification of PAHs exhibiting extensive peak overlap. The effluent stream was monitored using a diode-array spectrophotometer. With their system, absorption spectra could be recorded between 220 nm and 400 nm at 1, 2, or 5 second intervals. They then used multiwavelength fitting methods for data processing and multicomponent

analysis. Table 5 shows the detection limits that were achieved by using absorption measurements at the wavelengths of maximum absorptivity, and also by using peak integration at maximum wavelengths.

Fluorescence Detection

All PAHs fluoresce to some extent when excited by UV radiation due to their π -electron configuration. Because of the diversity within the PAH class of compounds, their fluorescence emissions occur over a wide range of wavelengths. Fluorescence detection, because of its inherent selectivity and sensitivity, is widely used for monitoring PAHs separated by HPLC (52,53). The selectivity is achieved because, although many molecules absorb UV-VIS light, far fewer molecules show appreciable fluorescence emission. The sensitivity is greater than that of UV-VIS absorption because in absorption measurements, it is necessary to distinguish a small difference between two relatively large signals. Absorption is only dependent on the concentration of the analyte, the cell pathlength, and the molar absorptivity. In contrast, fluorescence measurements detect an emitted signal above the dark-current background in the detector (a relatively large signal in the presence of the low background signal). Fluorescence can also be increased by increasing the excitation intensity, thereby adding more sensitivity as is

TABLE 5
DETECTION LIMITS USING A DIODE-ARRAY
ABSORBANCE DETECTOR

Compound	Detection limits ($\mu\text{g ml}^{-1}$)			λ_{max} (nm)
	Without integration		With integration	
	254 nm	λ_{max}	λ_{max}	
Acenaphthylene	1.1	0.02	0.006	227
Fluorene	0.07	0.06	0.011	262
Phenanthrene	0.06	0.06	0.004	254
Fluoranthene	0.27	0.10	0.005	287
Pyrene	0.49	0.07	0.003	241
Benzo(b)fluorene	0.13	0.08	0.006	264
Benz(a)anthracene	0.19	0.10	0.003	288
Benzo(b)fluoranthene	0.20	0.17	0.007	258
Benzo(k)fluoranthene	0.16	0.11	0.005	308
Benzo(ghi)perylene	1.4	0.40	0.005	304
Benzo(a)pyrene	0.14	0.10	0.003	296

From ref. 51.

illustrated in the following equation for fluorescence intensity:

$$I_F = kQ_F I_0 \epsilon bc$$

where I_F is the fluorescence emission intensity, Q_F is the quantum yield, I_0 is the excitation intensity, ϵ is the molar absorptivity, b is the cell pathlength, c is the concentration of the analyte, and k is a constant that includes factors such as the geometry and efficiency of detection, etc.

There are several types of fluorescence detectors commercially available and these can employ filters for both excitation and emission, a monochromator for excitation or emission only, or monochromators for both excitation and emission. Due to the separation provided by the HPLC column, wavelength selection with filters is often adequate. The use of filters also offers higher excitation and emission throughput which will lower detection limits if the separation is acceptable. However, the analytes are often in a more complex matrix and monochromatic light is sometimes essential for good selectivity. A combination of monochromatic excitation and long-pass emission filters is often used for complex samples.

The most common excitation sources include the mercury lamp, which emits narrow bands of high intensity radiation, and continuous source lamps such as deuterium or xenon arc lamps. The most frequently-used lamp is the xenon arc

lamp, which has a relatively continuous spectrum from 260 nm to 660 nm.

The total fluorescence intensity for an analyte eluting from the HPLC column depends on several variables, including filter quality, purity of the mobile phase (which may contain quenchers, absorbers), quantum yields, and potential quenching effects by other species such as oxygen. Self-absorption or the inner-filter effect can affect the detector response at high concentrations but this is usually not a problem with trace analysis. Because of these variables, the need for calibration is especially important. A standard should be available for each PAH analyte to generate calibration curves for concentration determinations.

Peak Purity Determination. Many of the techniques for determining peak purity that have been applied to UV-VIS absorbance detection have also been applied to fluorescence detection. The simplest approach to identifying peak heterogeneity using fluorescence is to change either the excitation wavelength, emission wavelength, or both between chromatographic runs to see if hidden peaks become visible. However, since this is often tedious and time consuming, a procedure is needed to obtain all the information desired "on-the-fly" and in a single run. Although rapid scanning has been investigated (54), there is often significant loss of spectral resolution due to the fast scan speeds involved (10 nm/s). This spectral resolution problem can be

overcome through the use of electronic array detectors (55), intensified vidicon multichannel analyzer systems (56), or rapid scanning video fluorometer detection schemes.

Warner and co-workers (57,58) have investigated the use of a rapid scanning video fluorometer as an HPLC detector. This approach is very useful for identification of well-separated compounds; However, problems arise when there is incomplete separation. As Warner states, "deriving the contribution of each component to the total signal at any point in time becomes extremely difficult when components coelute and overlap spectrally". In this case, algorithms for the deconvolution of the data sets have to be utilized. Warner illustrated the resolution of a three-component system using these procedures, but the three components were not significantly overlapping spectrally, and no quantitation was described.

Another fluorescence technique that has been used to investigate peak heterogeneity is synchronous fluorescence spectroscopy. In this technique, instead of keeping the excitation wavelength constant and scanning the emission or vice versa, both the excitation and emission are scanned within a given spectral acquisition. Two approaches have been developed for synchronous scanning.

The first, constant wavelength synchronous luminescence spectroscopy (CWSLS), was originally described by Lloyd (59), and later developed by Vo-Dinh (60,61,62)

into a selective tool for quantitative multicomponent analysis of complex mixtures. A constant wavelength difference is maintained between the excitation and emission monochromators. In the majority of cases, this constant wavelength difference is optimal when it is equal to the Stoke's shift. Vo Dinh (60) reported that a wavelength difference of three nanometers is appropriate for many PAHs. However, the optimal difference may vary substantially and depends on the particular spectral characteristics of the PAHs under investigation. Spino et al (63) used CWSLS in combination with a micellar mobile phase to identify unresolved PAHs in chromatographic peaks. They found that optimum wavelength differences ranged from 10 to 50 nm. They were able to identify several coeluting PAHs, but no quantitation was shown. Figure 15 shows a chromatogram with overlapping peaks using a fixed wavelength absorbance detector at 254 nm. Using CWSLS, eight components could be identified from the three unresolved peaks.

The second approach to synchronous scanning fluorescence is called constant energy synchronous luminescence spectroscopy (CESLS). In this approach, developed by Inman and Winefordner (64,65,66), instead of keeping a constant wavelength difference between the excitation and emission monochromators, a constant energy difference is maintained corresponding to a vibrational energy difference. Kerkhoff et al. (67) demonstrated the

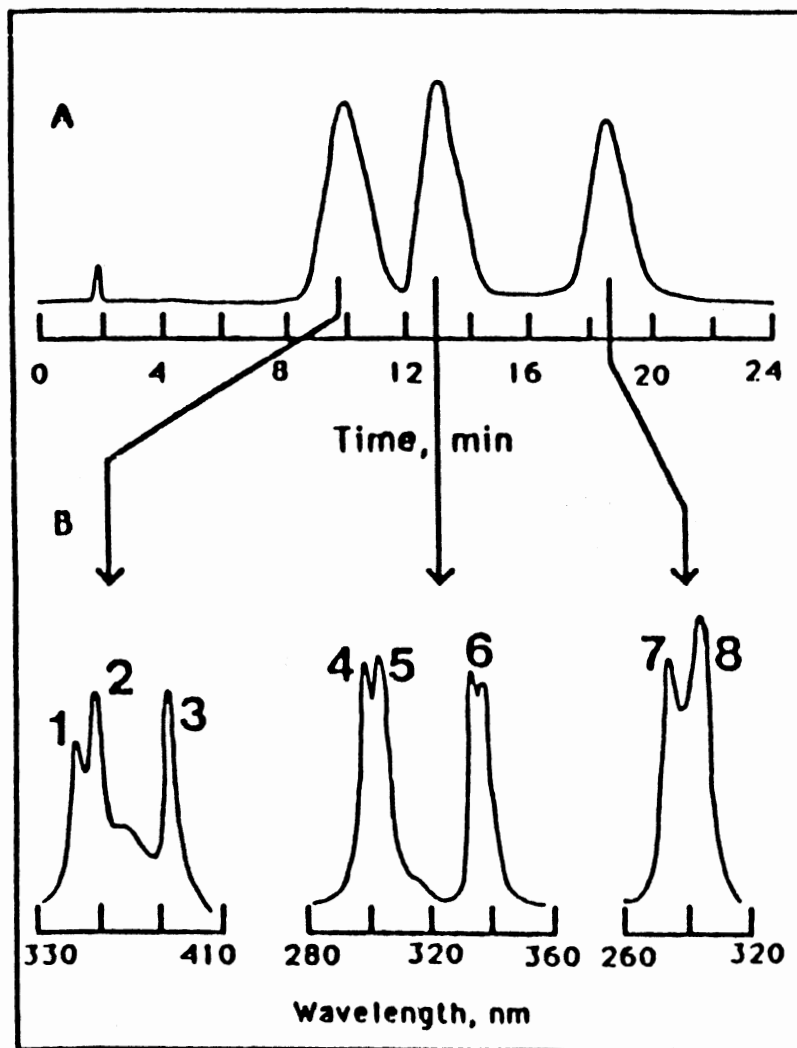


Figure 15. Separation of (1) Pyrene, (2) Fluoranthene, (3) Benzo(e)pyrene, (4) Biphenyl, (5) Fluorene, (6) Phenanthrene, (7) Naphthalene, (8) Acenaphthylene. (A) UV Detection at 254 nm Showing Only Three Peaks, (B) Synchronous Luminescence of the Three Peaks in (A) Using Wavelength Differences of 20, 10, and 5 nm, Respectively. From Ref. 63

use of this technique for several mixtures of PAHs. Their computerized system scanned at a rate of 200 nm s^{-1} and collected data in the forward and reverse directions. Figure 16 illustrates the chromatogram of a three-component mixture of PAHs. Figure 17 shows the CESLS spectra of the three PAHs plotted out after the run was finished. The authors stated that the loss in the detection limits observed in the rapid-scanning system compared to a variable wavelength fluorescence system could be as large as a factor of 3200, but the CESLS system obtained the result 200 times faster and, in addition, provided the CESLS spectra.

An overall comparison of the minimum detectable quantities for each of the detectors described above is difficult due to the many variations available for each technique. Nevertheless, Yeung and Synovec (68) presented a general comparison of the capabilities of commercially available detectors and state-of-the-art detectors. These minimum detectable quantities (amounts injected) for commercially available detectors are as follows, with the state of the art values in parentheses: mass spectrometry, 100 pg - 1 ng (1 pg); absorbance, 100 pg - 1 ng (1 pg); and fluorescence, 1 - 10 pg (10 fg).

PAHs are ubiquitous pollutants and therefore the identification and quantitation of these compounds is of utmost importance. There are a variety of detection methods available that will provide the needed information

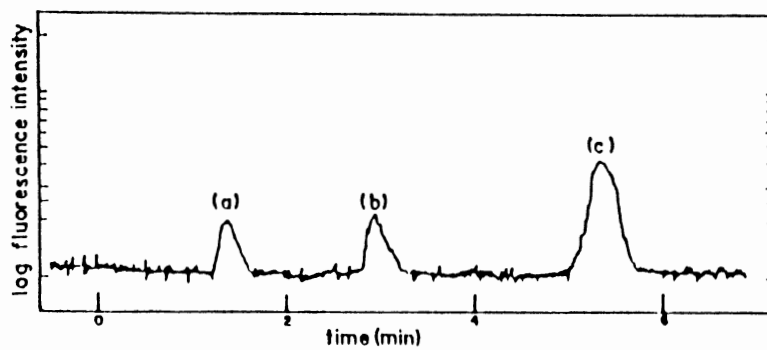


Figure 16. Fluorescence Chromatogram of (a) Anthracene, (b) Chrysene, and (c) Benzo(a)pyrene. From Ref. 68.

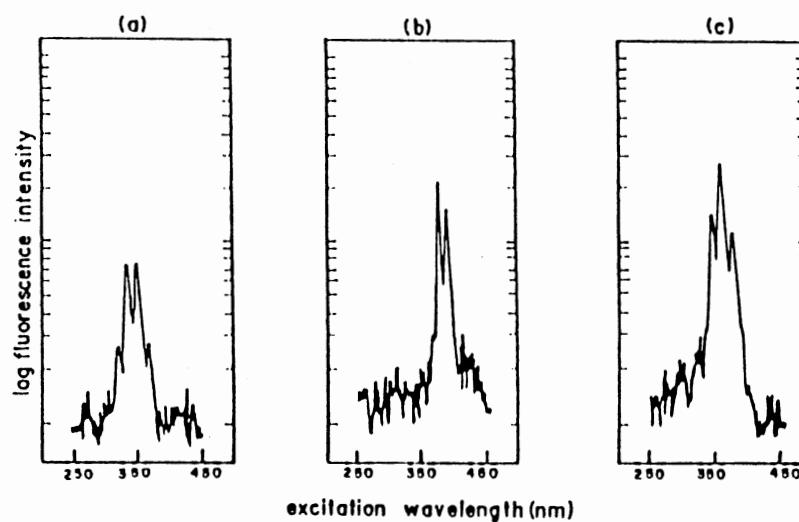


Figure 17. Constant Energy Synchronous Luminescence Spectra of The Three Peaks in Figure 16. From Ref. 67.

about the PAHs as long as sufficient separation is achieved. Unfortunately, the biggest problem in determining PAHs appears to be the coeluting isomers. Although several techniques seem capable of identifying compounds in coeluting peaks (even though much time and effort is often required), there is very little data that supports the quantitation of such peaks. The on-line phase-modulation fluorescence lifetime technique described in the Results section of this dissertation describes our approach, in which we first flag peak heterogeneity, identify the components present, and then quantitate the components in coeluting peaks, all based on the incorporation of fluorescence lifetime selectivity.

CHAPTER III

FLUORESCENCE LIFETIME THEORY AND APPLICATIONS

Fluorescence: A General Description

The fluorescence process involves the spin-allowed emission of electromagnetic radiation by a chemical species following promotion to an excited electronic state. Since fluorescence must necessarily begin by the absorption of a photon of light, one must consider the probability that a particular molecule has a potential electronic transition corresponding to a particular excitation energy. The probabilities for radiative transitions depend on several factors, including orbital overlap, molecular symmetry, and multiplicity (69). These factors result in typical molar absorptivity ranges for transitions to singlet $n\pi^*$, singlet $\pi\pi^*$, and triplet $\pi\pi^*$ excited states, of 10^1 - 10^3 , 10^3 - 10^5 , and 10^{-3} - 10^{-1} L cm⁻¹ mol⁻¹, respectively. The probabilities for $n\pi^*$ transitions are lower than $\pi\pi^*$ due to poor orbital overlap between the highly localized, nonbonding n orbitals and π^* orbitals. Radiative transitions involving electron spin (multiplicity) changes (triplet $\pi\pi^*$) are quantum-mechanically forbidden and therefore have very small molar absorptivities.

Once a molecule has been excited to an excited electronic state, the probability for fluorescence emission depends on which pathways are available for deexcitation other than fluorescence. The quantum efficiency of fluorescence emission is expressed as:

$$\Phi_F = \frac{k_F}{k_F + \Sigma k_d} \quad (1)$$

where k_F is the rate constant for fluorescence emission and Σk_d is the sum of the rate constants for all other processes that can depopulate the excited singlet electronic state, such as internal conversion which non-radiatively relaxes the molecule to the ground state, and intersystem crossing to a triplet state. From the triplet state, a molecule may either non-radiatively de-excite or emit radiation in the form of phosphorescence.

Fluorescence of PAHs

In taking into account the above considerations, it is obvious why PAHs are typically efficient fluorescent species. First, they contain extensive π -electron character due to conjugation, and therefore are efficiently excited by UV-VIS light. Furthermore, since most PAHs are relatively rigid, planar systems, there are considerably less vibrational pathways by which to non-radiatively de-excite.

The effect of increasing the number of fused rings in an unsaturated aromatic molecule is to increase fluorescence intensity and shift the excitation and emission spectral bands to longer wavelengths. For substituted aromatic molecules, substituents that are electron donating ($-\text{NH}_2$, $-\text{OH}$) enhance fluorescence, while electron withdrawing substituents ($-\text{NO}_2$, $-\text{CO}_2\text{H}$) decrease fluorescence. Heavy atom substituents such as $-\text{Br}$ and $-\text{I}$ tend to diminish fluorescence by increasing intersystem crossing to triplet states. For this reason, heavy atoms are often employed to encourage phosphorescence at the expense of fluorescence.

Molecules in excited electronic states generally possess molecular geometries and electronic charge distributions that are substantially different than in the ground state. In most instances, the excited state is more polar than the ground state and an increase in solvent polarity produces a greater stabilization of the excited state. For this reason, reversed-phase liquid chromatography, which employs typically highly polar mobile phases, is very desirable for the fluorometric detection of PAHs. However, one must always be alert to the possibility of changing fluorescence characteristics with different mobile phase compositions (70).

Fluorescence Lifetime Theory

In order to generally describe the fluorescence emission from a population of fluorescent molecules, one first assumes that the ground state population of molecules F are excited at a time dependent rate $f(t)$ directly to an excited state F^* . They return to the ground state from the excited state with a rate constant $K = k_E + k_S$, with k_E defined as the natural emissive rate constant and k_S the rate of radiationless deexcitation. Therefore, the equilibrium exists as follows:



The equation:

$$\frac{d[F^*]}{dt} = -K[F^*] + f(t) \quad (3)$$

relates the time dependence of the concentration of F^* to the rate constants for the absorption and emission.

Response To Pulsed Excitation

If one assumes that the excitation is instantaneous (i.e. the excitation pulse is infinitely narrow), then $f(t)$ will approach zero and equation 3 above becomes

$$[F^*] = [F^*]_0 e^{-Kt} \quad (4)$$

where $[F^*]_0$ is the initial concentration of excited-state molecules. The fluorescence response to pulsed excitation is shown in Figure 18. The mean lifetime, defined as $1/K$, corresponds to the time at which $[F^*]$ is equal to $1/e * [F^*]_0$. The mean lifetime is also referred to as the fluorescence lifetime, τ .

If the fluorescence emission is due to more than one component, and these components do not interact, then the time response to pulsed excitation is:

$$F(t) = \sum \alpha_i e^{-t/\tau_i} \quad (5)$$

where α_i is the fractional contribution of lifetime component τ_i . In order to resolve the individual decays from the multiexponential decay, one must first determine the lamp pulse profile. This can usually be measured in a separate experiment using a scatter solution, provided that the measurement is made as closely as possible in time to the measurement of the fluorescence decay. The observed fluorescence decay can then be fit by least-squares iterative reconvolution of the lamp pulse, using an assumed fluorescence decay law; these can be chosen as singly exponential, doubly exponential, and higher order exponential fits, until the best fit is obtained. This method is demonstrated for a mixture of anthracene and 9-cyanoanthracene in Figure 19 (71).

Alternately, if lifetimes are well separated and are sufficiently longer than the excitation pulse width, the

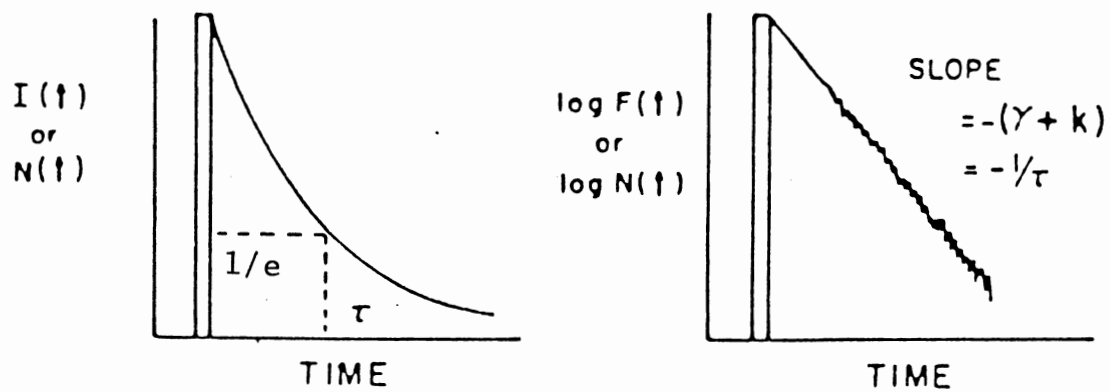


Figure 18. Exponential Fluorescence Decay After Pulsed Excitation. From Ref. 71.

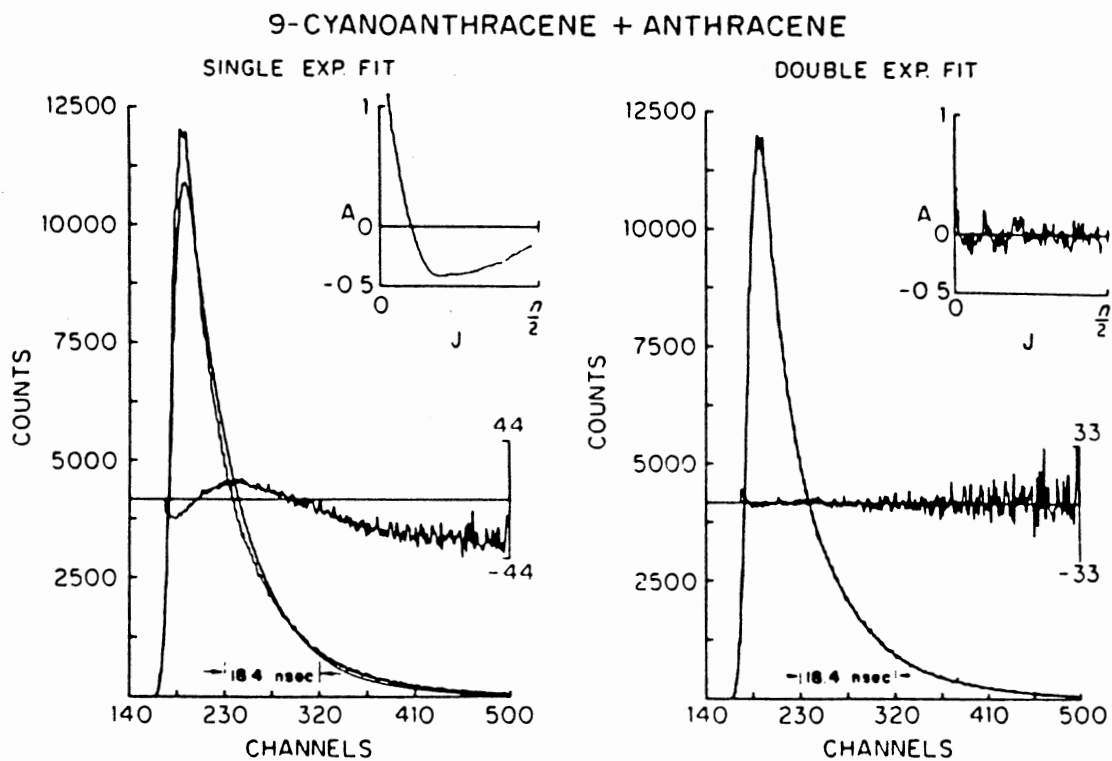


Figure 19. Least-Squares Reconvolution of a Two-Component Decay Using Single and Double Exponential Decay Laws For Fitting. From Ref. 71.

fluorescence decay curves can be obtained by component stripping. In this approach, the lifetime of the longest-lived component is determined after the shorter-lived components have decayed. The decay due to this component can then be subtracted from the total observed decay and so on. As would be expected, this method tends to fail when more than two components are present. The results for this method are shown in Figure 20 for two components (72).

Response To Harmonic Excitation

If the intensity of the excitation beam is sinusoidally-modulated at an angular frequency ω , then the time-dependent excitation function has the form:

$$E(t) = A(1 + m_{ex}\sin\omega t) \quad (6)$$

where $E(t)$ is the total intensity at time t , A is the steady state (d.c.) intensity, and $m_{ex}\sin\omega t$ is the time-dependent (a.c.) component. The modulation depth, m_{ex} , is the ratio of the a.c. amplitude to the d.c. intensity.

Upon excitation with light of the form $E(t)$, a fluorescent species will emit a signal with the same sinusoidal modulation frequency; however, it will be phase-shifted (ϕ) and demodulated (M), relative to the excitation:

$$F(t) = A'\{1 + m_{ex}M\sin(\omega t - \phi)\} \quad (7)$$

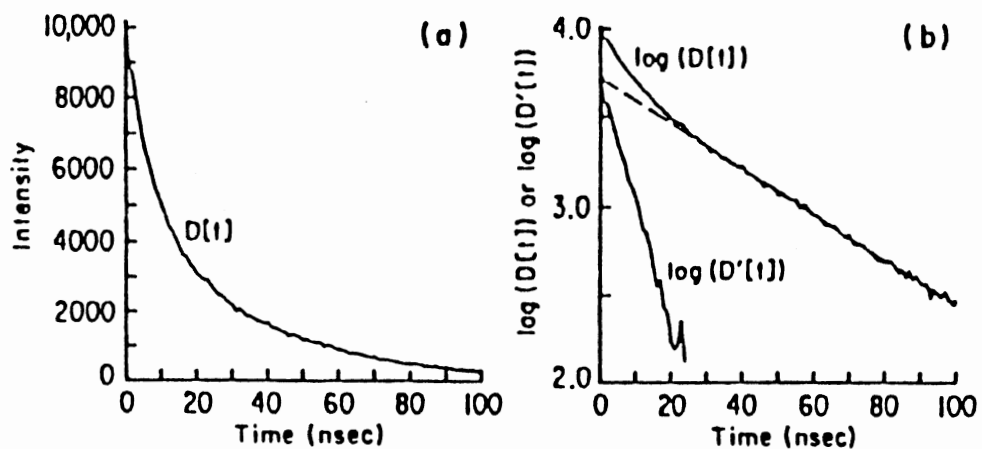


Figure 20. Component Stripping For Two-Component Decay. (a) Exponential Decay Showing Apparent Single Exponential. (b) Non-Linearity Indicates Two Components ($D(t)$) and Resulting Decay After Subtracting Long-Lived Component ($D'(t)$). From Ref. 72.

Figure 21 illustrates the excitation and emission functions graphically. The degree of phase-shift and demodulation is related to the fluorescence lifetime of the emitting species and the excitation modulation frequency used. The steady state term, A' , is related to k , an instrumental response constant, I , the excitation intensity, Φ_F , the fluorescence quantum yield, ϵ , the molar absorptivity of the compound, b , the cell pathlength, and c , the concentration of the compound, as follows:

$$A' = kI\Phi_F\epsilon bc. \quad (8)$$

The two parameters, ϕ and M , allow two convenient and independent calculations of the fluorescence lifetime of a species: the phase lifetime, τ_p , and the modulation lifetime, τ_M .

$$\tau_p = (1/\omega)\tan\phi \quad (9)$$

$$\tau_M = (1/\omega)\{(1/M^2)-1\}^{1/2} \quad (10)$$

In practice, measurement of ϕ and M requires some sort of reference in order to calibrate the phase and modulation of the excitation light. Two methods are available for calibration. One uses a scattering solution such as glycogen or kaolin solution, which has a radiative lifetime of zero by definition. Alternatively, one can choose a well-characterized reference fluorophore with a known fluorescence lifetime. The equations for the fluorescence lifetimes then take the form:

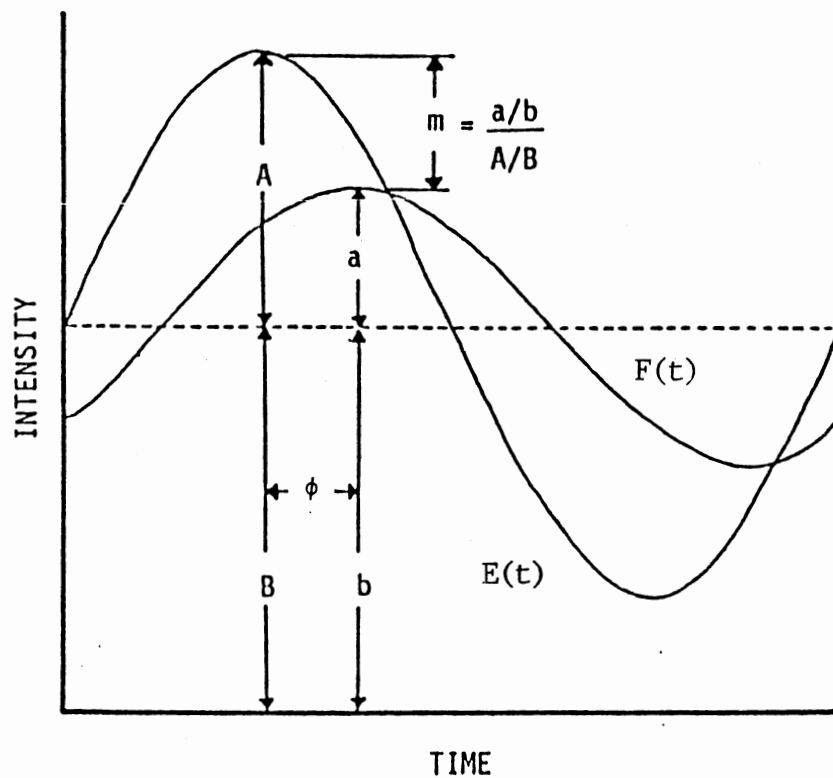


Figure 21. Excitation ($E(t)$) and Emission ($F(t)$) Functions For Harmonic Excitation Showing The Demodulation M and Phase Shift ϕ .

$$\tau_P = (1/\omega) \{ \tan[(\phi_S - \phi_R) + \tan^{-1}(\omega\tau_r)] \} \quad (11)$$

$$\tau_M = (1/\omega) [\{ (1 + \omega^2\tau_r^2)/D^2 \} - 1]^{1/2} \quad (12)$$

where $D = M_S/M_R$
 s corresponds to sample
 r corresponds to reference

For very accurate lifetime determinations, it is best to use a reference fluorophore which has excitation/emission wavelengths in similar regions as the sample (73) and also has a lifetime similar to that of the sample (74).

The previous discussion has assumed a homogeneous population with a single fluorescence lifetime. When dealing with a heterogeneous population, the total emission is the sum of emissions of the individual populations. However, using the phase-modulation approach, the mean lifetimes, τ_p and τ_m are not the arithmetic mean of the individual lifetimes. The mean tangent of the observed phase angle is less than the arithmetic mean of tangents, and the lifetime determined by the phase-shift is therefore shorter than the arithmetic mean lifetime. The lifetime determined by the demodulation is weighted more by the longer lifetime components and is therefore greater than the arithmetic mean lifetime. This weighting of the mean lifetimes measured by the phase-modulation technique is illustrated for a two component system in Figures 22 and 23. These "Christmas tree" and "banana" diagrams show again that the phase lifetime for a heterogeneous population is shortened while the modulation lifetime is

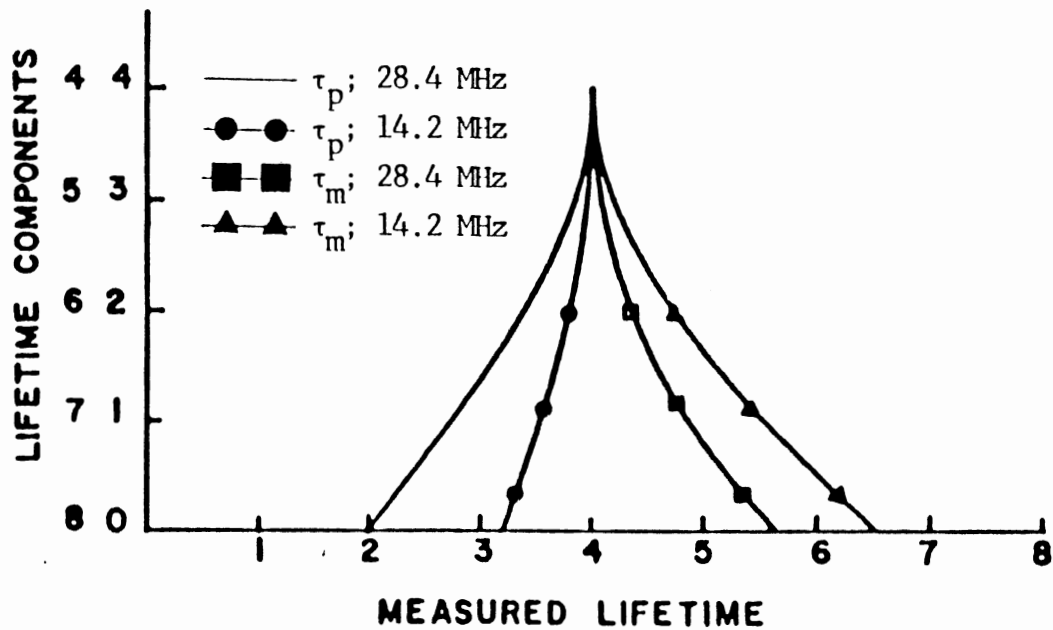


Figure 22. Divergence of Calculated Lifetimes From An Arithmetic Mean of 4 ns in Heterogeneous Systems of Two Components of Equal Intensity. From Ref. 75.

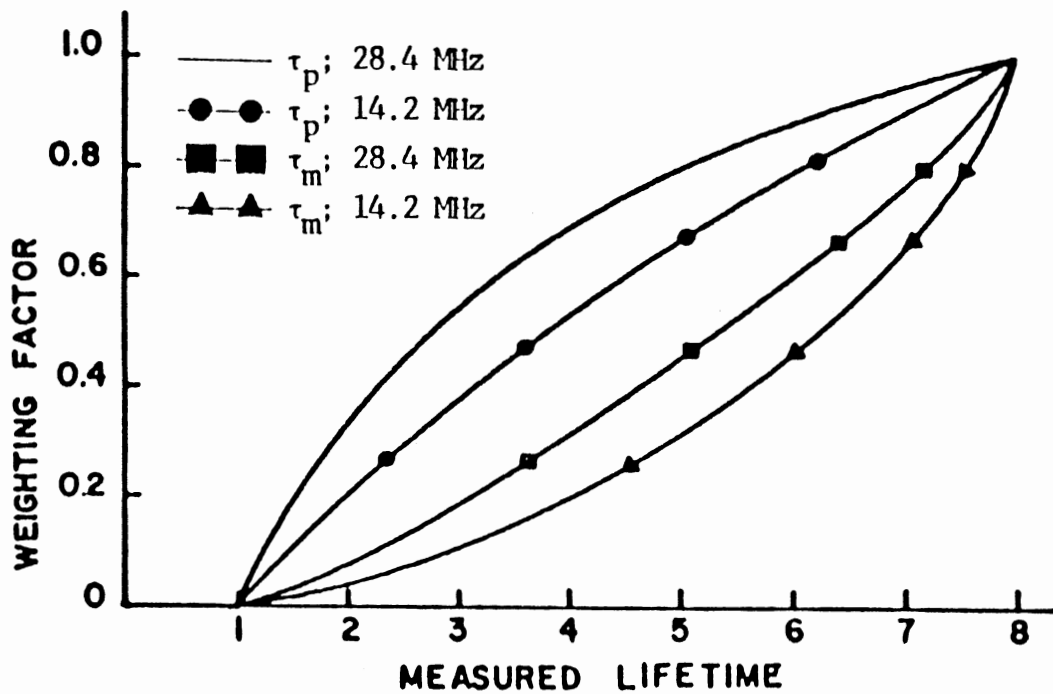


Figure 23. Divergence of Lifetimes in Two-Component Systems of 1 and 8 ns but different relative intensity (weight). From Ref. 75.

lengthened with respect to the arithmetic mean. Detailed derivations of the above theory have been presented by Spencer (75).

Heterogeneity Analysis Based On Phase-Modulation Lifetimes

Weber (76) described a closed-form analytical solution to calculate fractional intensity and lifetime values for two- and three-component systems from the phase and modulation values at N frequencies, where N equals the number of components in the sample. He expressed the phase-shift (ϕ) and demodulation (M) as follows:

$$\tan \phi = S/G = \omega\tau_p \quad (13)$$

$$M = [S^2 + G^2]^{1/2} = [1 + \omega^2\tau_M^2]^{-1/2} \quad (14)$$

where

$$S = \sum f_i \sin\phi_i \cos\phi_i \quad (15)$$

$$G = \sum f_i \cos^2\phi_i \quad (16)$$

The fractional intensities (f_i) are related to the preexponential factors (α_i) by:

$$f_i = \alpha_i\tau_i / \sum \alpha_i\tau_i. \quad (17)$$

The closed-form analytical solution, known as Weber's algorithm, was used by Jameson and Weber (77) to investigate the two forms of tryptophan at neutral and high pH. The relative yield and fluorescence lifetimes of

tryptophan vs. pH are shown in Figure 24. Table 6 shows lifetimes at each pH and Table 7 shows resolved lifetimes using data at 6 and 30 MHz. They found that the errors in the determination of the phase and modulation lifetimes were dependent on the choice of frequency pair and the proportions of the compounds. As a general rule, the lifetimes of the components were resolved with a precision which was degraded by a factor of 5-15 with respect to the precision of the input lifetimes. The authors note that the data acquisition and computation for the phase-modulation method is much faster and more direct than for pulse techniques and don't require fitting to ad hoc instrumental response parameters as is necessary in pulsed experiments.

Jameson and Gratton (78) further investigated heterogeneity analysis and developed a non-linear least squares approach to solve for lifetimes and fractional contributions of components present in a heterogeneous sample. They noted that, for the system previously described by Weber, if more than two modulation frequencies were used while solving the closed-form equations for two components using Weber's algorithm, the relative uncertainty in the resolved lifetimes increased. Since this result was unexpected, they looked at how the resolved lifetimes for a two component system of 3.1 and 8.7 ns would come out using several different sets of frequency pairs. As Figure 25 shows, the distribution of the

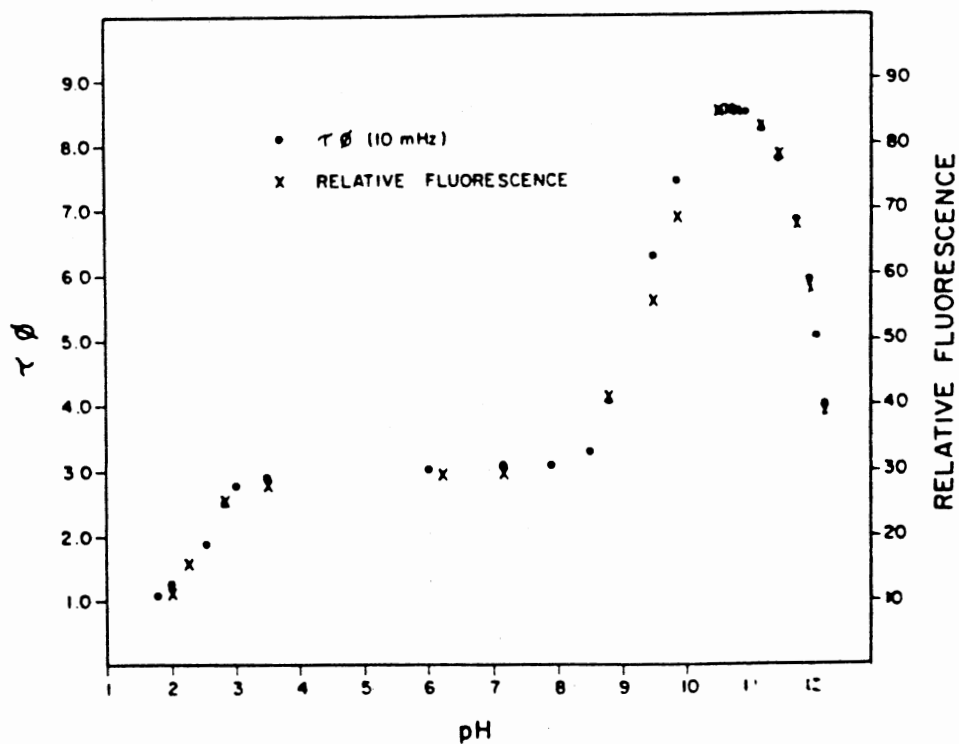


Figure 24. Relative Fluorescence Intensity and Fluorescence Lifetimes as a Function of pH For Tryptophan. From Ref. 78.

TABLE 6
 FLUORESCENCE LIFETIMES OF TRYPTOPHAN
 AT DIFFERENT PH VALUES

pH	6 MHz		18 MHz		30 MHz	
	τ^P , ns	τ^M , ns	τ^P , ns	τ^M , ns	τ^P , ns	τ^M , ns
8.27	3.84 ± 0.07	4.18 ± 0.26	3.50 ± 0.02	3.83 ± 0.02
8.56	4.37 ± 0.02	5.10 ± 0.11	4.04 ± 0.03	4.90 ± 0.03	3.85 ± 0.05	4.38 ± 0.03
9.04	5.76 ± 0.01	6.91 ± 0.27	5.20 ± 0.05	6.63 ± 0.05	4.60 ± 0.11	5.82 ± 0.08
9.44	7.21 ± 0.01	8.03 ± 0.09	6.53 ± 0.06	7.49 ± 0.05	5.62 ± 0.01	7.27 ± 0.03
9.74	7.89 ± 0.04	8.12 ± 0.08	7.41 ± 0.03	8.01 ± 0.12	7.08 ± 0.02	7.92 ± 0.03
9.96	8.27 ± 0.01	8.39 ± 0.05	7.76 ± 0.03	8.35 ± 0.04

From ref. 78.

TABLE 7
 RESOLVED LIFETIMES FOR DATA IN TABLE 6
 USING WEBER'S ALGORITHM

pH	τ_1 , ns	τ_2 , ns	f_1	f_2
8.27	3.28	9.34	0.923 (0.824)	0.077 (0.176)
8.56	3.41	8.84	0.824 (0.707)	0.176 (0.293)
9.04	3.09	8.62	0.498 (0.444)	0.502 (0.556)
9.44	2.77	9.16	0.314 (0.241)	0.686 (0.759)
9.74	2.96	8.60	0.140 (0.137)	0.860 (0.863)
9.96	2.04	8.58	0.056 (0.088)	0.944 (0.912)

From ref. 78.

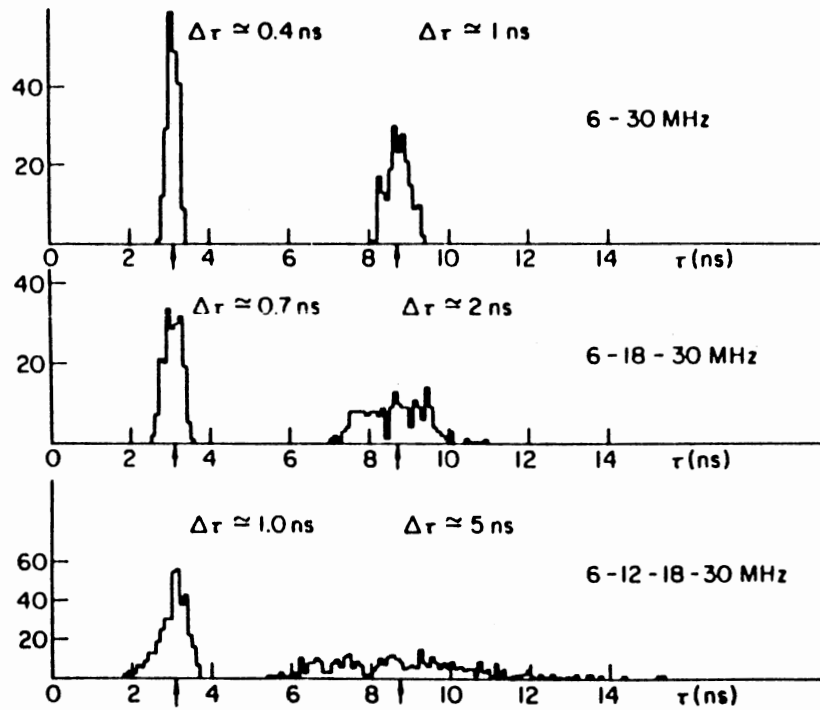


Figure 25. Distribution of Resolved Lifetimes Using Weber's Algorithm With More Than Two Frequencies For a Two-Component System of 3.1 and 8.7 ns. From Ref. 79.

resolved lifetimes increased as more frequencies were used. This was due to the fact that high frequency data is weighted more than low frequency data in the algorithm. They concluded that, given the accuracy of modern instrumentation, the closed solution becomes practically inapplicable for the case of three or more modulation frequencies. The authors then sought to determine theoretically what the optimum modulation frequencies would be in order to determine a two component system of 3.1 and 8.7 ns using two frequencies. Figure 26 shows that 30 MHz gave the largest separation, and Figure 27 shows that the best second frequency of the 6, 18 and 30 MHz available was 6 MHz.

After having evaluated Weber's algorithm, the authors introduced a non-linear least squares approach to analyze a two-component system. The function which was minimized during the analysis was:

$$F = \sum \{ (1-W) [(\phi_r^c - \phi_r^m) / \sigma_\phi]^2 + KW [(M_r^c - M_r^m) / \sigma_m]^2 \} \quad (18)$$

where ϕ_r^c and M_r^c are the calculated values of phase-shift and demodulation, ϕ_r^m and M_r^m are the measured values at ω_r , W is a weighting parameter which takes into account the inherent statistical accuracies associated with phase and modulation values, K is a normalization factor to account for phase data being in degrees while modulation data is in percentage units, and σ_ϕ and σ_m are the errors associated with phase and modulation data. Figure 28 shows

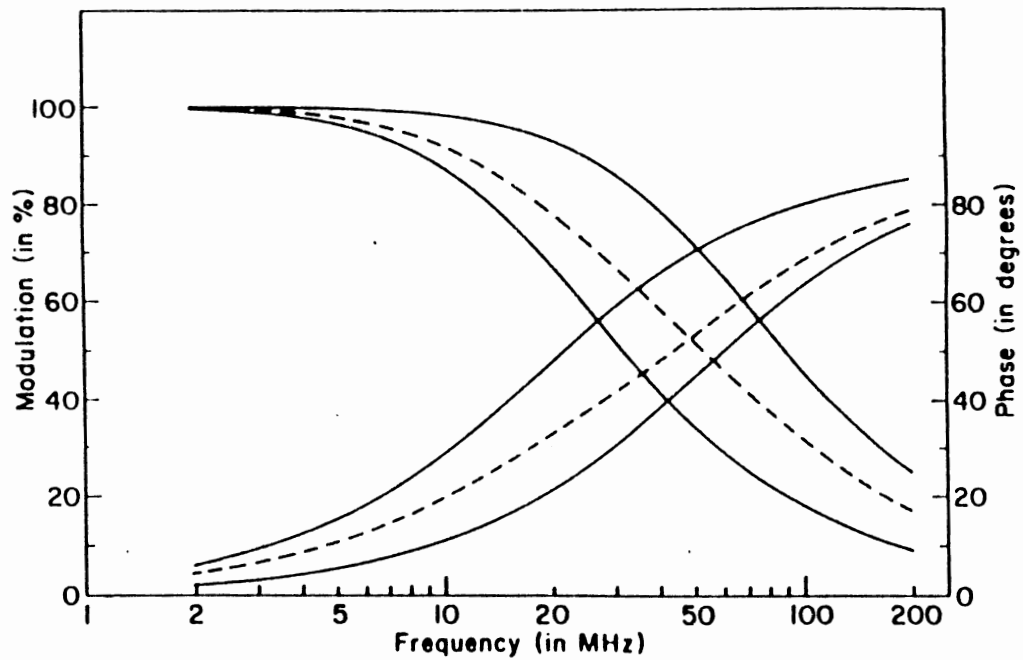


Figure 26. Phase and Modulation as a Function of Modulation Frequency For a Two-Component System of 3.1 and 8.7 ns. From Ref. 79.

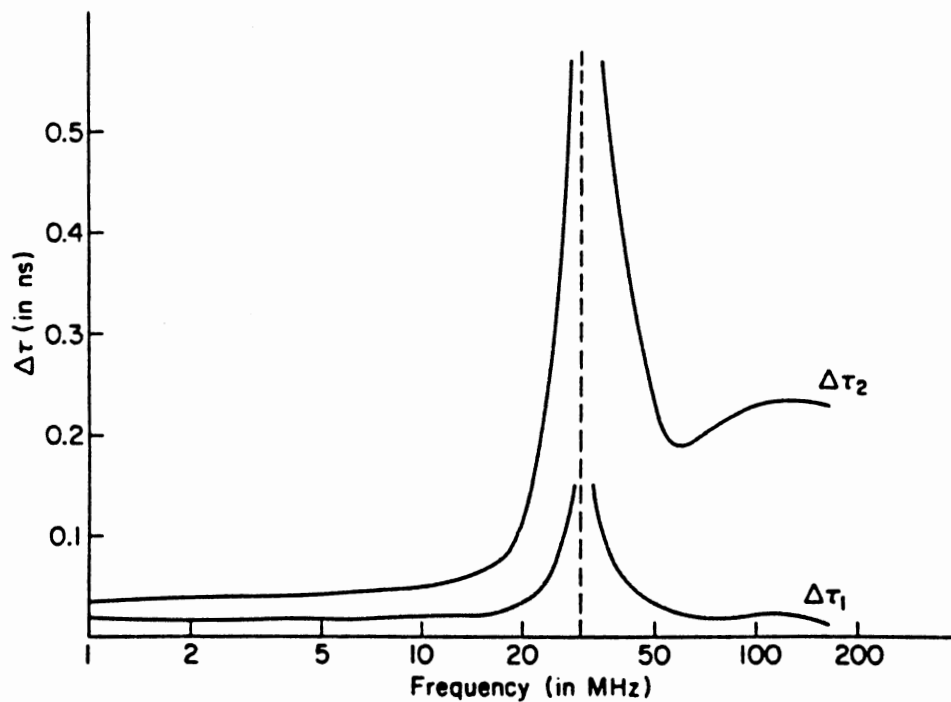


Figure 27. Errors in Resolved Lifetimes Using Weber's Algorithm as a Function of Frequency With One Frequency Fixed at 30 MHz. Same System as in Figure 26. From Ref. 79.

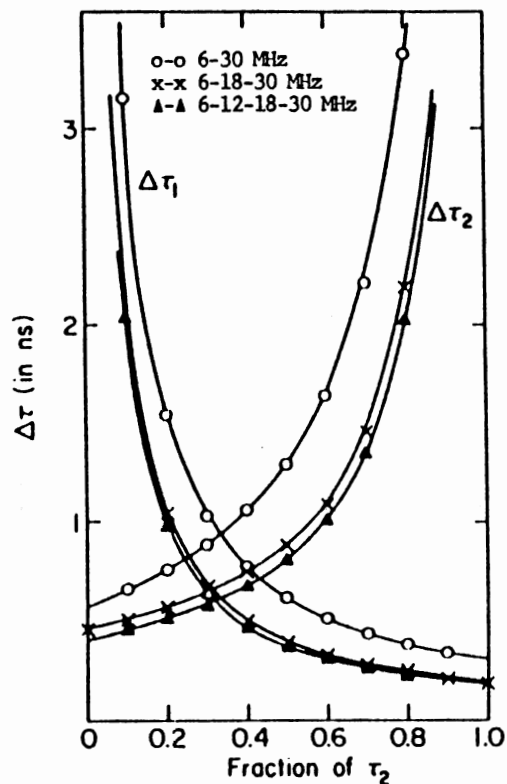


Figure 28. Uncertainty in the Resolved Components of the 3.1 and 8.7 ns System Using NLLS. From Ref. 79.

TABLE 8

RESOLVED LIFETIMES FOR 1:3 MIXTURE OF PERYLENE AND 9-AMINOACRIDINE USING NLLS WITH 5, 10, 20, AND 80 MHZ

Components	τ_1 , ns	f_1	τ_2 , ns	f_2
Perylene	4.33 ± 0.02	1.00
9-aminoacridine	10.99 ± 0.03	1.00
Mixture (1:3)	3.76 ± 0.06	0.26 ± 0.01	10.59 ± 0.10	0.74 ± 0.01

From ref. 79.

a plot of the uncertainty in the determination of the previously described two-component system of 3.1 and 8.7 ns. The errors in determinations of the phase and modulation were assumed to be ± 0.1 degree and ± 0.002 , respectively. For the two-frequency approach, the NLLS routine gave results similar to Weber's. Increasing the number of frequencies decreased the uncertainty with the NLLS approach, in contrast to Weber's closed-form solution. Finally, they were able to demonstrate the resolution of a 1:3 mixture of perylene and 9-aminoacridine. The results obtained using at 5, 10, 20, 40 and 80 MHz on a multifrequency instrument are shown in Table 8.

Dalbey and co-workers (79) investigated the use of phase-modulation fluorimetry to resolve binary and ternary systems of carbazole, pyrene, and POPOP. They first used Weber's closed-form solution and found that for a two-component system, the closed form gave lifetimes that varied markedly from independently measured lifetimes. For example, phase and modulation data at 18 and 30 MHz gave a value of 64.67 ns for pyrene, compared to the actual lifetime of 22.8 ns. They found that fixing the lifetime of one of the components that improved results under some circumstances, but for others results varied. The authors attempted to overcome this problem by writing computer programs which were able to utilize data at all three of the available frequencies (6, 18, 30 MHz). The programs used an iterative Monte Carlo method to find the best fit

to all of the multifrequency input data. They adapted the programs to allow different input and output parameters as shown in Table 9. Data was obtained at 6, 18 and 30 MHz for several solutions of pyrene (22.8 ns) and carbazole (8.7 ns) and fit to two-component systems using the Fit 1 and Fit 2 routines. The results are shown in Table 10. The average lifetime calculated for carbazole (τ_2) by Fit 1 was 8.86 ns when the pyrene lifetime (τ_1) was fixed at 22.8 ns. The average resolved lifetimes from FIT2 were 23.09 and 9.06 ns. For both of these analyses, the resolved lifetimes were within 0.4 ns of the "true" values and the fractional contributions were within 10% of their predicted values, except those for which the predicted fractional contributions were small ($\alpha < 0.05$). The authors then investigated a three component system of pyrene, carbazole, and POPOP ($\tau = 1.25$ ns). The solutions were made up to have equal intensity contributions from pyrene and carbazole, with a varying contribution from POPOP (0 to .718). Table 11 shows the results. The average resolved lifetime of POPOP determined by the FIT3 routine (τ_1 and τ_2 were fixed at 22.8 and 8.7 ns) was 1.4 ns, compared to the predicted value of 1.2 ns, when the data from solution two was omitted. In addition, the fractional contributions of POPOP, carbazole, and pyrene resolved by FIT3 and FIT3a were within an average of 7% of their expected values.

Beechem and co-workers (80) investigated global resolution of heterogeneous decay by phase-modulation

TABLE 9
COMPUTER PROGRAM ROUTINES^b

Name	Data input	Output ^a
FIT 1	τ_1, τ_p, τ_m at 6, 18, 30 MHz	$\tau_2, \alpha_1, \alpha_2, * \chi^2$
FIT 2	τ_p, τ_m at 6, 18, 30 MHz	$\tau_1, \tau_2, \alpha_1, \alpha_2, * \chi^2$
FIT 3	$\tau_1, \tau_2, \tau_p, \tau_m$ at 6, 18, 30 MHz	$\tau_3, \alpha_1, \alpha_2, \alpha_3, * \chi^2$
FIT 3a	$\tau_1, \tau_2, \tau_3, \tau_p, \tau_m$ at 6, 18, 30 MHz	$\alpha_1, \alpha_2, \alpha_3, * \chi^2$

a $* \chi^2$ is the sum of squares of differences between predicted and experimental τ_p and τ_m values at each frequency.

b All data from ref. 85.

TABLE 10
RESOLVED FLUORESCENCE LIFETIMES OF
PYRENE AND CARBAZOLE^c

Solution	τ_1	τ_2^a	α_2, true^b	α_2, calc^b	$^*\chi^2$
1	22.80	—	—	—	—
2	22.83	9.09 (9.06)	0.045	0.059 (0.058)	0.052 (0.053)
3	22.98	9.27 (8.87)	0.086	0.110 (0.099)	0.190 (0.195)
4	23.30	9.28 (8.65)	0.16	0.182 (0.153)	0.217 (0.247)
5	23.46	9.19 (8.71)	0.27	0.299 (0.263)	0.111 (0.141)
6	23.30	9.72 (9.41)	0.35	0.353 (0.325)	0.176 (0.187)
7	22.81	8.62 (8.61)	0.43	0.404 (0.404)	0.019 (0.019)
8	22.71	9.10 (9.16)	0.45	0.416 (0.422)	0.199 (0.200)
9	23.88	9.35 (9.09)	0.52	0.531 (0.489)	0.091 (0.116)
10	23.06	8.57 (8.49)	0.55	0.510 (0.500)	0.016 (0.018)
11	22.66	8.69 (8.72)	0.62	0.581 (0.586)	0.061 (0.062)
12	23.05	8.81 (8.77)	0.77	0.751 (0.745)	0.009 (0.010)
13	—	8.7	—	—	—

^a Values in parentheses were determined using the FIT1 routine with τ_1 (pyrene) set at 22.8 ns.

All other values were determined using the FIT2 routine with τ_1 for pyrene and τ_2 for carbazole.

^b α_2 is the fractional contribution of carbazole.

^c All data from ref. 85.

TABLE 11
RESOLVED FLUORESCENCE LIFETIME OF POPOP IN THE
PRESENCE OF PYRENE AND CARBAZOLE^{a, b}

Sol.	τ_3	α_1 values		α_2 values		α_3 values	
		True	Calc.	True	Calc.	True	Calc.
1	—	0.51	0.550 (0.543)	0.49	0.450 (0.457)		
2	(2.05)	0.483	0.522 (0.515)	0.467	0.413 (0.432)	0.05	0.064 (0.053)
3	1.51	0.464	0.496 (0.492)	0.44	0.403 (0.413)	0.096	0.102 (0.096)
4	1.45	0.42	0.461 (0.456)	0.405	0.353 (0.366)	0.175	0.186 (0.179)
5	1.57	0.357	0.395 (0.386)	0.345	0.305 (0.331)	0.298	0.300 (0.282)
6	1.40	0.275	0.300 (0.304)	0.265	0.260 (0.256)	0.46	0.440 (0.440)
7	1.30	0.188	0.22 (0.216)	0.182	0.180 (0.17)	0.63	0.60 (0.614)
8	1.20	0.138	0.14 (0.155)	0.14	0.190 (0.146)	0.718	0.67 (0.699)

^a Results from FIT3 routine with τ_1 fixed at 22.8 ns and τ_2 at 8.7 ns. Values in parentheses were determined using the FIT3a routine with $\tau_1 = 22.8$ ns, $\tau_2 = 8.7$ ns, and $\tau_3 = 1.25$ ns.

^b All data from ref. 85.

fluorometry. They attempted to resolve heterogeneous systems using information from several data sets differing only by an experimental parameter such as emission wavelength. Anthracene and 9-cyanoanthracene were evaluated at two frequencies, 30 and 18 MHz, and three emission wavelengths, 410, 420, and 430 nm. Figure 29 shows results comparing the global analysis with conventional NLLS analysis on individual data sets and with Weber's algebraic solution. The improvement of the global analysis over the other two techniques is apparent. Figure 30 shows the results with a more difficult data set, in which KI was added to the anthracene/9-cyanoanthracene mixture to dynamically quench the lifetimes. From this data it appears that the global analysis approach is the most useful of the three. The results of Beechem et al. appear very convincing, but no reference was made to getting the fractional contributions back out of the analysis for quantitative purposes.

On-line Fluorescence Lifetime

Detection For HPLC

Preliminary investigations into the incorporation of fluorescence lifetime selectivity into HPLC detection centered around time-resolved fluorescence detection. Richardson and co-workers (81) used time-resolved laser-induced fluorescence to enhance the selectivity for HPLC-separated PAHs. A pulsed nitrogen dye laser was used to

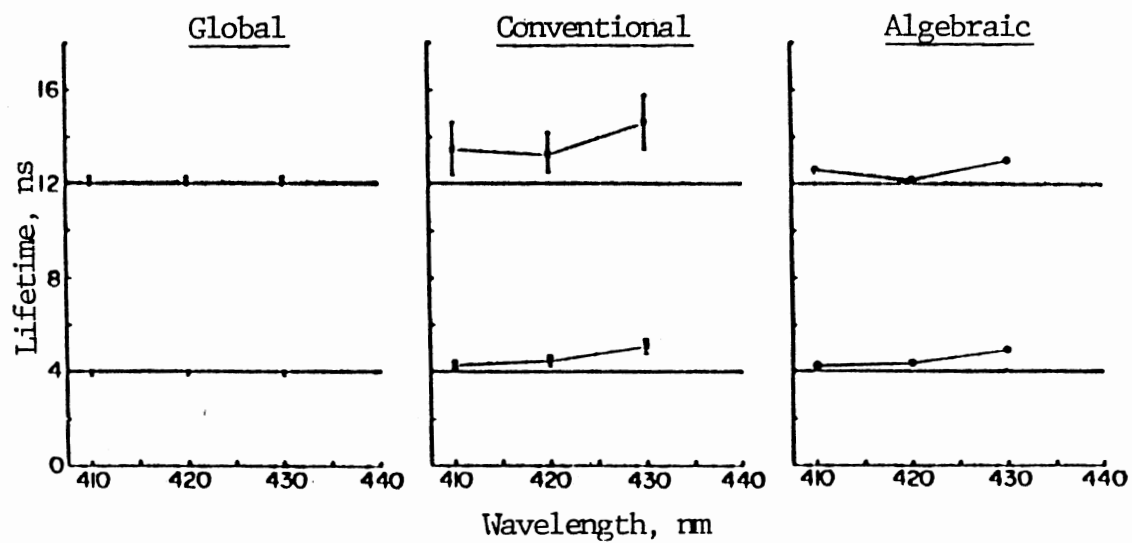


Figure 29. Resolved Lifetimes for Anthracene (4 ns) and 9-CNA (12 ns) Using Global, Conventional, and Algebraic (Weber's) Heterogeneity Analyses. From Ref. 81.

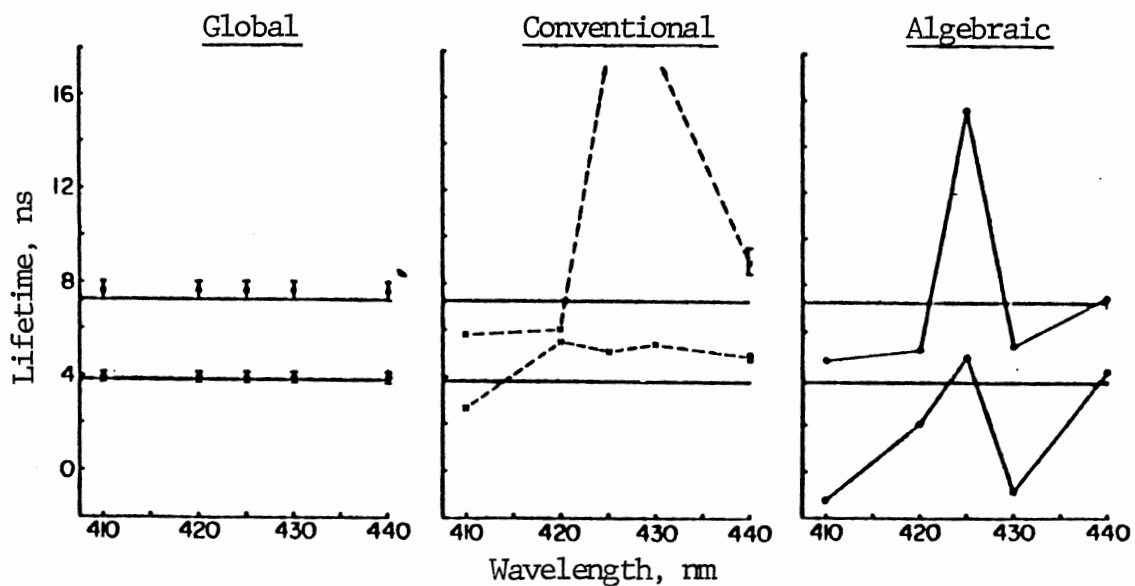


Figure 30. Resolved Lifetimes For System in Figure 29 With Dynamic Quencher Added to Yield Lifetimes of 3.9 and 7.2 ns for Anthracene and 9-CNA. From Ref. 81.

detect PAHs after a specific time delay, which enabled the rejection of scattered light and very short-lived interfering background signals in the chromatogram, thereby increasing the signal-to-noise ratio for the longer-lived analytes. The changes in selectivity are shown in Figure 31 for delay times of 0, 15, and 45 ns. The authors reported detection limits of the order of 1-10 pg for the longer-lived PAHs; however, the pulse width of the nitrogen pumped dye laser (10 ns) precluded the use of this system for shorter-lived PAHs.

Imasaka et al. (82) used a sub-nanosecond dye laser which consisted of a transversely excited atmospheric pressure nitrogen laser as the pumping source, a sub-nanosecond response PMT, and a fast sampling oscilloscope to achieve nanosecond time resolution for time-resolved fluorometric detection of HPLC-separated PAHs. Figure 32 shows the reduction in background noise achieved with a 20 ns time delay.

Furuta and Otusuki (83) also used time-resolved fluorescence detection in combination with HPLC for determination of PAHs in lake waters. Again, the use of a time delay allowed lower detection limits than with steady-state fluorescence, and some selectivity was obtained by using different delay times, but the lifetime information from the compounds was not fully exploited. The above time-resolved detection methods do increase signal-to-noise by reducing short-lived background signals in

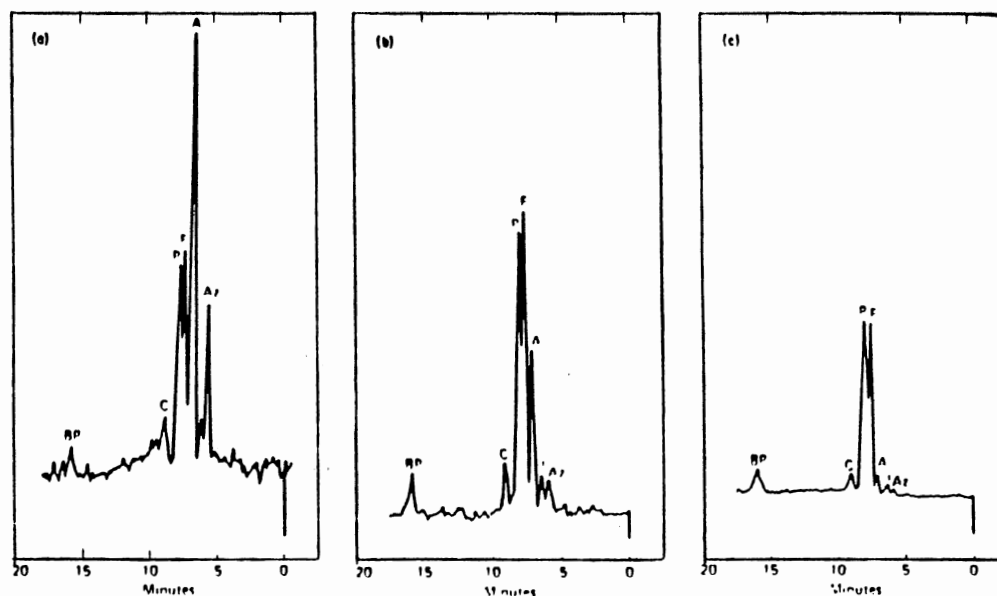


Figure 31. Fluorescence Detection of Six PAHs Using Pulsed Excitation and Time Delays of (a) 0 ns, (b) 15 ns, and (c) 45 ns. From Ref. 82.

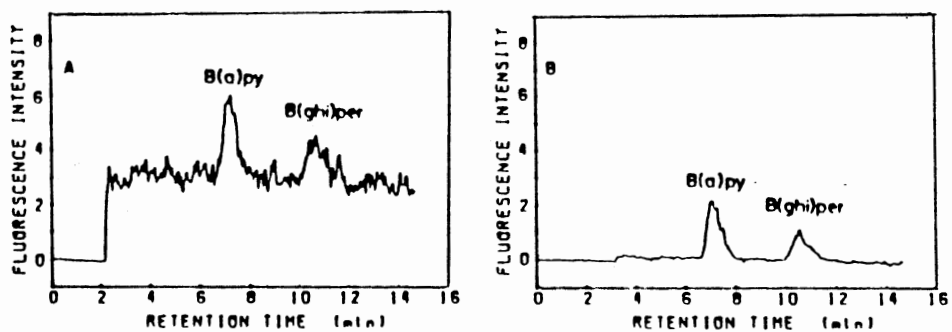


Figure 32. Fluorescence Detection of B(a)P and B(ghi)P Using Pulsed Excitation and Time Delays of (a) 0 ns and (B) 20 ns. From Ref. 83.

chromatograms. Although this is helpful, what is really needed is information regarding peak heterogeneity, component identification, and component quantitation.

In an attempt to make further use of fluorescence lifetime information, Desilets and co-workers (84,85) developed a technique, again using pulsed laser excitation, whereby peak heterogeneity and fluorescence lifetimes could be determined from data obtained from HPLC eluents. The authors used a pulsed nitrogen laser operating at 10 Hz with a 1.5 ns pulse width. The signal from the PMT detector was equally split and one of the outputs was delayed by running it through a longer coaxial cable, before both inputs were put into a dual channel sampling oscilloscope. This produced an approximately 10 ns delay between the two signals (Figure 33), thus enabling the fluorescence decay to be monitored at two points on the decay curve (Figure 34). The ratio of these two points was found to be largely independent of concentration and could be correlated to the fluorescence lifetime of the compound under study because, under identical experimental conditions, a given lifetime would produce a given ratio. Figure 35 shows how the ratio is relatively invariant with sample intensity and concentration, and Figure 36 illustrates the ability of the ratio approach to spot peak heterogeneity. This technique provides much more information than earlier time-resolved methods, but disadvantages include: (a) the lifetimes must be

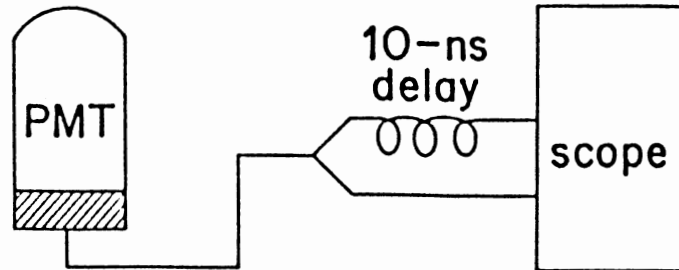


Figure 33. Instrumental Setup to Obtain 10 ns Delay Between Oscilloscope Inputs. From Ref. 86.

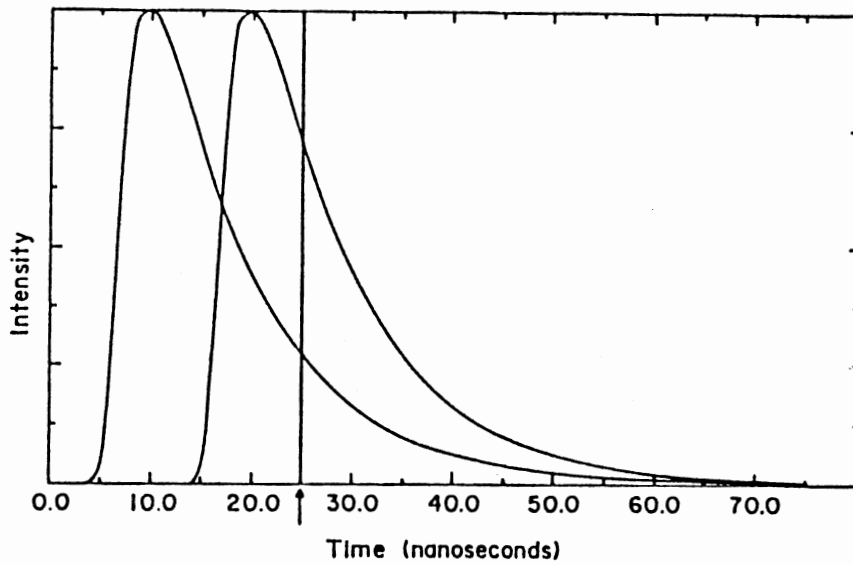


Figure 34. Position of Oscilloscope Apertures For Ratio Measurement. From Ref. 86.

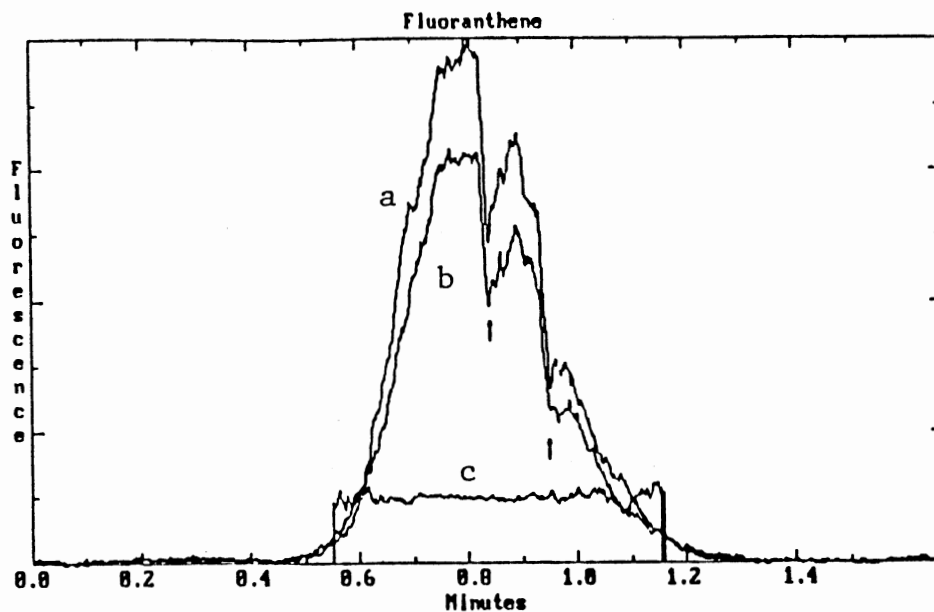


Figure 35. Illustration of the Two Channels of Raw Data (a,b) and Their Ratio (c) For Fluoranthene. The Arrows Correspond to Points Where Neutral Density Filters Were Placed in the Collection Optics. From Ref. 86.

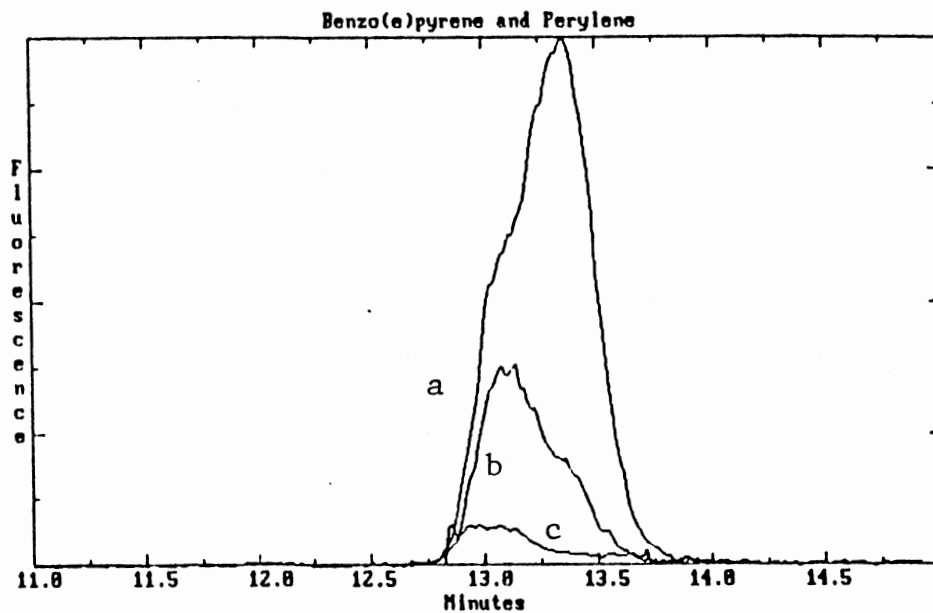


Figure 36. Two-Component Peak consisting of Perylene and Benzo(e)pyrene Showing How the Ratiogram Can Resolve Overlapping Peaks. (a,b) Two Channels of Raw Data, (c) Ratio. From Ref. 86.

calculated from calibration curves correlating lifetimes with the two-point ratios, (b) completely overlapping peaks will simply show a constant ratio corresponding to some lifetime between those of the two compounds present, thus appearing to be a homogeneous, single-component peak, and (c) since the ratios are independent of concentration, no quantitative information is suggested for overlapping peak components.

The determination of PAHs by the phase-modulation technique, on the other hand, allows direct indication of peak heterogeneity at each point on the chromatogram (even for completely overlapping peaks and/or completely overlapping spectral characteristics), direct determination of fluorescence lifetimes in most cases, and quantitative determination of the incompletely-separated compounds.

CHAPTER IV

EXPERIMENTAL

Chemicals

Stock Solutions

The polycyclic aromatic hydrocarbons used for this research were purchased from either Accustandards (New Haven, CT) or Analabs (North Haven, CT) at >99% purity and used without further purification. Solvents, including spectral grade acetonitrile, methanol, and water were purchased from Burdick and Jackson and were all HPLC certified. Stock solutions were prepared as follows: appropriate amounts of each PAH were weighed out, diluted with solvent in volumetric flasks, and sonicated for at least 30 minutes using an ultrasonicator to ensure complete dissolution. The stock solutions were then stored in rinsed brown glass bottles with Teflon-lined lids.

HPLC Mobile Phases and Samples

HPLC certified spectral grade solvents (acetonitrile, methanol, and water) were purchased from Burdick and Jackson. All HPLC mobile phases were vacuum filtered through 0.45 micron filters using an all-glass HPLC

filtration funnel and flask. Samples, both standards and mixtures, were diluted and then filtered through 0.45 micron filters using a luer-lock syringe and disposable filters. The filtered mixtures and standards were stored in rinsed brown glass vials with Teflon-lined caps for eventual injection into the HPLC. This commitment to filtering mobile phases and samples extended the lifetime of the column and improved stability of the HPLC system.

Instrumentation

HPLC System

A general diagram of the instrumental set-up is shown in Figure 37. The complete HPLC system was purchased from Waters Chromatography. The system utilized two model 501 pumps capable of flow rates from 0.1 to 9.9 ml/min. A U6K injector was used which allows syringe injections of samples sizes up to 1 ml. The pumps were controlled by a model 680 Automated Gradient Controller. This microprocessor-based controller manages the flow rates of the two pumps to allow constant isocratic proportioning or full gradient control of a binary solvent system. The controller provides linear, convex, concave, and step-wise gradient programs, which can be designed by the user; up to 10 can be stored in the memory of the controller. In addition to the pump control, the 680 has seven contact-closure switches which can be opened, closed, or pulsed as desired by designing timed-event programs. These switches

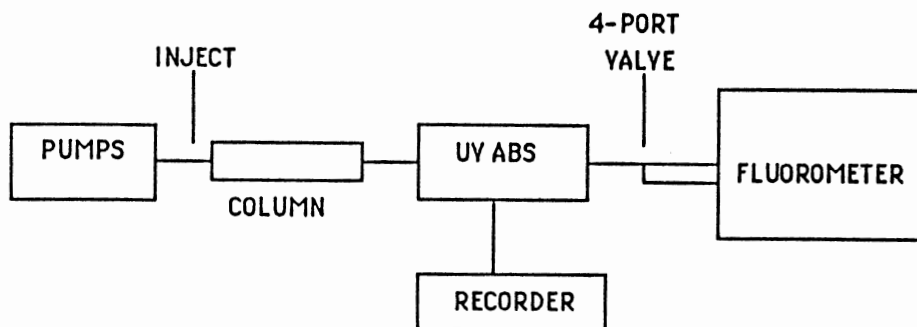


Figure 37. General Diagram of HPLC/UV/Spectrofluorometer Setup.

can be used to run auto-injectors, fraction collectors, etc. The HPLC column consisted of a ChromSep cartridge column assembly which utilizes glass column inserts. The columns were 0.3 cm in diameter and either 10 or 20 cm long. The reversed phase packing was 5 micron Vydac 201TP, which is a C₁₈ bonded phase packing developed especially for the separation of PAHs. A 1 cm guard column, also packed with C₁₈ bonded phase, was used before the analytical column to extend column life. The use of the cartridge column assembly allowed columns to be replaced rapidly and easily without having to disconnect any tubing, thus avoiding undue leakage, and was also much more cost effective than typical stainless-steel columns. A Waters model 440 fixed wavelength absorbance detector, which monitors absorbance at 254 nm, was used for detection for studies independent of the spectrofluorometer. The absorbance detector was also used in series with the spectrofluorometer as a universal detector, thus picking up any compounds which absorbed UV light but were not fluorescent. Outputs from the absorbance detector were connected to an analog chart recorder. The incorporation of the four-port valve between the UV absorbance detector and the spectrofluorometer (see Figure 37) enabled a peak or peak portion to be trapped in the spectrofluorometer for stopped-flow studies. The flow from the HPLC was diverted to waste, therefore the HPLC pumps were not required to be stopped during the stopped-flow measurements. Two

different types of flow cells were used and these will be described in the Results section.

Spectrofluorometers

SLM 4800S. All steady-state, lifetime, and phase-resolved intensity measurements were acquired using one of two phase-modulation spectrofluorometers, both of which are commercially available from SLM Instruments in Urbana, Illinois. Initial work done at Oklahoma State University was with the SLM 4800S phase-modulation spectrofluorometer. A diagram of this particular instrument is shown in Figure 38. The excitation source is a 450 watt ozone-free Xenon arc lamp manufactured by Osram with replacements supplied by The Second Source (Duarte, CA). The Xenon arc source provides a continuous excitation power spectrum from the ultraviolet to the near infra-red, and therefore is appropriate for scanning the excitation spectrum as well as for constant wavelength work. The output from the lamp is focused into an excitation monochromator employing a holographic grating (1500 groves/mm). The excitation and emission monochromators can be scanned at a maximum rate of 100 nm/sec. The monochromators allow variable entrance and exit slit widths ranging from 0.5 nm to 16 nm.

After the appropriate excitation wavelength has been selected by the excitation monochromator, the further propagation of the exciting light depends upon whether steady-state or dynamic measurements will be made. If

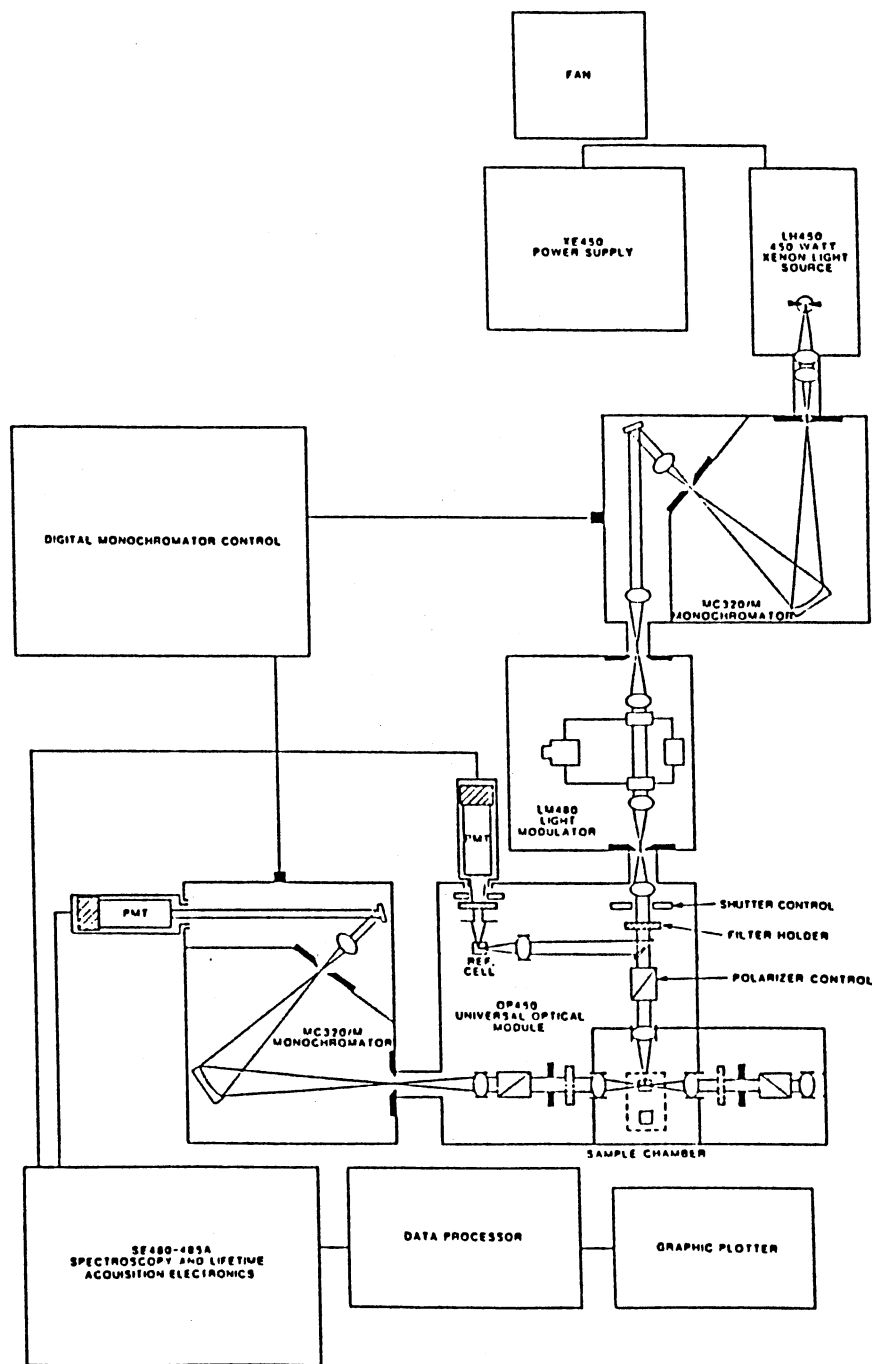


Figure 38. SLM 4800S Phase-Modulation Spectrofluorometer. From Instrument Manual.

steady-state measurements are required, the light simply transverses the modulation tank and enters the sample chamber. A small portion of the excitation beam is split off by a beam splitter and sent to a reference PMT (Hamamatsu R928) for ratiometric measurements to correct for any lamp fluctuations or drift. The major portion of the excitation beam illuminates the sample compartment, where the sample can be contained in a cuvette, an HPLC flow cell, or any other particular sample holder such as a front surface fluorescence sample holder. As can be seen in Figure 38, the fluorescence emission is monitored at right angles to the excitation through one of two pathways: the emission can be monitored through the emission monochromator, which is identical to the excitation monochromator, or it can be monitored through one or more emission filters, which allow greater through-put of the emission intensity, but decrease the selectivity available. An Apple IIe computer with software supplied by SLM was used for data acquisition and manipulation. In the steady-state mode, excitation/emission spectra, polarization measurements, and kinetic (intensity vs. time) data can be acquired.

In the dynamic or lifetime mode, the excitation intensity is sinusoidally modulated as it passes through the Debye-Sears acousto-optic light modulator. A standing wave is created in a solution (19% ethanol in water) contained in the modulator, acting as a diffraction grating

as a result of the alternating regions of compression and rarefaction in the solution. This causes the light transversing the solution to be intensity modulated. The modulation compartment is shown expanded in Figure 39. The tank's ultrasonic transducer is a very thin plate of gold-coated quartz. A quartz standing wave plate is opposite the transducer. The position of the wave plate in the tank is controlled by three micrometers (M1,M2,M3): M1 controls the angle of the tank in the light beam, M2 controls the horizontal position of the standing wave plate, and M3 controls the vertical position of the standing wave plate. Proper adjustment of the above micrometers allows optimum modulation at the desired modulation frequency. Three modulation frequencies were available on this instrument: 6, 18, and 30 MHz. After passing through the tank, the light is focused by a lens, L2, onto the exit slit, S2.

SLM 48000S. An SLM 48000S multi-frequency phase-modulation spectrofluorometer was used for work completed after September, 1987. Although the 48000S contains many of the same features of the 4800S, there are some fundamental differences, and these will be described. Figure 40 shows the general instrumental diagram. The major instrumental differences are the modulation hardware and electronics. Instead of the Debye-Sears acousto-optic modulation, the 48000S uses a Pockel's cell for electro-optic modulation. The Pockel's cell is driven by a frequency synthesizer which allows modulation at

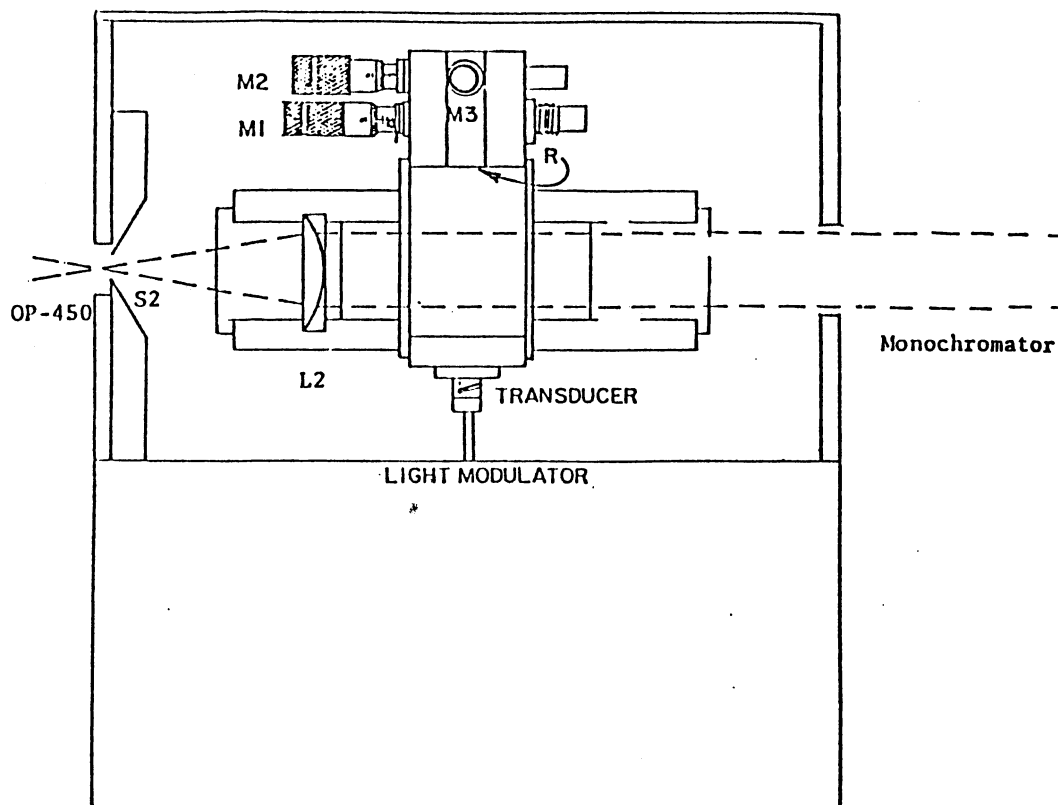


Figure 39. Debye-Sears Modulation Tank for SLM 4800S. M1 Controls the Angle of the Tank in the Light Beam. M2 and M3 Control the Horizontal and Vertical Positions of the Standing-Wave Plate. From Instrument Manual.

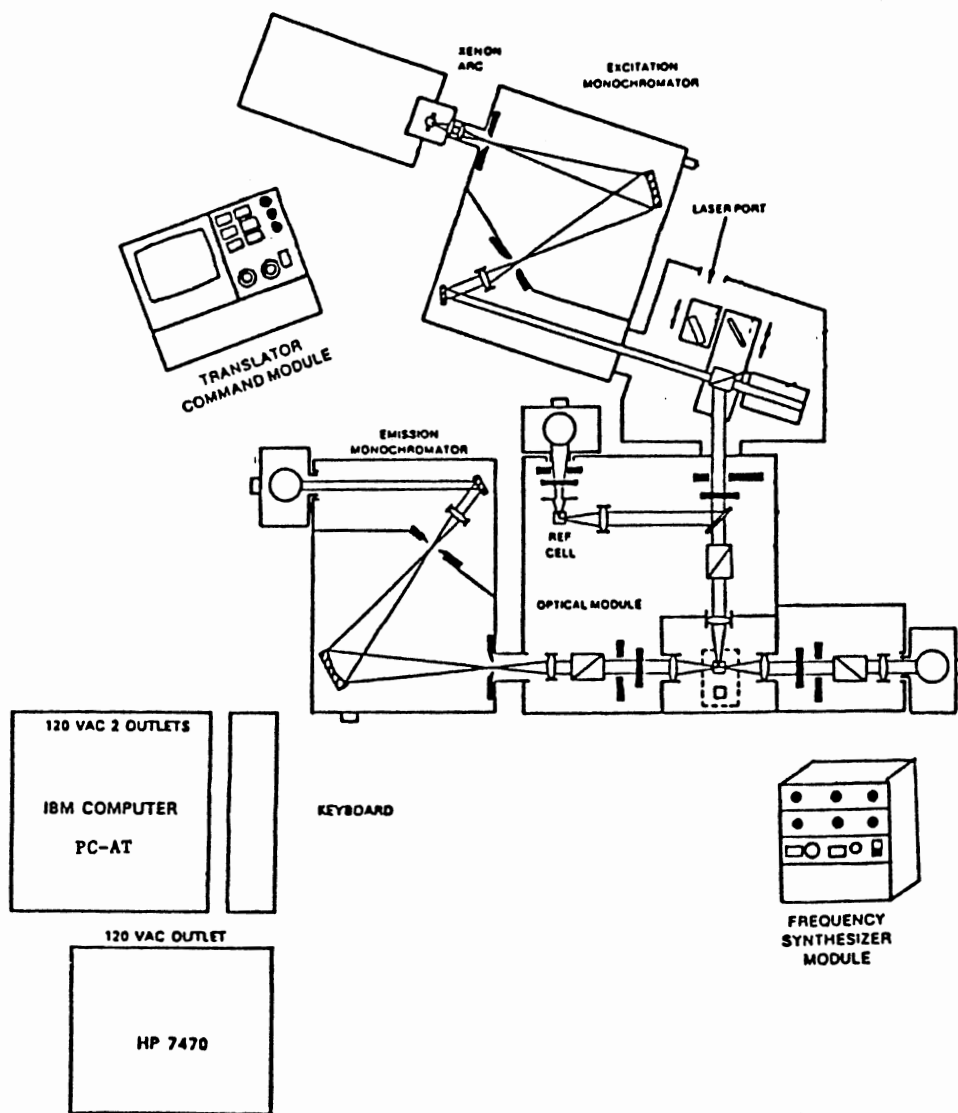


Figure 40. SLM 48000S Multifrequency Phase-Modulation Spectrofluorometer. From Instrument Manual.

frequencies from 1 to 250 MHz in 100 KHz increments. Figure 41 shows the light path through the modulation compartment when the Pockel's cell is in use. The light from the excitation monochromator passes through a Q-switch polarizer, creating horizontally polarized light which is partially vertically polarized at the applied modulation frequency by the Pockel's cell. This beam then exits the Pockel's cell and again hits the Q-switch polarizer, which passes the horizontally polarized component and reflects all other components of the light through to the sample module.

When steady-state measurements are desired, the light from the excitation monochromator is simply reflected off of a mirror into the sample module, thus by-passing the Q-switch polarizer and the Pockel's cell altogether, as can be seen in Figure 42. The remaining portions of the 48000S are similar to the 4800S, including Hamamatsu R928 photomultiplier tubes for detection, except with respect to the computer hardware and software for instrument control and data acquisition and treatment. An IBM PC AT is used, which allows input and control of all PMT voltages, monochromator settings, and data acquisition parameters.

Data Acquisition and Manipulation

Batch Analysis. The data acquisition and analysis will be described only for the 48000S, since at present the same computer hardware and software are available for both

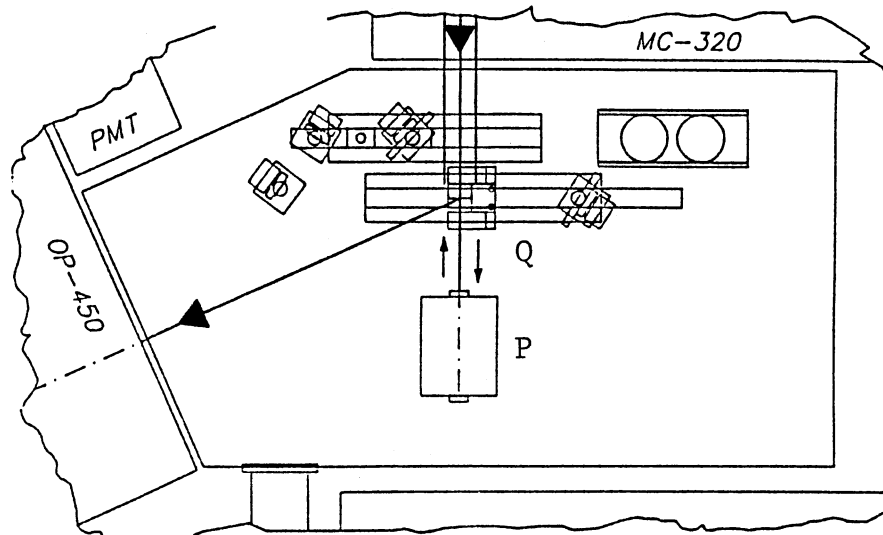


Figure 41. Beam Path Through Modulation Compartment for Dynamic Measurements Showing Q-Switch Polarizer (Q) and Pockel's Cell (P). From Instrument Manual.

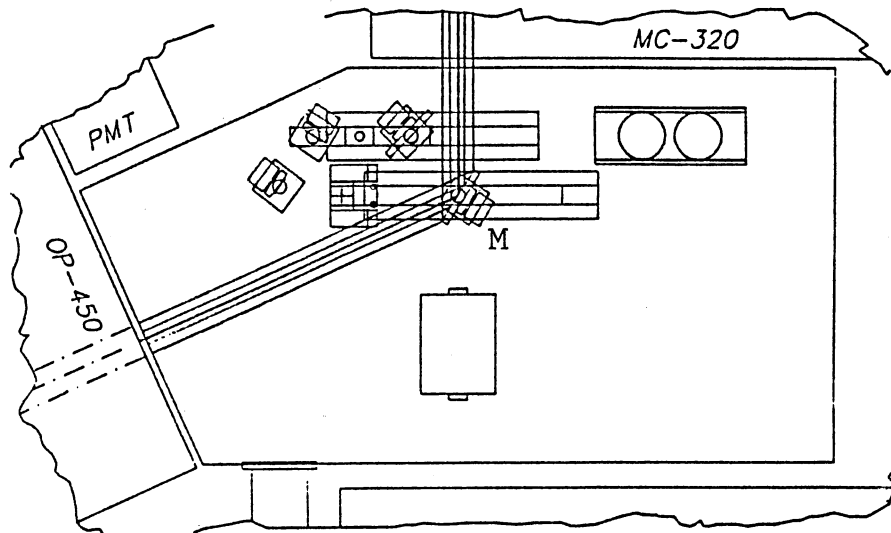


Figure 42. Beam Path Through Modulation Compartment for Steady-State Measurements Showing Mirror (M). From Instrument Manual.

the 4800S and the 48000S. All data was acquired in the ratiometric mode to correct for any lamp fluctuations or drift. Fluorescence lifetimes of standards were measured at approximately optimum modulation frequencies, corresponding to $1/(2\pi\tau)$. Usually, a reference fluorophore was used as the reference; however, scatter was sometimes taken as the reference, as will be discussed in the Results section. Typically 10 measurements were taken per solution (5 measurements each of sample and reference, alternating between the two). Each measurement consisted of the average of 100 samplings. If lifetimes at one particular frequency only were desired, the software would calculate the lifetimes and these could be copied from the computer display or printed out on paper. If data at several modulation frequencies was being acquired for heterogeneity analysis, the SLM software stored the phase-shift and demodulation values at each frequency in a user-named file for later retrieval and use in the non-linear least squares (NLLS) heterogeneity analysis routine.

For heterogeneity analysis using the NLLS routine, data was acquired at an appropriate number of frequencies. The SLM software for the NLLS heterogeneity analysis first suggests either a one component fit with a particular lifetime or a two-component fit with suggested first guess lifetimes and fractional contributions. The user has the option of supplying alternate first guesses for the number of components, the lifetimes, and the fractional

contributions. Both the lifetimes and fractional contributions can be allowed to float, or the lifetimes can be fixed if the values are known. The output from the NLLS heterogeneity analysis consists of the lifetimes and fractional contributions of each of the components as well as measures of the "goodness of fit" of the calculated values to the experimental values, in the form of a reduced chi-squared value. Overlay plots of the phase and modulation vs. frequency data for both the experimental and calculated results are also available, with residual errors plotted out separately for phase and modulation.

Data acquired on-line with HPLC. The software provided by SLM for the 48000S, besides allowing for complete spectral acquisition, also contains a slow-time kinetics mode (data vs. time). This allows both the d.c. intensity and the dynamic information to be acquired as a function of time, which is what is necessary for collecting data on-line with an HPLC. Although no strictly chromatographic software was used, the SLM software for most purposes was found adequate for the particular need of this research. A contact closure switch, accessed by the timed-events program on the Waters 680 gradient controller and connected to the SLM controller, allowed the SLM to be triggered by the HPLC at each injection, thus maintaining consistent time synchronization between the two instruments as well as between runs.

Due to the need for a reference in order to calculate the phase and modulation lifetimes, fluorescence lifetimes were not calculated in real time; however, additional programming could be done to permit on-line calculations in future applications, provided the source code for the SLM software is available.

For a typical run, d.c. intensity, phase and modulation data were acquired on-the-fly at fixed time increments, typically 1 to 5 seconds, as the chromatographic peaks were eluted. Measurements for the reference, usually a reference fluorophore, were also acquired. The phase-shift and demodulation were calculated post-acquisition from the analyte and reference data, and then the phase and modulation lifetimes were calculated. The fluorescence lifetimes vs. time were then plotted using commercial plotting routines.

If heterogeneity analysis were performed, the "true" phase-shift and demodulation values, ie., those corresponding to the calculated lifetime irrespective of the reference fluorophore, were then calculated from the lifetimes at each point along the chromatogram that was desired. These "true" phase-shift and demodulation values were input into the SLM NLLS heterogeneity analysis routine, and the heterogeneity analysis performed. As was discussed under the batch data manipulation section above, the lifetimes and fractional contributions were found from the heterogeneity analysis. In order to translate these

values into intensity values at each point along the chromatogram, i.e. "reconstruct" the resolved chromatogram, the calculated fractional contributions were multiplied by the d.c. intensity of the corresponding point in the chromatogram. This reconstructed chromatogram could then be compared to chromatograms obtained for the same amount of the individual components injected separately, and the quality of the results determined. Initially, all of the post acquisition calculations were done point-by-point with a hand-held Hewlett Packard programmable calculator. Later, spreadsheets were used to do all of the data manipulations, but increasing complexity of chromatograms resulted in lack of sufficient memory to handle the data laden spreadsheets. Eventually, algorithms were written in Quickbasic, which greatly simplified the process and reduced the data manipulation time significantly.

CHAPTER V

RESULTS AND DISCUSSION

The following results represent steps taken to achieve the overall goal of determining phase-modulation fluorescence lifetimes on-line with HPLC for qualitative and quantitative analysis. This chapter is divided into sections, each of which describes a logical grouping of experiments designed to minimize errors and interferences due to chemical, physical, instrumental, or mathematical processes. The experiments are presented in approximately chronological order due to the evolving nature of the research. Experimental details will be provided only when clarification of information provided in Chapter 4 is deemed necessary.

Characterization Of Test Compounds

Members of the set of sixteen EPA priority pollutant PAHs were characterized in terms of their fluorescence spectra, lifetimes, and HPLC chromatographic properties. The structures, molecular weights, abbreviated names, and other relevant information was provided in Table 1, Chapter 1.

Experimental

Stock solutions and samples were made up in 80% aqueous acetonitrile (MeCN). For batch fluorescence studies (spectra, lifetime determinations) concentrations on the order of 1×10^{-6} M were used. For the HPLC sample mixture, the concentration of each component was approximately 1×10^{-5} M. The mobile phase consisted of a gradient from 40% to 100% aqueous MeCN with a flow rate of 0.5 ml/min. The SLM 4800S was used to acquire the fluorescence data. An excitation modulation frequency of 18 MHz was used for the fluorescence lifetime determinations.

Fluorescence Spectral Characteristics

Fluorescence excitation and emission spectra were acquired for each of sixteen PAHs. Their excitation and emission maxima are given in Table 12. Since these compounds were chosen to be used for fluorescence detection in HPLC, it was important to group them with respect to compromise wavelengths such that several of the PAHs could be monitored with a particular excitation wavelength / emission filter pair. Table 12 also shows that two main groups can be chosen, one with excitation at 270 nm and emission using a 320 nm long pass (LP) filter, and the other with excitation at 360 nm and emission using a 400 nm LP filter. The choice between employing the selectivity of monochromatic emission or the more general response from

TABLE 12
 FLUORESCENCE EXCITATION AND EMISSION MAXIMA

#	Name	Ex	Em
1	Naphthalene ^a	275	330, 400
2	Acenaphthylene ^a	280	325
3	Acenaphthene ^a	285	320, 340
4	Fluorene ^a	260, 295	320
5	Phenanthrene ^a	250	350, 370, 385
6	Anthracene ^b	340, 355, 375	380, 400, 425
7	Fluoranthene ^b	280, 355	460 broad
8	Pyrene ^a	270, 320, 330	380, 395
9	Benz (a) anthracene ^b	285	390, 410
10	Chrysene ^a	270, 320	360, 385, 400
11	Benzo (b) fluoranthene ^b	255, 300, 350	440 broad
12	Benzo (k) fluoranthene ^b	305, 380, 400	410, 435
13	Benzo (a) pyrene ^b	290, 360, 380	410, 430
14	Dibenz (a, h) anthracene ^b	290, 330, 340	400, 420
15	Benzo (ghi) perylene ^b	295, 360, 380	410
16	Indeno (123-cd) pyrene ^b	300, 360, 380	475, 510

^a Compromise wavelengths; 270 nm ex., 320 nm LP em.

^b Compromise wavelengths; 360 nm ex., 400 nm LP em.

using an emission filter involves a compromise. As is often the case, one is faced with reducing the selectivity in order to improve the overall detectability of the PAHs.

Table 13 shows the phase and modulation lifetimes obtained on the SLM 4800S at 18 MHz, along with their standard deviations. The samples were not deoxygenated, and therefore some of the lifetimes may be somewhat shorter than those typically reported for these particular compounds. As can be seen in Table 13, the range in fluorescence lifetimes for the PAHs is from 4 to 31 nanoseconds. The relative standard deviations are generally less than 2% of the fluorescence lifetimes.

HPLC Characteristics

The separation of eleven PAHs obtained using gradient elution with aqueous MeCN (40-100%) and UV absorption detection at 254 nm is shown in Figure 43, along with relative retention times. All components were well resolved under these conditions except for Acenaphthene which appears as a shoulder on the fluorene peak. Figure 44 illustrates the resultant selectivity achieved by combining fluorescence lifetime information with chromatographic retention time for a set of 11 PAHs separated by gradient elution. It is evident, especially in cases of similar retention times, that the fluorescence lifetime domain increases selectivity over that obtainable by steady-state fluorescence intensity detection alone.

TABLE 13
PHASE AND MODULATION FLUORESCENCE LIFETIMES^a

	Name	Phase Lifetime ^b	Modulation Lifetime ^b
1	Naphthalene	20.58 ± 0.83 (4.0)	22.43 ± 0.36 (1.6)
2	Acenaphthylene	14.28 ± 0.27 (1.9)	15.49 ± 0.32 (2.1)
3	Acenaphthene	15.77 ± 0.22 (1.4)	16.25 ± 0.09 (0.6)
4	Fluorene	5.57 ± 0.10 (1.8)	6.43 ± 0.09 (1.4)
5	Phenanthrene	20.16 ± 1.43 (7.1)	20.26 ± 0.42 (2.1)
6	Anthracene	4.00 ± 0.04 (1.0)	3.91 ± 0.08 (2.0)
7	Fluoranthene	31.13 ± 0.15 (0.5)	31.27 ± 0.25 (0.8)
8	Pyrene	26.91 ± 0.21 (1.2)	26.67 ± 0.15 (0.6)
9	Benz (a) anthracene	18.37 ± 0.22 (1.2)	18.26 ± 0.20 (1.1)
10	Chrysene	21.88 ± 2.16 (9.9)	21.33 ± 0.36 (1.7)
11	Benzo (b) fluoranthene	29.84 ± 0.28 (0.9)	29.29 ± 0.19 (0.6)
12	Benzo (k) fluoranthene	8.20 ± 0.04 (0.5)	8.29 ± 0.09 (1.1)
13	Benzo (a) pyrene	17.02 ± 0.05 (0.3)	17.24 ± 0.14 (0.8)
14	Dibenz (a,h) anthracene	14.60 ± 0.21 (1.4)	15.09 ± 0.16 (1.1)
15	Benzo (ghi) perylene	24.55 ± 0.54 (2.2)	25.94 ± 0.13 (0.5)
16	Indeno (123-cd) pyrene	6.91 ± 0.05 (0.7)	7.07 ± 0.03 (0.4)

^a In 80% aqueous acetonitrile without deoxygenation.

^b Lifetimes ± one standard deviation (n = 5) in ns; relative standard deviations (%) are shown in parentheses.

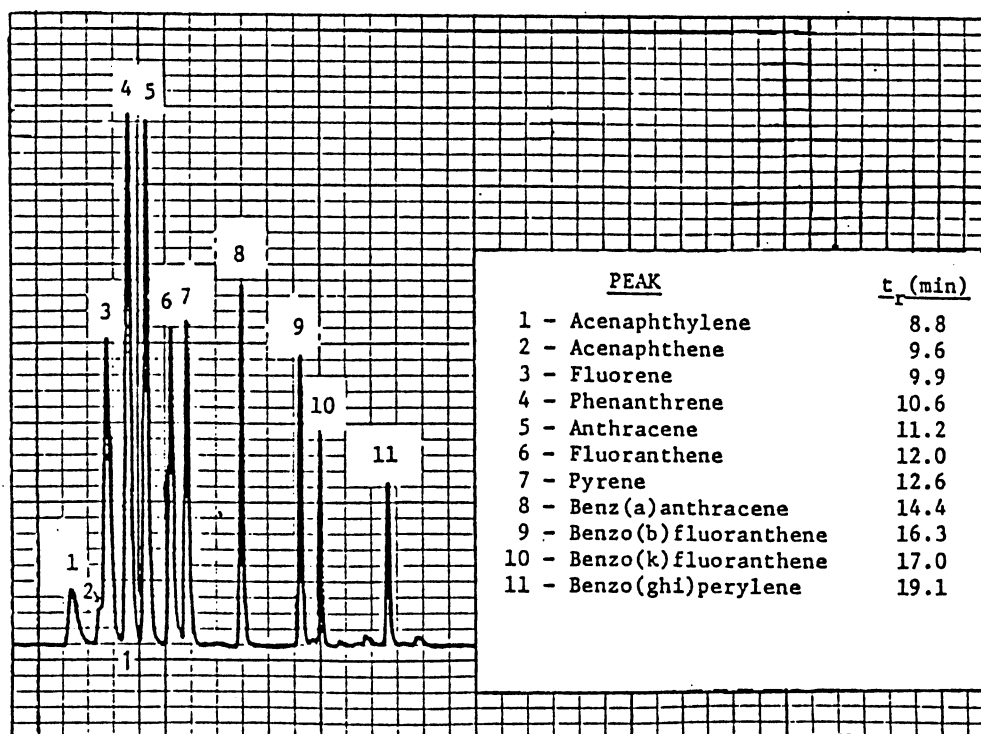


Figure 43. Chromatogram of 11 PAHs Using Gradient Elution and UV Absorbance Detection at 254 nm.

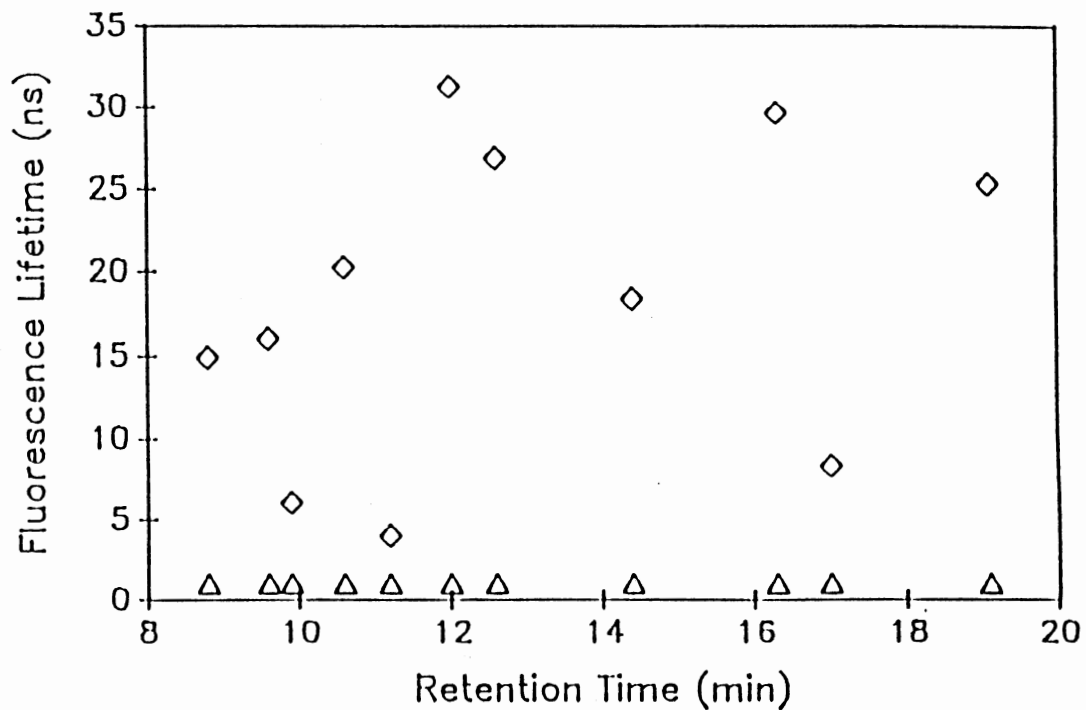


Figure 44. Fluorescence Lifetimes vs. HPLC Retention Time for PAHs. (Δ) One-Dimensional Retention Time Data. (\diamond) Two-Dimensional Lifetime Data as a Function of Retention Time.

The above experiments verified that fluorescence lifetime information on-line would indeed permit much more selectivity for the determination of PAHs, thereby affirming the initial goal of the research project: to determine phase-modulation lifetimes on-line with HPLC.

On-Line Fluorescence Lifetime Determinations

The first use of a phase-modulation spectrofluorometer is described for the measurement of fluorescence lifetimes on-line with HPLC. Parameters such as mobile phase composition and references used for lifetime calculations were investigated, as well as the problems caused by interfering signals.

Experimental

Stock solutions of PAHs were made up in 80% aqueous MeCN. Sample solutions of PAH mixtures for HPLC runs were made up with concentrations on the order of 1×10^{-6} M. The Waters HPLC system was used in the isocratic mode with a mobile phase of either 90% or 80% aqueous MeCN, and a flow rate of 0.5 mL/min. The SLM 4800S was used along with a modified, custom-made 20 μ L quartz flow cell (NSG Precision Cells) for HPLC detection. A low-fluorescence black quartz flow cell was also used for some experiments. Fluorescence excitation wavelength was selected with the excitation monochromator, while emission was observed with long pass filters and a 600 nm short-pass filter. All

lifetime determinations were made using an excitation modulation frequency of 18 MHz.

Effects of Solvent Composition on Lifetimes

The effect of changing solvent composition on the fluorescence lifetimes of several PAHs was determined. In going from 100% MeCN and increasing the water content of the solvent, the fluorescence lifetimes almost always increase, as one would expect, and as illustrated for B(k)F in Figure 45. As was discussed in Chapter III, this apparent increase in the excited state lifetime is due to the fact that molecules in excited electronic states generally possess molecular geometries and electronic charge distributions that are substantially different than in the ground state. In most cases the excited state is more polar than the ground state and an increase in solvent polarity produces a greater stabilization of the excited state (75). To initially avoid another changing parameter, the isocratic mobile phase was used.

Investigation of Possible Interferences

The presence of interfering signals was also investigated, including scattered light, which is much greater for microvolume flow cells than for conventional cuvettes, fluorescence from filters, and solvent impurities. The presence of solvent impurities can cause both a relatively constant interfering background signal or

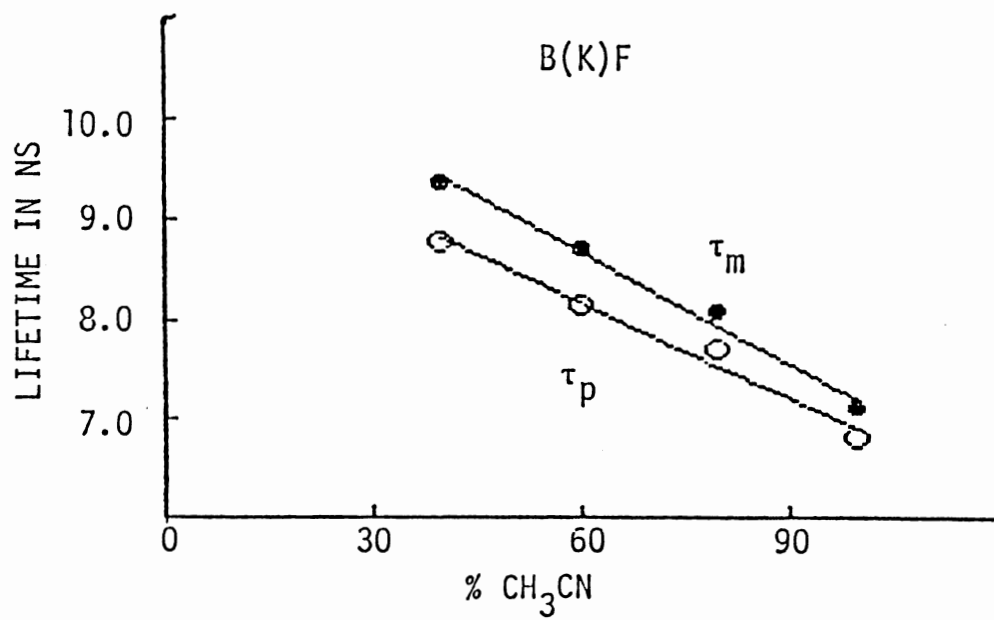


Figure 45. Lifetime vs. Percent Aqueous Acetonitrile as Solvent.

actual chromatographic peaks during a chromatogram. It is important to note that, while for steady-state intensity detection the constant fluorescence background can simply be offset or "zeroed-out", for fluorescence lifetime detection any fluorescence or scatter background will influence the phase and modulation which is observed, and therefore affect the calculated lifetimes . HPLC grade MeCN from several suppliers were investigated (Fisher, Mallinckrodt, Burdick and Jackson), and the Burdick and Jackson MeCN was found to be consistently superior. Water sources, including (1) distilled, de-ionized water directly from an in-lab water distillation apparatus, (2) this same water after passage through an activated charcoal column, and (3) B&J water were investigated. The activated charcoal-filtered water showed similar and only slightly higher impurity than the B&J water and therefore was used for further experiments. The long-pass filters that were initially used in the experimental arrangement were replaced by "low-fluorescence" long pass filters purchased from Oriel. The remaining source of unwanted signal was assumed to be due to scattered light. To solve the problem of scattered light, several adaptations were made to the flow cell and sample chamber, including the following: (1) covering and eventual removal of the reflective mirrors on the two sides of the flow cell mount; (2) addition of black tape to the quartz block encasing the actual capillary tube; and (3) construction of additional slits to be placed

in the sample compartment in order to further reduce any stray light present in the system. Although these measures helped in small amounts, scattered light was still found to contribute to the signal detected. The approach was then changed from attempting to physically reduce the scattered light to mathematically correcting for it by treating it as a component in a heterogeneous system.

Scattered Light Corrections

It was assumed that scattered light has a radiative lifetime of zero and was the only source of unwanted signal in the system. The fractional intensities of the scattered light and the fluorescence emission were found from the steady-state intensity information, since the scattered light intensity is the intensity measured between chromatographic peaks. The intensity of the fluorescence signal at any point in a chromatographic peak was found simply by subtracting the background scattered light intensity from the total intensity, and the fractional contributions of the scattered light and fluorescence emission were then calculated.

As was discussed in Chapter 3, the observed phase-shift ϕ and demodulation M for a two component system can be expressed as follows (82):

$$\tan \phi = S/G \quad (13)$$

$$M = [S^2 + G^2]^{1/2} \quad (14)$$

where

$$G = [f_A / (1 + \omega^2 \tau_A^2)] + [f_B / (1 + \omega^2 \tau_B^2)] \quad (19)$$

$$S = [f_A (\omega \tau_A / (1 + \omega^2 \tau_A^2))] + [f_B (\omega \tau_B / (1 + \omega^2 \tau_B^2))] \quad (20)$$

If the scattered light is taken as component A with a lifetime of zero, then equations 19 and 20 are reduced to:

$$G = f_A + [f_B / (1 + \omega^2 \tau_B^2)] \quad (21)$$

$$S = f_B \tau_B / (1 + \omega^2 \tau_B^2) \quad (22)$$

where component B is the fluorescence emission. Since f_A and f_B were known from the steady-state intensity data, the corrected phase and modulation lifetimes (τ_p' and τ_m' , respectively) of the fluorescence emission were calculated from the experimental phase and modulation data at a single modulation frequency by solving the quadratic expressions derived from equations 13, 14, 21, and 22 above:

$$\tan\phi (f_A \omega^2 \tau_p'^2) - f_B \omega \tau_p' + \tan\phi = 0 \quad (23)$$

$$\omega^4 (f_A^2 - M^2) \tau_m'^4 + \omega^2 (f_B^2 + 2f_A - 2M^2) \tau_m'^2 + (1 - M^2) = 0 \quad (24)$$

Synthetic data was used to verify the above equations, and gave the correct, hypothetical results. The scatter correction was then applied to real data.

Values for the uncorrected phase and modulation lifetimes, the corrected modulation lifetimes, and the fractional contributions of scattered light are shown in Table 14. Clearly, the corrected modulation lifetimes are

TABLE 14
 FLUORESCENCE LIFETIMES FOR B(k)F^a

n ^b	F _S ^c	τ_m^d	$\tau_m'^e$	τ_p^f
*	1.000	—	—	—
1	.870	2.97	7.47	0.41
2	.810	3.47	7.03	0.74
3	.782	3.87	7.44	0.99
4	.790	3.90	7.73	0.96
5	.818	3.52	7.43	0.91
6	.853	3.21	7.64	0.74
7	.890	2.48	8.01	0.64
8	.922	2.37	7.93	0.40
9	.940	2.14	8.40	0.33
10	.958	1.84	8.94	0.14
11	.966	1.50	7.46	0.12

- a Excitation = 380 nm; Emission = 385 nm LP.
 b Position along the chromatographic peak.
 c Fractional contribution of scattered light.
 d Uncorrected modulation lifetime.
 e Scatter-corrected modulation lifetime.
 f Uncorrected phase lifetime.

much closer to the expected 8.25 ns lifetime for B(k)F under these conditions. Also, the corrected values are essentially constant over the entire peak, which is expected for a single component, since as soon as any intensity is measured for a peak, it should have a single lifetime value corresponding to that component regardless of concentration. The uncorrected values, on the other hand, rise and fall in a manner reflecting the chromatographic peak shape, since the fractional contribution of the second component (scattered light) is decreasing and then increasing along the peak profile. The wavelengths used to collect the data in Table 14 were very close to the scatter peak in order to test the ability to correct for large amounts of scattered light. Corrected values are not shown for the phase lifetime because meaningful values were not obtained under these conditions. A second set of data for B(k)F was collected further away from a scatter peak, and the results are shown in Table 15. The corrected phase and modulation lifetimes are in good agreement with each other and are fairly constant over the peak, but the values are about one-half of the expected lifetime for B(k)F. The scatter corrections definitely improved the results for lifetime determinations, since constant values were obtained across the peak. However, some other factor was evidently also present which caused inaccurate values to be calculated for the lifetimes.

TABLE 15
 FLUORESCENCE LIFETIMES FOR B(k)F
 ALONG A PEAK

n ^a	m ^b	p ^b
1	4.58	2.82
2	4.36	4.22
3	4.16	4.04
4	4.00	4.24
5	3.55	4.21
6	3.42	4.20
7	3.20	4.00
8	2.98	3.93
9	3.22	4.31
10	2.83	3.69
11	2.94	3.62
12	3.00	4.17
13	3.77	2.96
14	3.37	3.52
	<u>3.53±0.56</u>	<u>3.92±0.37</u>

^a Chromatographic peak position.
^b Scatter-corrected lifetimes
 in ns.

Comparison of References

In a second set of experiments, steps were taken to further reduce the amount of scatter interfering with the analyte signal. A self-masking black-quartz flow cell with a 20 μL volume (Hellma Cells) was purchased. This cell was specifically designed to block any stray light except that which directly impinges on the observation volume. In addition to the flow cell, the excitation wavelength used was 360 nm with both a 399 nm low-fluorescence long-pass filter and a 600 nm short-pass filter for emission. This arrangement significantly reduced the scattered light present in the experiment.

A mixture of five components, fluoranthene, benzo(b)fluoranthene (B(b)F), benzo(k)fluoranthene (B(k)F), benzo(a)pyrene (B(a)P), and benzo(ghi)perylene (B(ghi)P) was investigated under mobile phase conditions of 80% aqueous MeCN and a flow rate of 0.5 mL/min. The use of dimethylPOPOP ($\tau=1.45$ ns) was compared to the use of scattered light off of the flow cell as the reference. The advantage of using the scatter from the flow cell as the reference is that no additional compound needs to be added to the mixture for the lifetime determinations. The scatter from the flow cell was observed by removing the filters from the emission path and collecting data for the scatter under baseline chromatographic conditions.

The following figures show lifetimes vs. relative time measurements taken across individual peaks. The zero point

indicates a point in time just before the peak is detected. Figure 46 shows the lifetime vs. time for the five completely separated compounds using the scatter reference. Figure 47 shows the same using dimethylPOPOP as the reference. The lifetimes acquired on-line with the HPLC are reasonably constant, especially for the shorter-lived components, and close to the values shown in Table 13 above. There are at least two reasons the lifetimes are more constant for the shorter-lived components: first, the modulation frequency used in this experiment was 18 MHz, which is optimal for a lifetime of 8.8 ns; second, the references, both the scatter ($\tau=0$) and the dimethylPOPOP ($\tau=1.45$ ns), are very short-lived and therefore the differences between the lifetimes of the references and the analytes are less for the short-lived compounds. In general, it appears that the lifetimes were more constant when dimethylPOPOP was used as the reference, although for all examples the lifetimes came together at the correct value in regions close to the peak maxima.

The above sets of experiments identified many initial problems related to acquiring lifetime data on-line with HPLC. The scatter correction procedure is applicable not only to the problems related to this particular instrumental arrangement, but to any experiment where the phase-modulation technique is being used to determine lifetimes in a scattering environment such as front surface fluorescence or other similar arrangements.

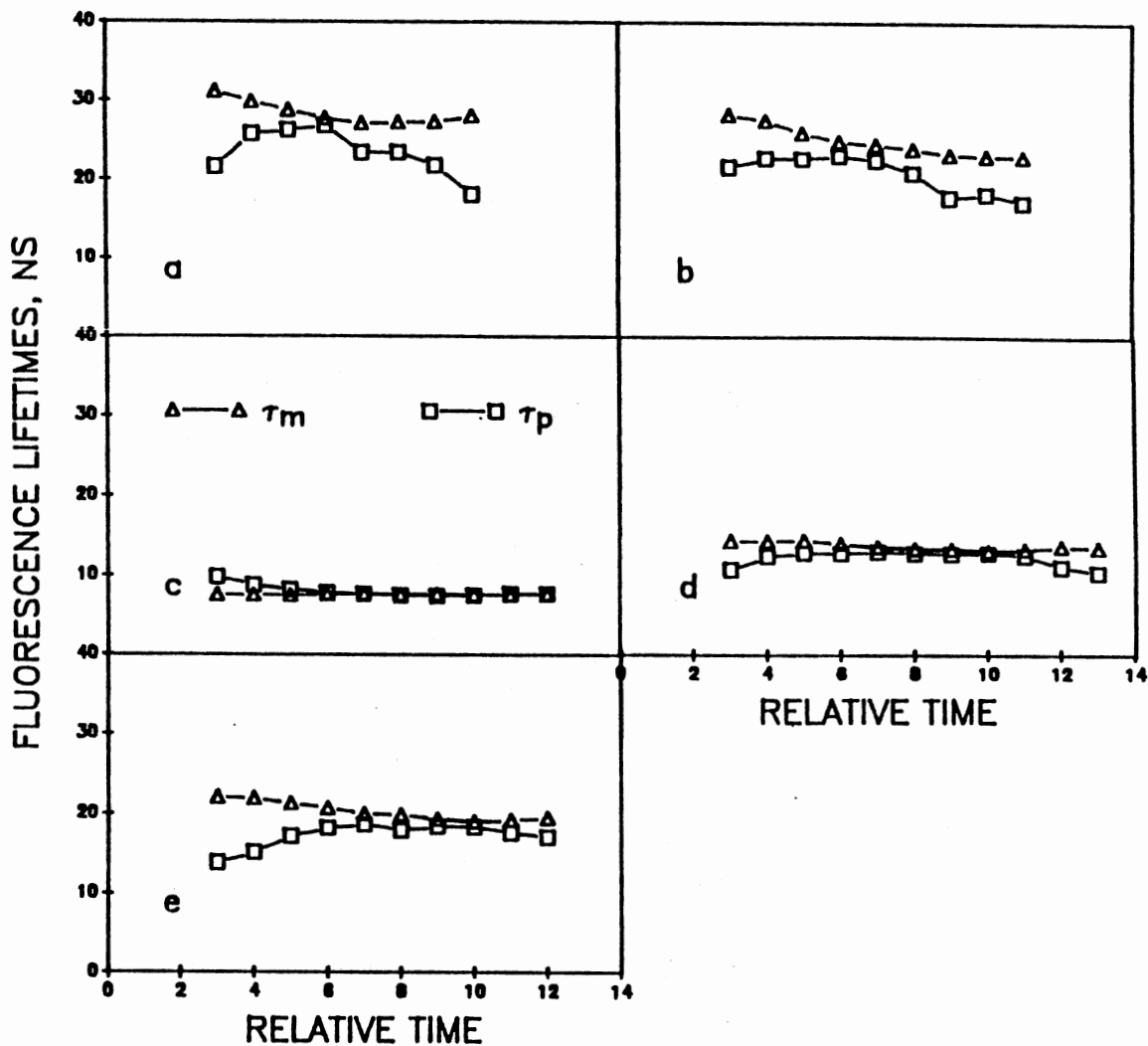


Figure 46. Lifetimes vs. Time Using Scatter as the Reference. (a) Fluoranthene, (b) B(b)F, (c) B(k)F, (d) B(a)P, and (e) B(ghi)P.

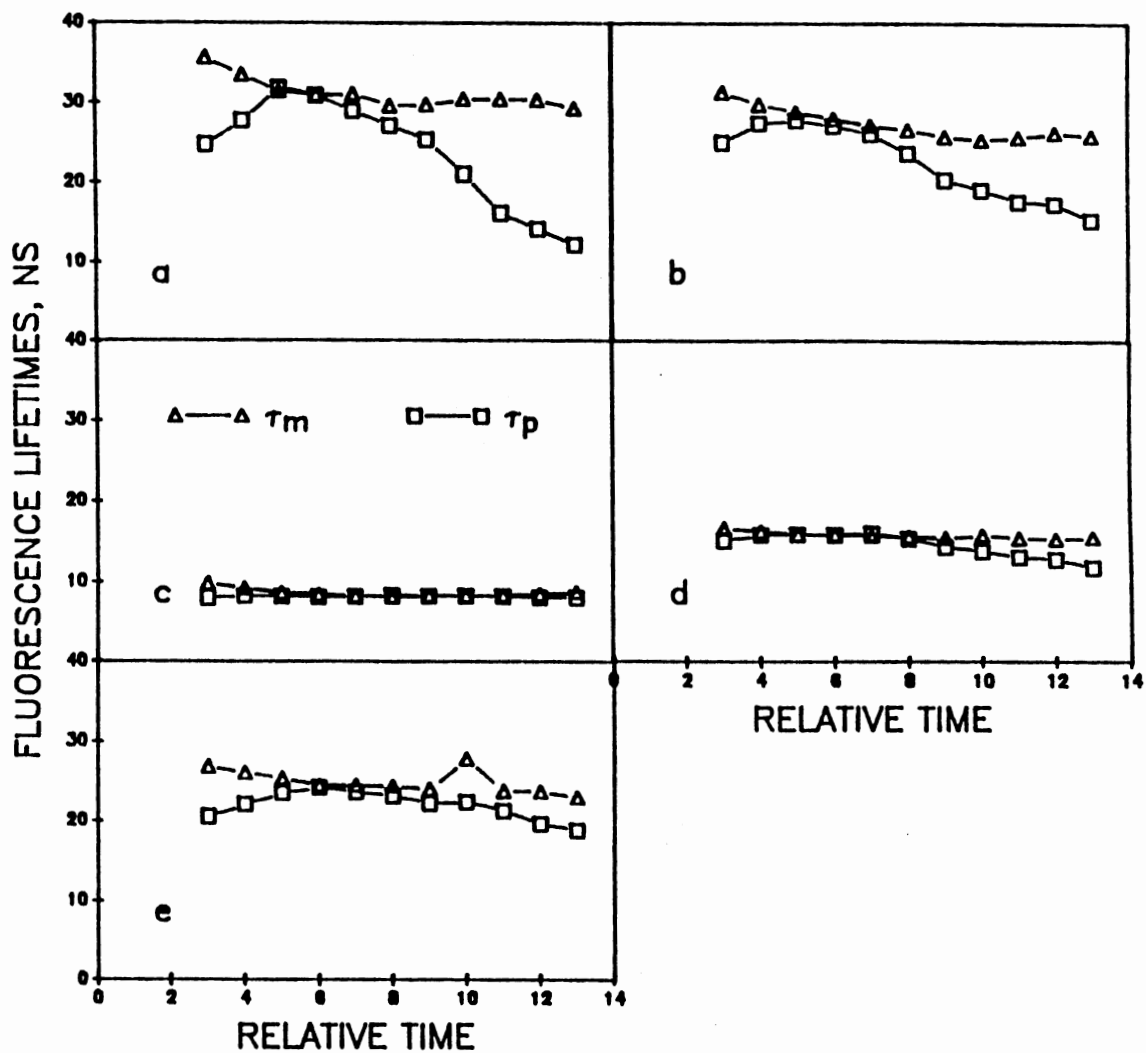


Figure 47. Lifetimes vs. Time Using DimethylPOPOP as the Reference. PAHs are the Same as in Figure 46.

Application of Phase-Modulation Fluorescence
Lifetime Determinations and Heterogeneity
Analysis To Mixtures of B(k)F and B(b)F

Steady state intensity information from compounds separated by HPLC is useful for identification and quantification; however, one must be reasonably convinced that the peaks are due to only one component. Also, in areas where more than one component is contained in a chromatographic peak or peak portion, some means of quantitation of those components must be available.

In this set of experiments the apparent lifetimes were calculated from the phase-shift and demodulation of the emission signal relative to the exciting light, as was discussed in the fluorescence lifetime theory section (Chapter 3, equations 9 and 10). The degree of agreement between the apparent phase and modulation lifetimes was used as an indicator of chromatographic peak overlap, ie., the presence of more than one fluorescent component at a given point along the chromatogram. Phase-modulation fluorescence chromatograms collected at more than one modulation frequency were used to perform heterogeneity analysis, in which the fluorescence lifetimes and fractional contributions to intensity of the components at each point along the chromatogram were calculated.

The use of phase-modulation measurements for the chromatographic detection of a binary system of benzo(k)fluoranthene (B(k)F) and benzo(b)fluoranthene

(B(b)F) is described. Both on-line HPLC detection and batch mode simulations were used to demonstrate the ability of phase-modulation fluorometry to resolve the fluorescence contributions of the two components in overlapping chromatographic peaks. Solvent composition was varied in order to create different degrees of peak overlap ranging from zero to essentially complete overlap. B(k)F and B(b)F were chosen for this work because of the similarity in their chromatographic retention properties and their spectral absorption and fluorescence characteristics. The difference between their fluorescence lifetimes is large, thereby facilitating the resolution of their chromatographic peak intensity contributions by the use of phase-modulation fluorescence detection.

Experimental

Stock solutions of B(k)F (5.07×10^{-5} M) and B(b)F (9.91×10^{-5} M) were prepared in 100% MeCN. Standards and mixtures were prepared by dilution of the stock solutions. The concentrations in the mixture used for HPLC were 2.38×10^{-6} M for B(b)F and 1.50×10^{-6} M for B(k)F. This resulted in amounts injected of 11.5 ng and 7.6 ng for B(b)F and B(k)F respectively. The HPLC separations were performed with isocratic solvent systems of 75% and 90% MeCN in water and 100% MeCN. Samples were manually injected by syringe in 20 μ L volumes. Phase, modulation, and steady state measurements were made with the SLM 4800S,

which was described in the general instrumentation section. A 20 μ L self-masking black quartz flow cell (Hellma Cells) was used in the fluorescence instrument. Excitation wavelength was selected at 360 nm by the excitation monochromator, and a combination of a 399 nm low fluorescence long pass filter with a 600 nm short pass filter (Oriel) was used to pass the fluorescence emission. A kaolin (Aluminum Silicate) scattering solution was used as the reference for batch fluorescence lifetime determinations, and scatter from the flow cell without filters in the emission path was used as the reference for the on-line fluorescence lifetime determinations. Solutions were not deoxygenated.

The phase-modulation chromatographic and batch simulation experiments were all performed as five replicate runs, and the results are expressed as the averages of the runs. Chromatographic data and batch simulation data was collected with fluorescence detector in the "10 average" mode, and fluorescence lifetime determinations in the batch mode were performed in the "100 average" mode. Heterogeneity analysis using Weber's algorithm was performed on an APPLE IIe computer using the SLM software. Weber's algorithm requires only two modulation frequencies, so results for Weber's algorithm shown in this experiment are for 6 MHz and 18 MHz data, which was found to give the best overall results for the B(k)F/B(b)F system. The nonlinear least squares (NLLS) heterogeneity analyses were

performed on an IBM PC-AT, also using SLM software. Data for the NLLS analyses was acquired at all three modulation frequencies (6, 18, and 30 MHz). In cases for which the NLLS program suggested a one-component solution, both the one-component and two-component solutions were found. Only the two-component solutions are reported here, as the one-component solutions did not give any overall improvement in the results.

Batch Experiments

A series of six solutions in 100% MeCN were studied in a batch mode, in order to test the ability of the heterogeneity analysis experiments to resolve the contributions of B(k)F and B(b)F in mixtures of the two. The solution compositions were chosen to represent the relative fluorescence intensity contributions of B(k)F and B(b)F, represented by α_A and α_B , respectively, at successive points along a chromatogram. Measurements of phase-shift and demodulation for each solution at 6, 18, and 30 MHz were used to calculate τ_p and τ_m values at each frequency. Heterogeneity analyses were then performed to find α_A , α_B , τ_A , and τ_B , using both Weber's algorithm for exact solutions and the NLLS approach. Results, expressed as the relative errors in the α and τ values for each component, are shown in Table 16. Results are also shown in Table 16 for NLLS analyses in which the fluorescence

TABLE 16
RESULTS FOR BATCH HETEROGENEITY ANALYSIS FOR B(k)F AND B(b)F

True Value		% Error									
		Exact (6,18 MHz)				NLLS1 (6,18,30 MHz)				NLLS2 (6,18,30 MHz) ^a	
α_A	α_B	τ_A	α_A	τ_B	α_B	τ_A	α_A	τ_B	α_B	α_A	α_B
0.77	0.23	-2.5	-4.8	-5.0	22	-2.6	-4.2	-4.4	21	0	5.3
0.58	0.42	-3.9	-3.2	-4.5	11	-0.9	1.7	2.1	3.5	3.2	1.2
0.36	0.64	-6.1	-8.0	-1.5	8.9	2.0	3.7	5.3	4.3	-0.3	-2.0
0.19	0.81	-7.1	-7.3	-0.4	3.4	13	25	7.2	5.8	-1.3	0.7
0.08	0.92	-12	-16	0.2	1.0	--	-100	-16	8.7	-12	0.5
0.04	0.96	-32	-32	-0.8	1.4	--	-100	-8.7	4.3	-16	0.5

^a NLLS2 performed as with NLLS1 but with τ_A and τ_B fixed at 7.23ns and 25.24ns.

lifetimes of the two components were fixed at the values obtained for the B(k)F and B(b)F standard solutions.

Chromatographic Experiments

The chromatographic resolution of the B(b)F and B(k)F peaks is listed in Figure 48 for each of the three solvents used (75, 90 and 100% MeCN). Resolution R was calculated as the difference between the retention times of B(k)F and B(b)F, divided by the mean of the two peak widths. The resolutions for the UV absorption chromatograms were slightly greater than those of the fluorescence chromatograms, probably due to the positioning of the fluorometer after the absorption detector. The peaks were completely resolved with 75% MeCN, partially resolved with 90% MeCN and highly overlapping with 100% MeCN, as is also shown in Figure 48.

Six chromatograms (each the average of five replicates) were run for each of the three solvent compositions, including the steady state fluorescence intensity chromatograms of the individual B(k)F and B(b)F solutions and the B(k)F/B(b)F mixture, and the phase-modulation fluorescence chromatograms of the mixture at 6, 18 and 30 MHz modulation frequencies. Retention time reproducibility was within 1.3% relative standard deviation for each of the sets of five replicate chromatograms. Steady state fluorescence intensity chromatograms of the two individual components were constructed from the phase-

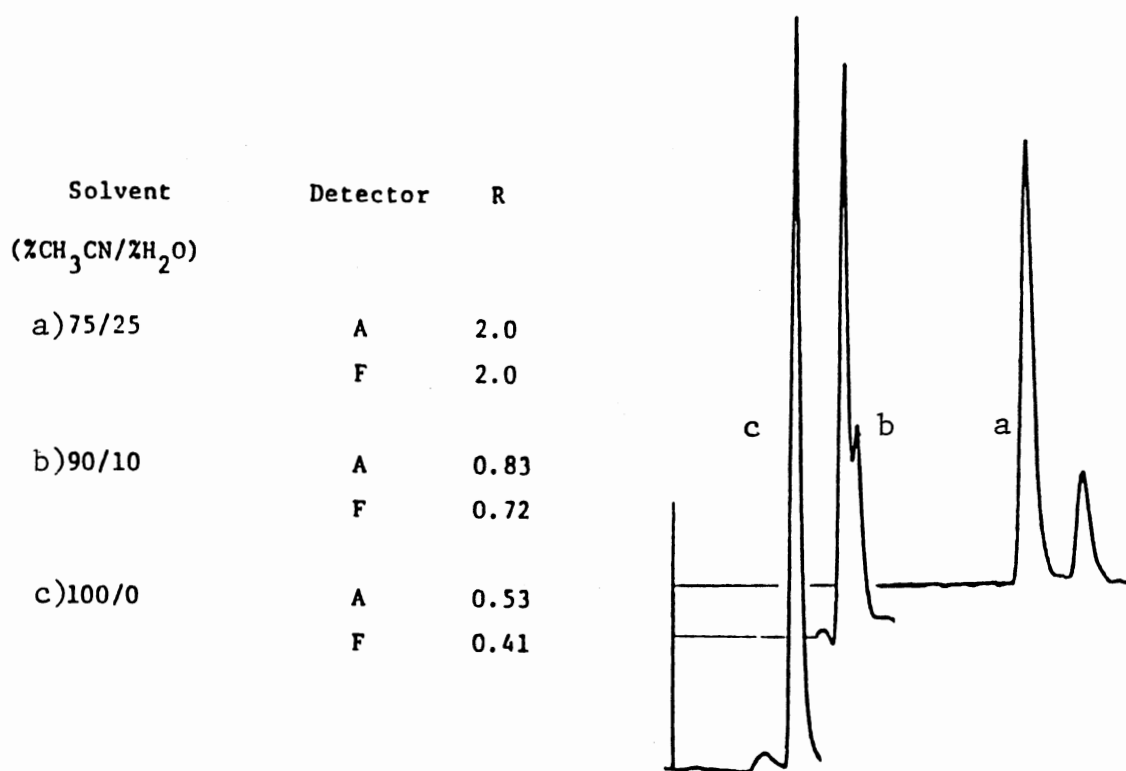


Figure 48. Chromatograms of B(k)F and B(b)F Using Different Mobile Phase Compositions With Isocratic Elution.

modulation chromatograms of the mixture as follows. The phase-shift and demodulation values recorded at each point along the phase-modulation fluorescence chromatograms were used to calculate the τ_p and τ_m values at each point, yielding three sets of τ_p and τ_m values per point (one set for each modulation frequency). Heterogeneity analysis of the fluorescence lifetime data was then used to find α_A , α_B , τ_A and τ_B at each chromatographic point. The steady state fluorescence intensity chromatograms for each component were constructed by multiplying the α value for the component at each point by the steady state intensity of the mixture chromatogram at that point. The reconstructed chromatograms were compared at each point with the steady state intensity fluorescence chromatograms of the individual components. The comparison was based on three criteria: the retention time (t_r), the fluorescence intensity (I_F), and lifetime (τ_F) at the peak. Results are summarized in Table 17 for both the exact solutions and NLLS analyses, in terms of the relative errors for each of the comparison criteria.

Discussion

The batch simulation experiments show the limiting accuracy that can be expected in resolving the fractional intensity contributions of B(k)F and B(b)F in 100% MeCN with the SLM 4800S. The accuracy with which the fluorescence lifetimes can be determined is also indicated.

TABLE 17
RELATIVE ERRORS FOR ON-LINE HETEROGENEITY ANALYSES

Solvent (%MeCN/ %Water)	Method	B(k)F			B(b)F		
		t_r	I_F	τ_F	t_r	I_F	τ_F
75/25	Exact ^a	1.5	8.5	0.4	4.0	9.2	6.3
	NLLS1 ^b	-3.0	15.8	0.7	-0.3	-12.6	-9.6
	NLLS2 ^c	-1.9	7.9	—	-5.7	-12.8	—
90/10	Exact	-0.5	23.4	2.2	0.8	-1.2	-17.1
	NLLS1	-0.9	16.8	16.8	0.1	2.1	-10.4
	NLLS2	-0.6	23.1	—	0.0	-4.3	—
100/0	Exact	1.3	16.2	-1.5	-2.1	-16.7	-9.2
	NLLS1	2.5	18.7	14.6	-1.1	-8.6	-8.9
	NLLS2	0.8	9.3	—	-1.3	-12.1	—
Average % error : ^d							
	Exact	1.1	16.0	1.7	2.3	9.0	11.0
	NLLS1	2.1	17.0	11.0	0.5	7.8	9.6
	NLLS2	1.1	13.0	—	2.3	2.3	—

^a Exact solution using Weber's algorithm at 6 and 18 MHz.

^b NLLS1 performed at 6, 18, and 30 MHz.

^c NLLS2 performed at 6, 18, and 30 MHz with lifetimes fixed.

^d Relative error magnitude averaged for the three solvent systems.

As would be expected, the accuracy of the fluorescence contributions and lifetime determinations decreases as the fractional intensity contribution of the component decreases. The magnitudes of the relative error for the exact solutions systematically increase, whereas the NLLS errors show random fluctuations except for the extreme cases of $\alpha_A \gg \alpha_B$ or $\alpha_A \ll \alpha_B$, for which the errors show a sharp increase.

For the chromatographic experiments, the relative errors in fluorescence contributions and lifetimes are lowest at the points in the chromatograms corresponding to the peaks of the components. The errors increase as the peripheral regions of the peaks are approached, as expected both intuitively and from the results for the batch simulations. For analytical purposes, the retention times and the fluorescence intensity and lifetime values at the chromatographic peaks of the components are of the most value in both quantitative and qualitative analysis.

Several interesting points can be made about the results shown in Table 17. Very good results were obtained for the retention times of the peaks that were constructed from the phase-modulation data. Errors in retention time were largest for the 75% MeCN, despite the fact that complete chromatographic separation is obtained with this solvent system. This indicates that the error is related to the magnitude of the retention time itself, which is much longer for the 75% MeCN solvent, rather than to the

errors in the phase-modulation reconstruction of the peaks. There appear to be systematic errors (positive for B(k)F and negative for B(b)F) in the peak intensity and lifetime determinations. The errors do not seem to be related to chromatographic resolution, i.e., errors do not decrease as the chromatographic separation improves. Overall, the exact solution results for B(k)F are better than the NLLS solutions, especially for the τ_F determinations in which the average magnitudes of the relative errors differ by an order of magnitude. On the other hand, the NLLS results (with variable τ_A and τ_B) are somewhat better than the exact solution results for B(b)F. These apparent biases may be the result of the modulation frequencies used for the experiments, since Weber's algorithm and the NLLS program weight the errors in the phase and modulation differently.

Fluorescence Lifetimes for PAHs On-line
With HPLC Using A Multifrequency
Phase-Modulation Fluorometer

The first use of a multifrequency phase-modulation fluorometer is described for the measurement of fluorescence lifetimes on-line with HPLC. Several considerations were addressed, including correction factors for instrumental problems, intensity matching of the reference and sample signals, and the effect of changing

the HPLC flow rates and mobile phase composition on the observed fluorescence lifetimes obtained.

As was noted in the previous section, there are several features of fluorescence lifetime measurements that are of particular importance for HPLC detection. First of all, fluorescence lifetime is generally independent of concentration; therefore, the lifetime for a single-component peak should attain a certain value as soon as the fluorescence intensity is detected, and remain constant over the entire peak. Second, phase-modulation lifetime determinations provide two independent lifetime values: τ_p , calculated from the phase-shift, and τ_m , calculated from the demodulation. For single-component peaks, τ_m has the same, constant value as τ_p over the entire peak. For overlapping peaks, on the other hand, τ_m will be greater than τ_p in the regions that are comprised of more than one fluorescent component. Phase-modulation fluorescence lifetime detection can therefore be used to indicate the presence of more than one fluorescent component at any point along the chromatogram.

Experimental

Stock solutions and samples were prepared as described in the general experimental section. Samples were manually injected by syringe in 20 μ L volumes. Isocratic elution was again used in this work, and the mobile phase compositions will be described later. A four-port valve

was used to connect the flow between the UV absorption detector and the fluorometer, in order to perform stopped-flow experiments. The valve had no noticeable effects on the chromatographic peak in the continuous flow experiments, and was therefore left in place for all HPLC experiments. The 20 μ L self-masking black-quartz fluorescence flow cell was used for flow and stopped-flow measurements.

Fluorescence lifetimes were determined on the SLM 48000S multifrequency phase-modulation spectrofluorometer (SLM Instruments, Inc.), described in the general instrumental section (Chapter 4), in which electrooptic modulation is used to provide essentially continuous frequency selection in the 1 - 250 MHz range. Wavelength selection was accomplished with the excitation monochromator set at 360 nm and a combination of a 399 nm long-pass and a 600 nm short-pass filter for emission. For batch measurements, 10 75-average measurements were used. The "slow time kinetics" mode of the instrument was used to acquire data with time under flow conditions. On-line measurements were acquired as a 3-average reading taken once per second. The raw data, including d.c. intensity, a.c. amplitude, and phase angle, was transferred to a spreadsheet (As Easy As, shareware) program for data manipulations. Scatter was used as the reference for the batch lifetime calculations, while 9-anthracenecarbonitrile

(9-AC, 97%, Aldrich) was used as the reference for the on-line work.

Batch Analysis

A batch heterogeneity analysis of B(k)F / B(b)F was repeated with the 48000S multifrequency instrument in order to determine how the new instrument compared with the 4800S used in previous experiments. Fluorescence lifetimes were obtained for several solutions containing mixtures of B(k)F and B(b)F. The concentrations and relative steady state fluorescence intensities are shown in Table 18. Excitation modulation frequencies used included 7, 15, 23 and 35 MHz. Table 19 shows the fluorescence lifetimes obtained at each frequency for each solution. Non-linear least squares (NLLS) heterogeneity analysis was used to determine the lifetimes and fractional contributions of each compound in each solution, and these results are shown in Table 20. Table 20 also shows the results when the lifetimes were fixed at 7.05 ns (B(k)F) and 24.89 ns (B(b)F). Overall, the errors are low and only get prohibitively large for the minor component when the fractional contributions get below 20%. The errors were significantly reduced for the fractional contributions when the lifetimes were fixed, as would be expected. The use of multifrequency instrumentation significantly improved the results for heterogeneity analysis over those using the 4800S where only 6, 18, and 30 MHz were available (compare Table 20 to

TABLE 18
MIXTURES OF B(b)F AND B(k)F
FOR HETEROGENEITY ANALYSIS

#	Concentration B(b)F (M)	Concentration B(k)F (M)	Relative Intensity
1	—	2.06×10^{-6}	.6094
2	1.31×10^{-7}	1.80×10^{-6}	.6179
3	2.41×10^{-7}	1.55×10^{-6}	.6036
4	3.73×10^{-7}	1.29×10^{-6}	.5891
5	4.84×10^{-7}	1.04×10^{-6}	.5936
6	6.17×10^{-7}	7.78×10^{-7}	.6021
7	7.28×10^{-7}	5.19×10^{-7}	.5878
8	8.62×10^{-7}	2.60×10^{-7}	.5863
9	9.96×10^{-7}	—	.5871

TABLE 19
 FLUORESCENCE LIFETIMES OF MIXTURES OF B(b)F AND B(k)F^a

Freq.	1	2	3	4	5	6	7	8	9	
7	τ_p	24.78	20.93	17.96	15.58	13.61	11.60	9.96	8.44	7.19
	τ_m	24.99	23.73	21.77	20.04	18.22	15.66	13.02	9.86	5.60
15	τ_p	24.70	17.80	14.49	12.22	10.75	9.47	8.50	7.72	7.16
	τ_m	24.93	22.08	19.74	17.09	14.98	12.67	10.69	8.69	6.73
23	τ_p	24.54	15.97	12.76	10.88	9.69	8.71	8.09	7.50	7.18
	τ_m	25.00	20.98	17.93	15.42	13.43	11.36	9.74	8.20	6.91
35	τ_p	24.91	14.79	11.82	10.11	9.13	8.38	7.90	7.43	7.18
	τ_m	24.97	20.09	16.74	14.31	12.40	10.60	9.23	7.95	6.97

^a Lifetimes (in ns) calculated from the phase-shift and demodulation for each of the nine mixtures.

TABLE 20
RESULTS OF BATCH NLLS HETEROGENEITY ANALYSIS

#	"True" F_1 (B(k)F)	"True" F_2 (B(b)F)	% Error					
			F_1	τ_1	F_2	τ_2	$F_1'^a$	$F_2'^a$
1	0.00	1.00	—	—	—	—	—	—
2	0.13	0.87	7.7	6.2	0.0	2.0	-7.7	2.3
3	0.24	0.76	-4.2	-6.0	0.2	-1.3	0.0	0.0
4	0.37	0.63	-5.4	0.6	0.0	-1.2	-2.7	-1.5
5	0.48	0.62	-4.2	-0.3	3.8	-2.9	-2.1	1.9
6	0.60	0.40	0.0	0.9	5.3	-4.3	0.0	5.3
7	0.73	0.27	-1.4	0.3	7.7	-10.4	0.0	3.8
8	0.87	0.13	-2.3	-0.3	15.4	-22.9	0.0	0.0
9	1.00	0.00	—	—	—	—	—	—

^a NLLS performed with τ_1 and τ_2 fixed at 7.05 ns and 24.89 ns.

Table 16 in last section). Due to the multifrequency capabilities of the SLM 48000, the 250 frequencies (vs. 3 on the SLM 4800S) provide for much superior optimization in the number and selection of frequencies.

Fluorescence Lifetimes On-line With HPLC

Initial investigations. Fluorescence lifetimes were obtained on-line with the HPLC. The figures for all of the continuous-flow experiments represent relative time on the x-axis. It should be noted that zero on the relative time scale refers to a point just prior to elution of the peak, and does not indicate zero retention time.

It was determined that the use of the scatter from the flow cell was very dependent on the exact positioning of the flow cell, and also gave consistently poorer results ($\tau_m = \tau_p$) than when a reference fluorophore was used. 9-AC was chosen as the reference fluorophore since its lifetime ($\tau = 11.31$ in 100% MeCN) and spectral characteristics were in the same general range as most of the PAHs under investigation.

Figure 49 shows the fluorescence vs. time data for B(k)F at 0.5 mL/min and 100% MeCN. As can be seen, although the phase lifetimes are fairly constant over the peak, the modulation lifetimes are not only delayed but also highly sloping. Several experiments were done to determine if this behavior might be due to scattered light present in the system. Scatter corrections, described in

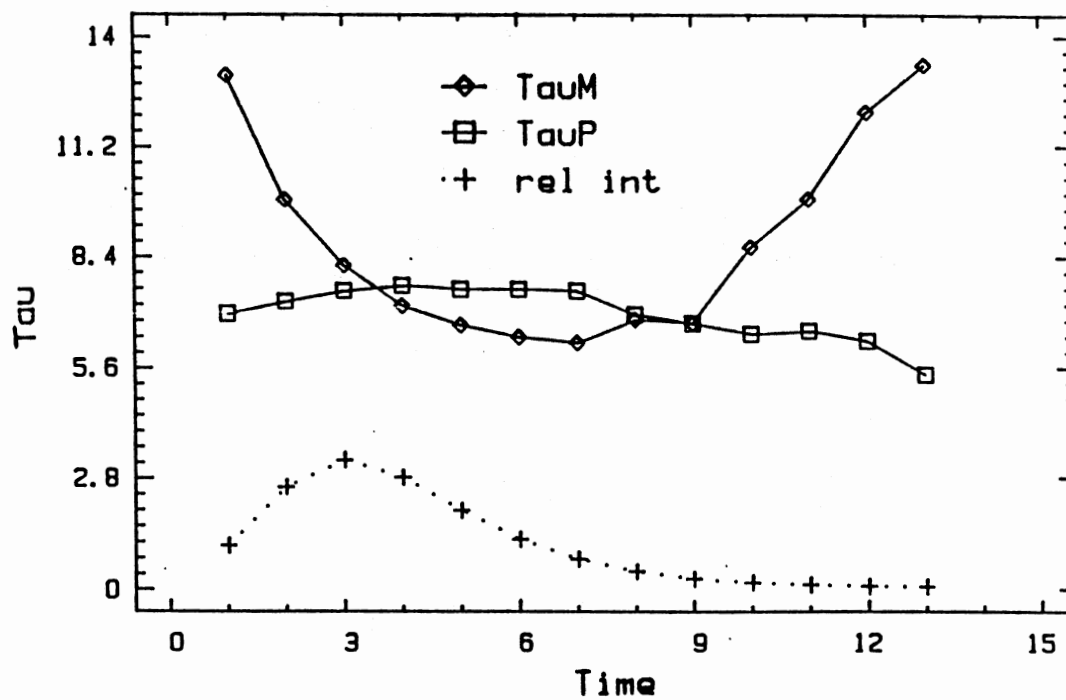


Figure 49. Fluorescence Lifetime Chromatogram for B(k)F at 0.5 mL/min and 100% MeCN.

the section ("On-line Fluorescence Lifetime Determinations"), were applied here as well as the use of crossed polarizers was investigated to cut out the scatter. These experiments all failed to improve results. Intuitively, it would seem that if scattered light were the problem, both the phase and modulation lifetimes at the peak periphery would fall to lower values because of the increasing contribution of the zero lifetime scatter. This is obviously not the case and therefore it was determined that scattered light was not the problem in this experimental arrangement.

Next, the possibility that the poor lifetime response was due to flow effects such as mixing in the flow cell was investigated. If the problems were caused by mixing in the flow cell, or by absorption of PAHs on the flow cell walls, then the response of the fluorescence lifetimes should change when the HPLC mobile phase flow rate was varied or when the mobile phase composition was changed. In order to test this hypothesis, the fluorescence lifetimes on-line were determined at flow rates from 0.2 mL/min to 1.2 mL/min with 100% MeCN. These are shown graphically for 0.2, 0.4, 0.6, and 0.8 mL/min in Figures 50 and 51. Besides the expected changes due to the sharper peaks at higher flow rates and therefore fewer points per peak, all the flow rates showed a similar response. The effect of changing the mobile phase composition while keeping the flow rate constant was determined for B(k)F and B(b)F at 0.5 mL/min.

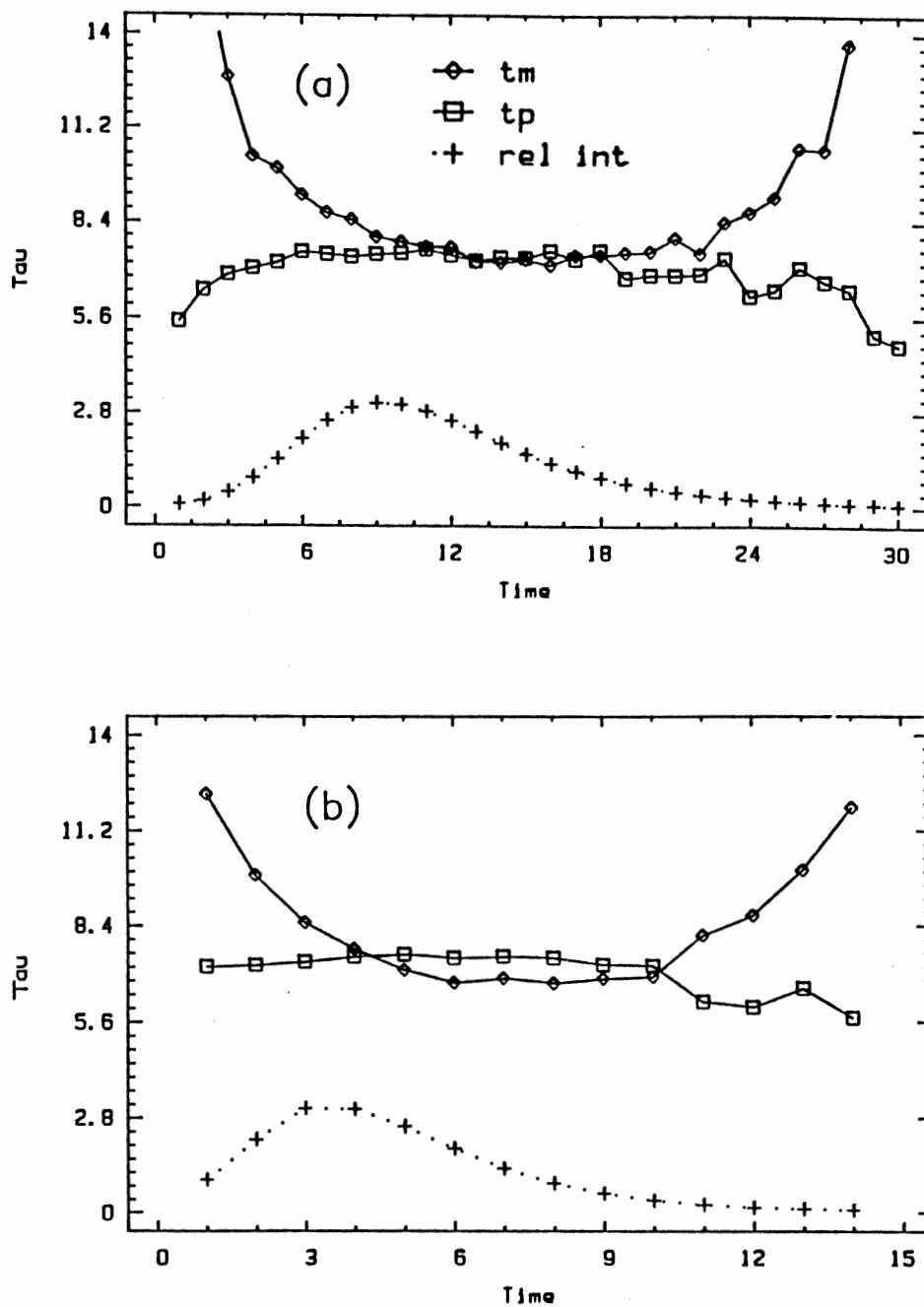


Figure 50. Fluorescence Lifetime Chromatograms of B(k)F Using 100% MeCN at (a) 0.2 and (b) 0.4 mL/min.

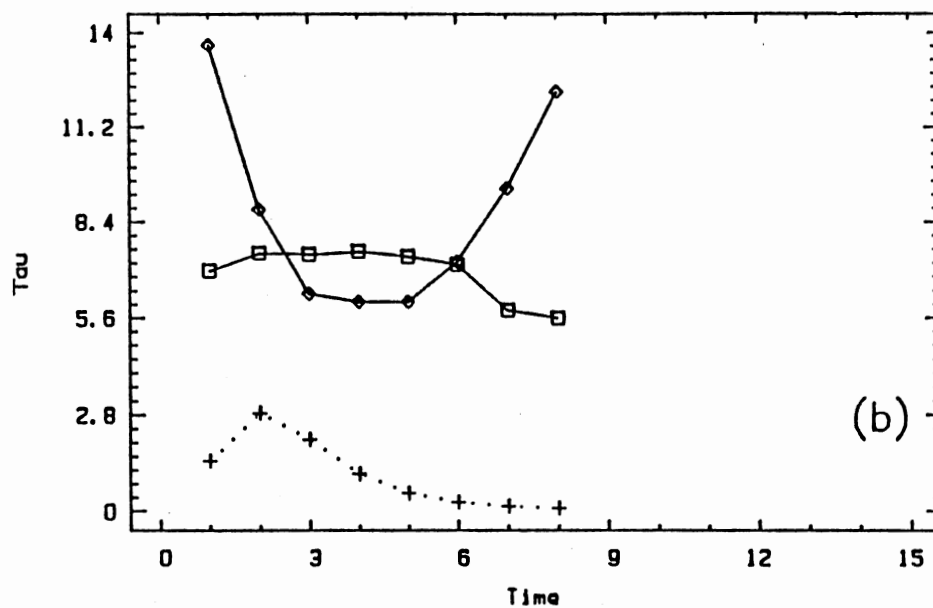
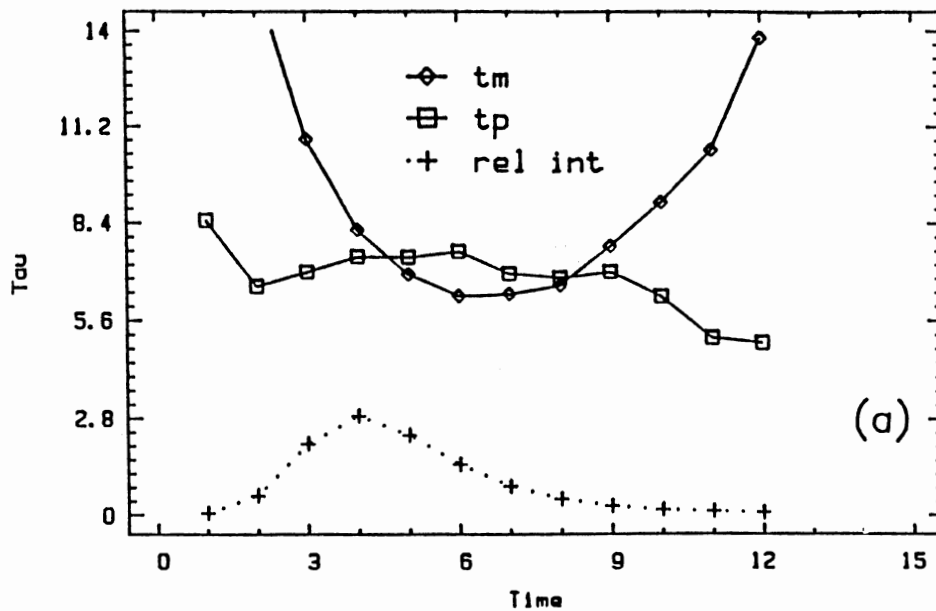


Figure 51. Fluorescence Lifetime Chromatograms of B(k)F Using 100% MeCN at (a) 0.6 and (b) 0.8 mL/min.

As can be seen in Figures 52-54, the only differences which can be seen in going from 100 to 80% MeCN is the peak broadening. Methanol was also used in place of the MeCN and gave very similar results. The incorrect behavior of the lifetimes, especially the modulation lifetimes, was shown not to be due to the presence of scatter, dynamic mixing, the particular compound, absorption effects, or other effects which can be traced to the analytes or to the solvent and solvent delivery. To determine if the effects could be tied to physical or mechanical problems instead of chemical problems, a series of experiments were done to pinpoint the exact cause of the incorrect lifetime behavior under flowing conditions.

Batch Mode Simulations. B(k)F was incrementally added to 100% MeCN in a quartz cuvette in order to simulate the concentration profile of the front edge of a chromatographic peak. Fluorescence intensity and phase and modulation lifetimes for each of the solutions are shown in Figure 55a. Over most of the "peak" edge, $\tau_p = \tau_m = 7$ ns, as expected for a peak containing B(k)F ($\tau = 7$ ns). However, τ_m was increasingly greater than τ_p as the intensity decreased (approaching the front of the "peak"). Since these measurements were under batch conditions, flow is not responsible for this effect. Further studies indicated the importance of intensity matching between the reference 9-AC solution and the sample. All of the lifetimes shown in Figure 55a were obtained by calibration

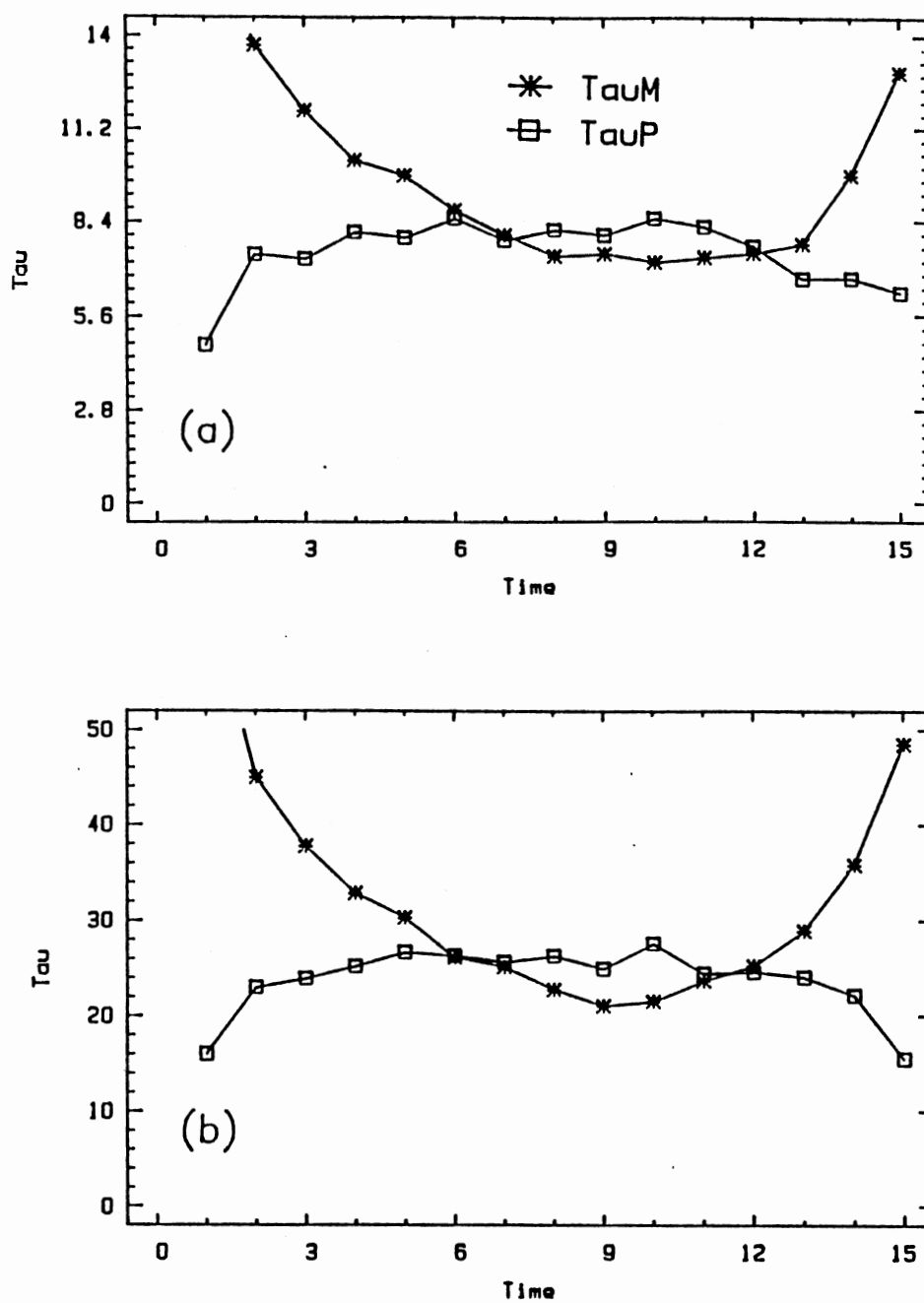


Figure 52. Fluorescence Lifetime Chromatograms at 0.5 mL/min and 80% Aqueous MeCN for (a) B(k)F and (b) B(b)F.

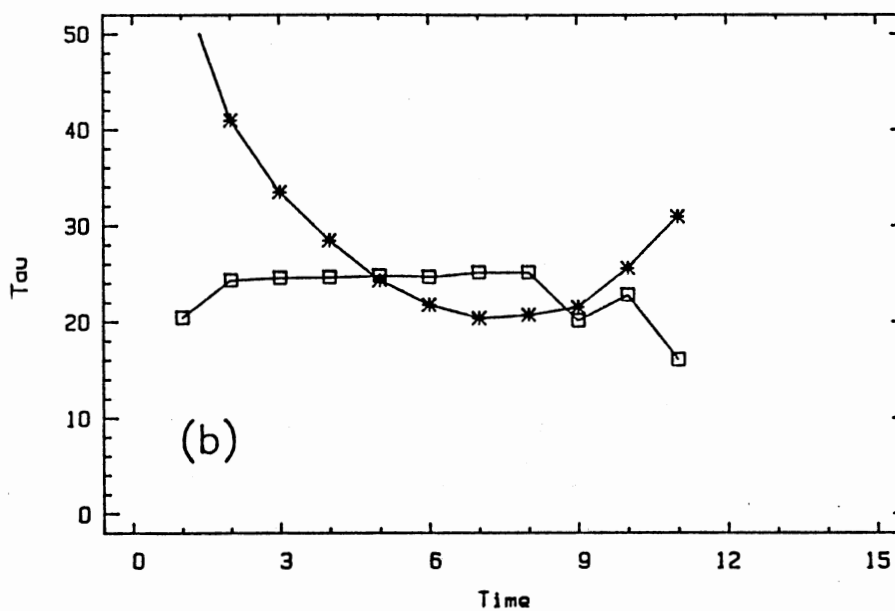
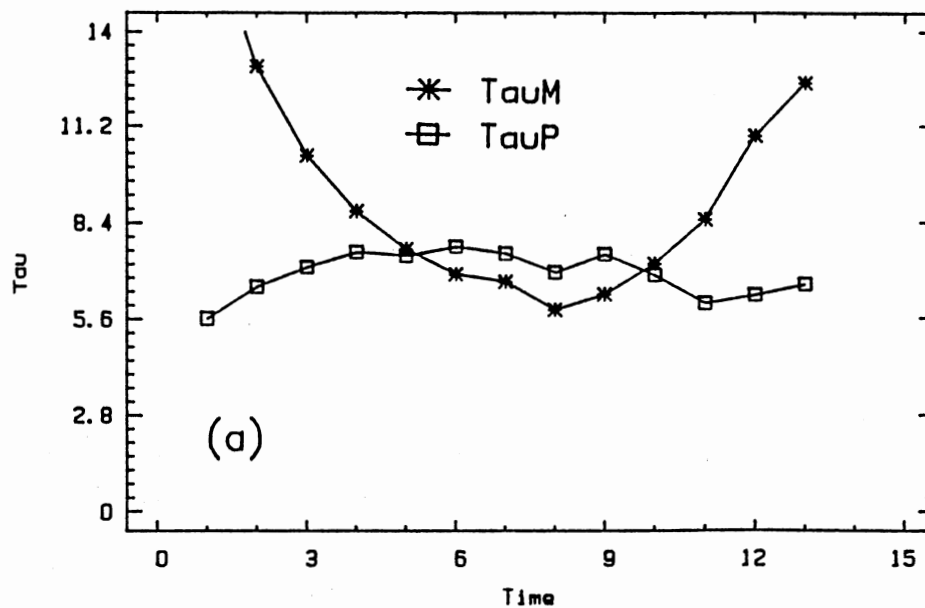


Figure 53. Fluorescence Lifetime Chromatograms at 0.5 mL/min and 90% Aqueous MeCN for (a) B(k)F and (b) B(b)F.

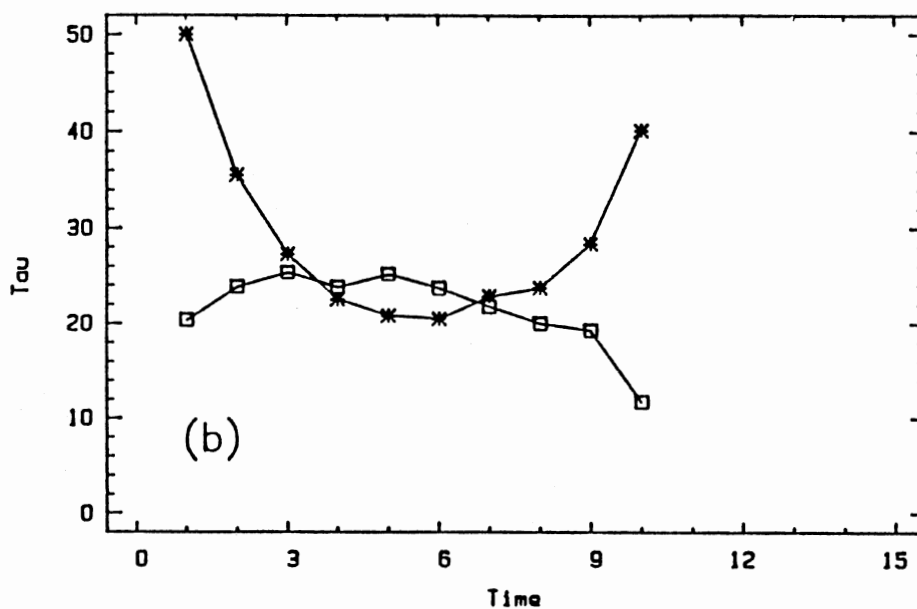
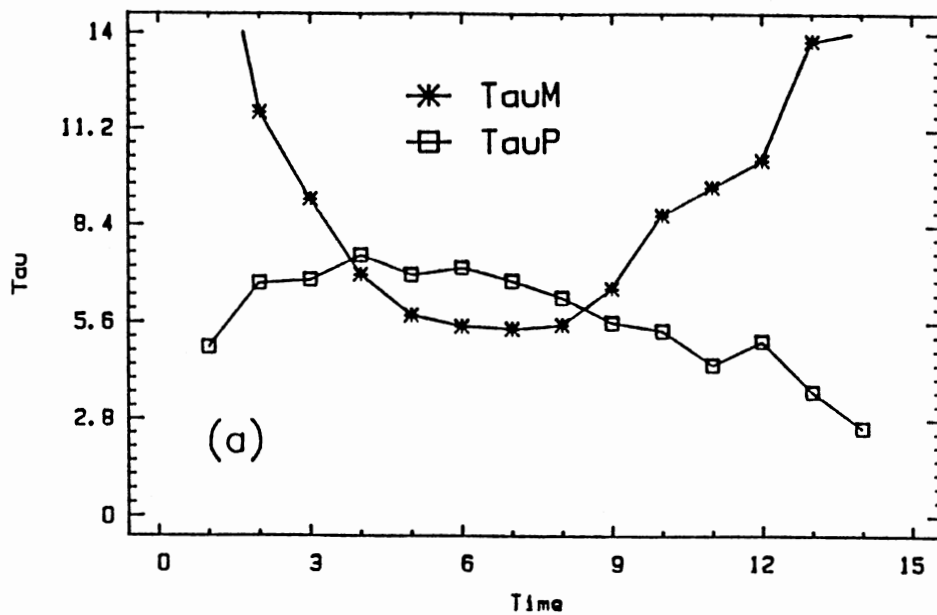


Figure 54. Fluorescence Lifetime Chromatograms at 0.5 mL/min and 100% MeCN for (a) B(k)F and (b) B(b)F.

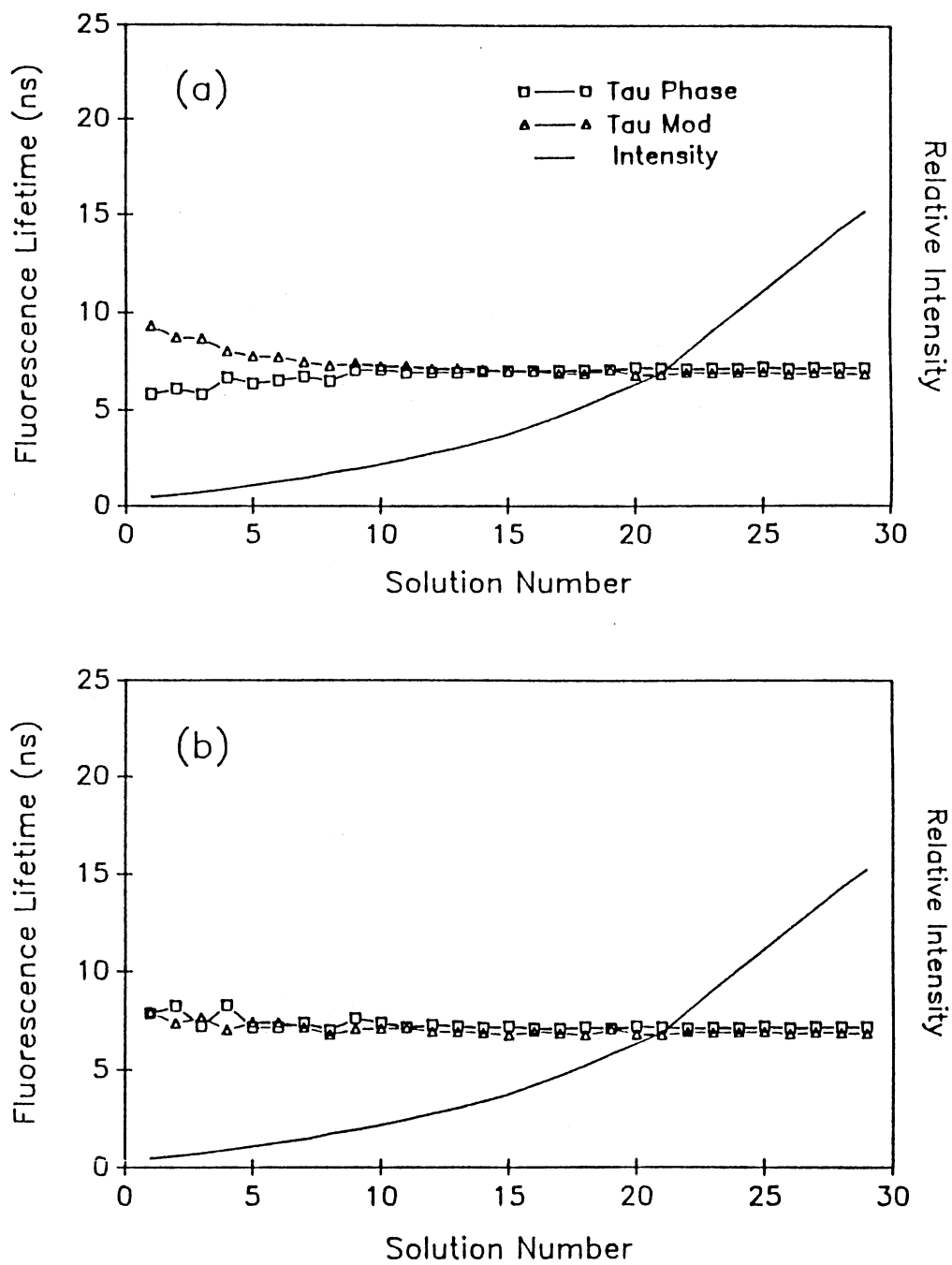


Figure 55. Batch Fluorescence Lifetime Chromatogram Simulations for B(k)F (a) Before and (b) After Reference Intensity Matching.

with a 9-AC solution that had an intensity similar to that of the highest concentration B(k)F solution. For these conditions, intensity matching is not important until the B(k)F intensity gets close to zero, at which point τ_m and τ_p become increasingly divergent. Figure 55b shows the improvement in lifetime determinations that is obtained when calibration is performed with a 9-AC solution that has the same intensity as the sample. Agreement between τ_m and τ_p occurs over the entire concentration range, yielding the correct value of 7 ns. The increase in random fluctuations of the observed lifetimes at the low intensity edge is due to the increased noise associated with the detection of low-level signals.

Stopped-flow Simulations. The next experiments used stopped-flow conditions to measure B(k)F as it was eluted from the HPLC, in order to evaluate the effects of the flow cell (but not flow conditions) on the lifetime determinations. The stopped-flow experiments used the same instrumental configuration as would be used for real-time chromatographic detection, but the flow from the HPLC was stopped for every measurement in order to eliminate effects due to flow. First, a single 9-AC reference solution, with an intensity similar to that of the B(k)F peak maximum, was used for lifetime calibration of all points. As shown in Figure 56a, there is excellent agreement between τ_p and τ_m across most of the chromatographic peak, and the only deviation occurs at the peak peripheries. Intensity-

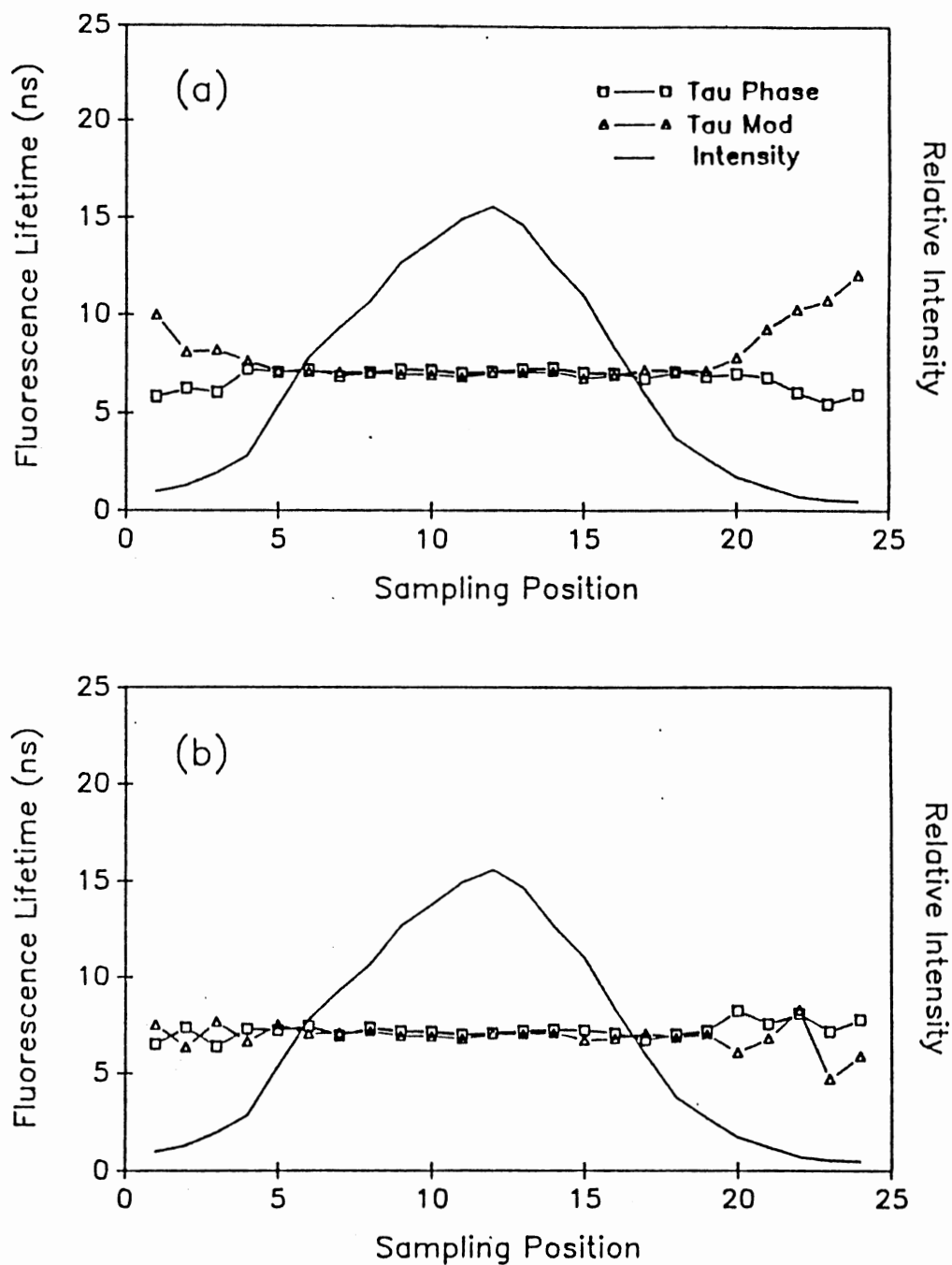


Figure 56. Stopped-Flow Fluorescence Lifetime Chromatogram Simulations for B(k)F (a) Before and (b) After Reference Intensity Matching.

matching helped to alleviate the deviation (Figure 56b). From this study, it was apparent that the flow cell itself introduced no new problems or artifacts in the intensity or lifetime determinations.

Flow Experiments. From the above batch and stopped-flow simulations it was clear that the lifetime response vs. intensity followed theory and the flow cell did not produce any serious problems for the lifetime determinations. These results, along with previous ones indicated that the problem was most likely due to an instrumental artifact rather than being due to something derived from the HPLC-imposed conditions.

To determine nature of the problem, both the a.c. intensity and the d.c. intensity were observed on-line under flowing conditions. This information was investigated due to the fact that the modulation lifetimes were the ones that were causing the problems, and the modulation lifetimes are calculated from the modulation ratio (a.c./d.c.) (see Figure 21). Figure 57 shows the a.c. and d.c. intensities for B(k)F at 23 MHz along with the modulation ratio (a.c./d.c.). The a.c. signal should be directly aligned the d.c. signal, and there should be a constant ratio of the a.c. to d.c. signals through the peak in order to get constant modulation lifetimes. Obviously, the a.c. signal is somewhat delayed, relative to the d.c. signal. Figure 57 also shows the modulation ratio after shifting the a.c. intensity to the left. A much flatter

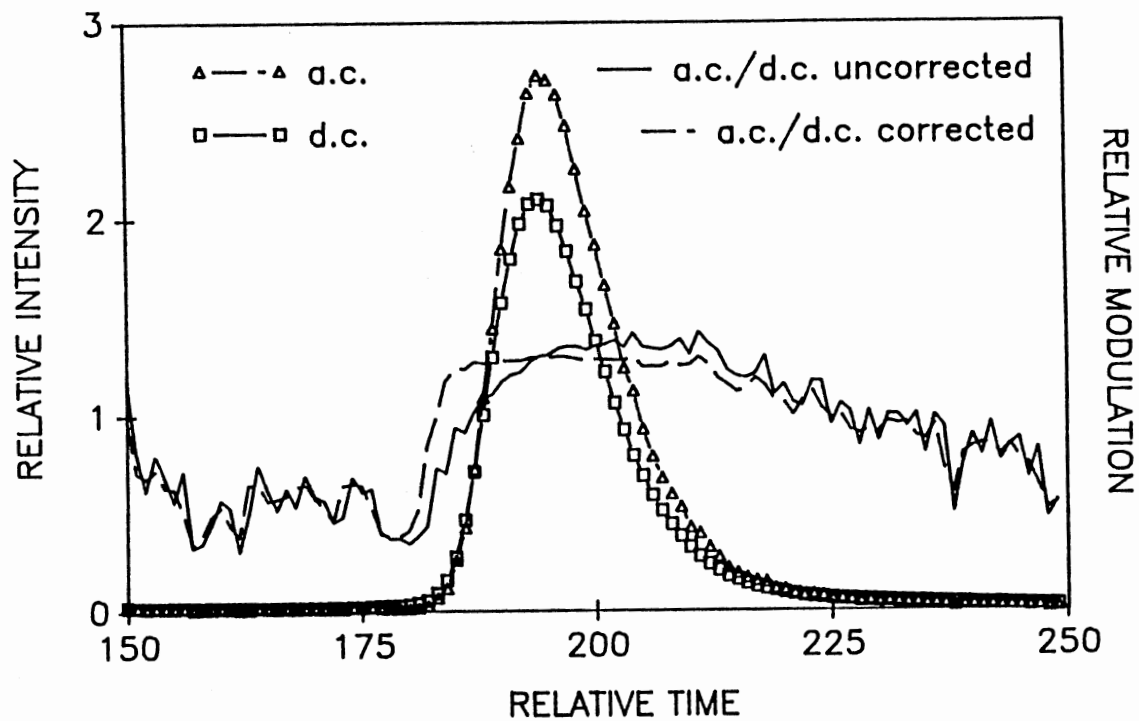


Figure 57. Dynamic (a.c.) and Steady-State (d.c.) Intensities and Modulation (a.c./d.c.) vs. Time for B(k)F.

"plateau-like" response is obtained after aligning the a.c. and d.c. peaks. The same shift is required for any data collected under the same conditions (number of points averaged, time step increment).

The cause of the problems was initially difficult to determine, but once we knew that it was caused by the fact that the a.c. signal is acquired by the electronics at a slightly later point in time than the d.c. signal, the problem was easily corrected. The reason the manufacturer was not aware of this problem is because the dynamic (lifetime) mode of the instrument was designed to be used only for static measurements, where the intensity would not significantly change with time. Our results were eventually confirmed by George Mitchell, the instrument electronics designer for SLM.

Figure 58 shows intensity and lifetimes, collected under flow conditions, for fluoranthene ($\tau = 29$ ns) that was eluted from the HPLC with a 100% MeCN mobile phase at a flow rate of 0.3 mL/min. The results shown in Figure 58a indicate two separate effects. First, this run used a single 9-AC reference instead of intensity matching, causing the lifetime divergence at the peak peripheries. Second, the modulation lifetime is not symmetric about the chromatographic peak and has a high, positive error at both the front and tail edges of the peak. Figure 58b shows the same data as for Figure 58a above, but with the a.c. intensity shifted 0.4 seconds to correctly line up with the

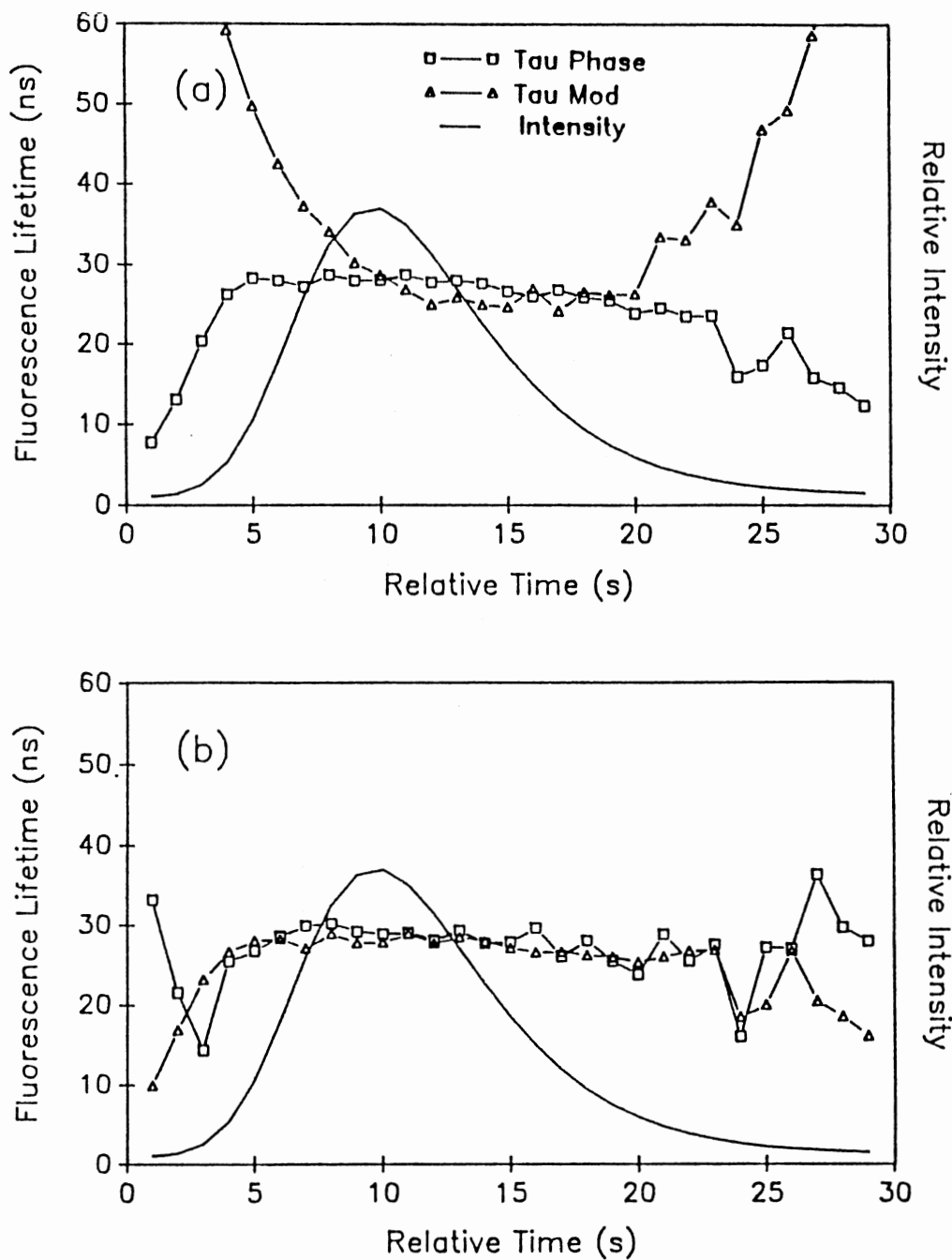


Figure 58. Fluorescence Lifetime Chromatograms for Fluoranthene at 0.3 mL/min and 100% MeCN (a) Before and (b) After Reference Intensity Matching and a.c. Correction.

d.c. signal, and with intensity matching of the reference to the analyte. To determine the correct amount to shift the a.c. signal under a particular set of experimental conditions, the a.c. and d.c. intensities for the chromatogram were collected. Using the "Edit a Spectrum" feature on the SLM software, the a.c. intensity chromatogram was shifted until it most closely aligned with the d.c. intensity chromatogram. The ratio of the two was then performed and the data manipulation continued. Once the required shift was found for a particular set of conditions, it was constant and did not need to be determined again.

The reference intensity matching was done by taking several stopped-flow measurements (intensity, phase, and modulation) of the reference fluorophore as it was eluted from the HPLC. The intensity of these stopped-flow measurements was then matched with the particular points in the chromatogram and the lifetime was calculated. This intensity matching was first done by hand, later by a search routine in the "As Easy As" spreadsheet program, and eventually by a program written in Microsoft Quickbasic.

Effects of Flow Rate and Mobile Phase Composition. In order for the on-line determination of lifetimes to be generally useful, the lifetime determinations must not be seriously degraded or changed with changes in HPLC mobile phase flow rate or mobile phase composition. Figure 59 shows the fluorescence lifetimes vs. time with changing

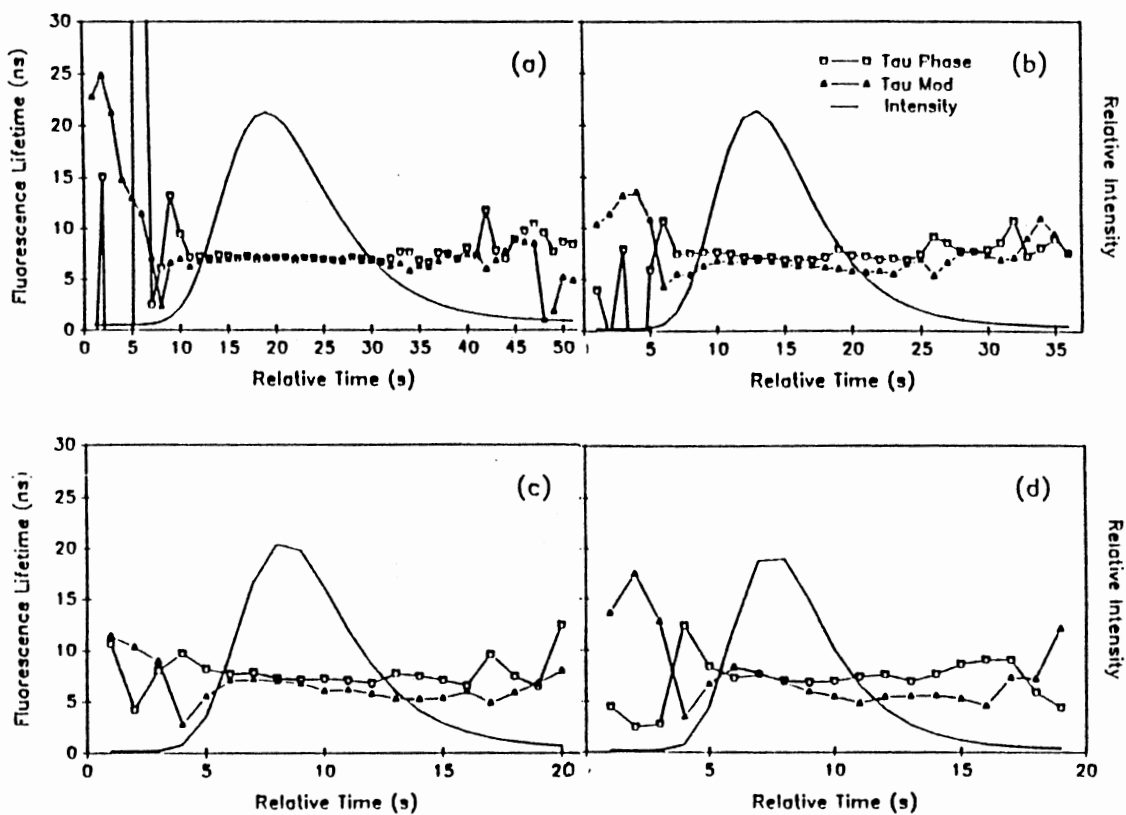


Figure 59. Fluorescence Lifetime Chromatograms for B(k)F With 100% MeCN at (a) 0.3, (b) 0.5, (c) 0.8, and (d) 1.0 mL/min.

mobile phase flow rates. The mobile phase was 100% MeCN and the data points were taken one every second. Relative to a flow rate of zero (stopped-flow), all of the flow rates used for on-line lifetime determinations exhibited increased noise that is especially evident at the edges of the peaks. As flow rate through the HPLC was increased, fewer points were collected per peak and the quality of the lifetime data was degraded. The best data was acquired at 0.3 mL/min, with systematic divergence at the higher flow rates. Figure 60 shows the results when the flow rate was held constant at 0.5 mL/min and the percent MeCN in water was varied for the mobile phase. Best results appear to be for the 90% MeCN chromatograms.

The effects of both flow rate and mobile phase composition can be attributed to similar causes. The systematic divergence of τ_m and τ_p , which increases with increasing flow rate or decreasing retention, appears to be related to the resulting increase in slope across the peak; this may be due to the difficulty in exactly compensating for the a.c. delay, which is more critical at higher slopes. The decrease in precision, which occurs with decreasing flow rate or increasing retention, appears to be related to the expansion of low-intensity regions that results from peak broadening.

In general, the fluorescence lifetimes were acceptable under all conditions investigated. There were errors at the higher flow rates; however, it must be noted that the

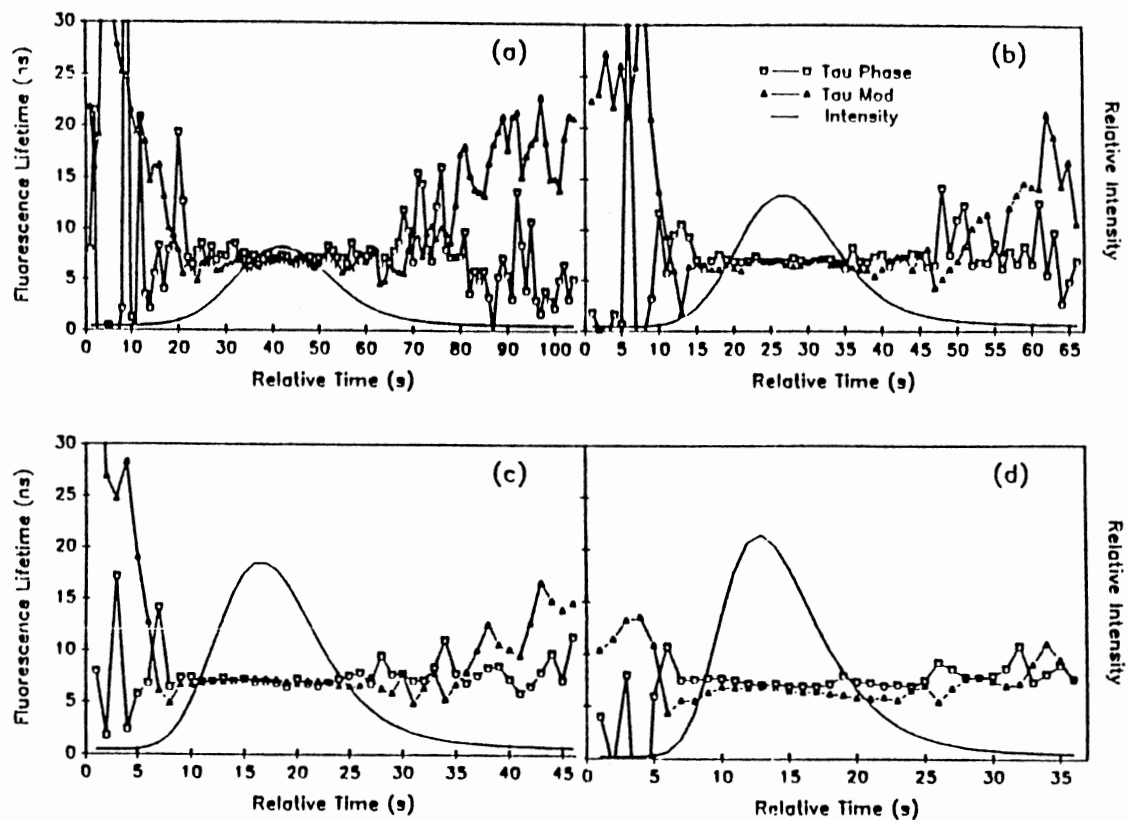


Figure 60. Fluorescence Lifetime Chromatograms for B(k)F at 0.5 mL/min With (a) 70%, (b) 80%, (c) 90%, and (d) 100% MeCN.

flow rate studies were done with 100% MeCN, which would most likely be replaced with a MeCN / water mobile phase for routine separations.

Conclusions.

Several substantial conclusions were identified with these experiments: (1) the major contributor to the error in the modulation lifetime was an instrumentation problem which was very difficult to find but proved relatively easy to solve; (2) intensity matching of the reference fluorophore to the analyte is important for both phase and modulation lifetime determinations at very low intensities for the SLM 48000S; (3) changing flow rates and mobile phase compositions have some effects on the fluorescence lifetime determinations, but not to an extensive degree; (4) the use of a moderately long-lived reference fluorophore (9-AC, $\tau=11.31$ ns) for the reference is preferred over short-lived fluorophores or scatter for the PAHs used in these studies, and (5) under correct conditions, phase-modulation fluorescence lifetimes can be accurately determined on-the-fly for components as they elute from an HPLC.

Fluorescence Lifetimes, Heterogeneity
Detection, and Heterogeneity Analysis
for Mixtures of PAHs Using HPLC
and Multifrequency Phase-
Modulation Fluorescence

Fluorescence lifetimes were determined at several modulation frequencies for a mixture of 6 PAHs which included: fluoranthene ($\tau = 28$ ns); benzo(b)fluoranthene ($\tau = 25$ ns); benzo(k)fluoranthene ($\tau = 7$ ns); benzo(a)pyrene ($\tau = 11$ ns); benzo(ghi)perylene ($\tau = 15$ ns); and indeno(1,2,3-cd)pyrene ($\tau = 7$ ns). The capability of the phase-modulation technique to determine fluorescence lifetimes on-line, to flag peak heterogeneity, and to determine fractional contributions of components in overlapping peaks is described.

Experimental

Data was acquired on the SLM 48000S using the "slow-time kinetics" portion of the acquisition software, including on-the-fly measurements of a.c. intensity, d.c. intensity, and phase. The a.c. signal was shifted to correctly calculate the modulation ratio, as described in the last section. 9-AC was used as the reference fluorophore, and a series of phase and modulation signals at changing intensities was acquired under stopped-flow conditions at each frequency for intensity matching of the 9-AC with the analyte intensities. Data was acquired as a

3-average reading (one per second) as the peaks were eluted. The HPLC was operated isocratically with 100% MeCN and a flow rate of 0.3 mL/min. These HPLC parameters were selected so as to create, in the same chromatogram, regions of no peak overlap, partial peak overlap, and almost complete overlap, amongst the six PAH components.

Fluorescence Lifetime and Peak

Heterogeneity Detection

The fluorescence lifetimes of the six-component mixture were determined on-line with HPLC at 4, 10, 15, 25, and 35 MHz. Figure 61 shows the lifetimes determined at 10 MHz. As predicted by theory, $\tau_m = \tau_p = \text{constant}$ in peak regions comprised of a single component, whereas $\tau_m > \tau_p$ in regions of overlapping peaks. For the former regions, agreement of the calculated lifetimes with "true" lifetimes (determined by phase-modulation measurements in batch experiments for the individual components) is excellent. For unresolved peaks, the calculated lifetimes across the peak clearly indicate the number of components and the regions of overlap. Even in the highly overlapping peaks of benzo(ghi)perylene and indeno(1,2,3-cd)pyrene, lifetime detection accurately indicates two components with lifetimes of 15 and 7 ns.

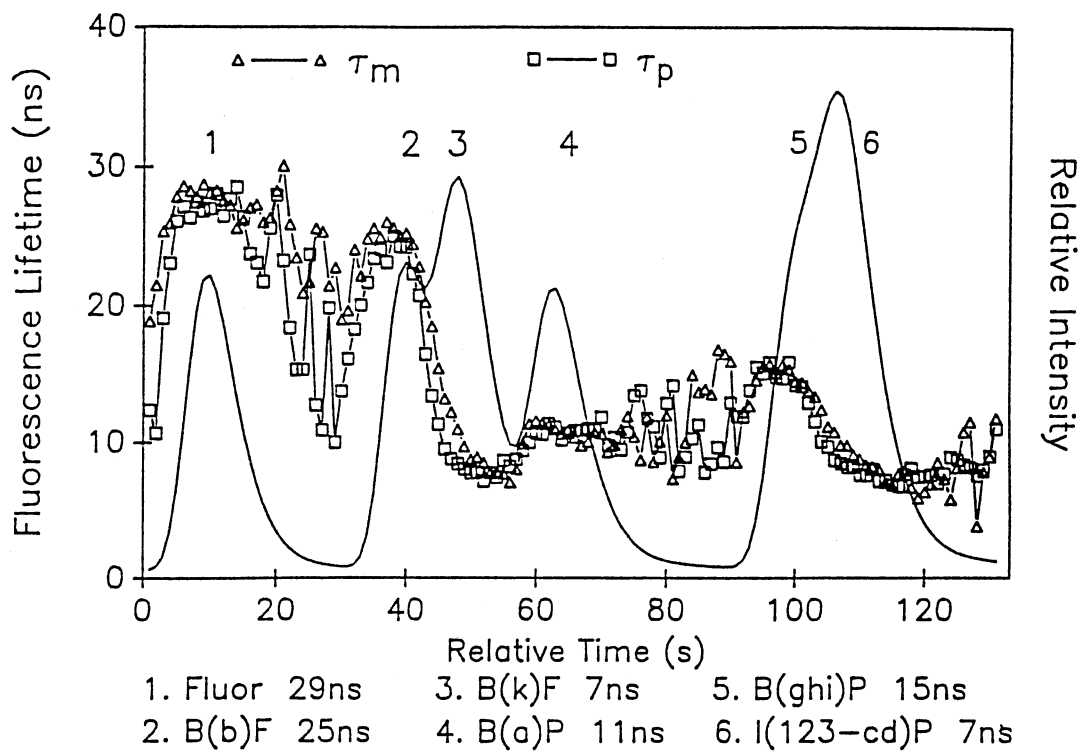


Figure 61. Fluorescence Lifetime Chromatogram Using 10 MHz Modulation Frequency, 100% MeCN, and 0.3 mL/min.

Heterogeneity Analysis

It is very important to be able to flag peak heterogeneity and get some information as to the identity of the overlapping compounds. Even more useful is the ability to obtain quantitative information from those overlapping compounds without having to completely separate them by much more exhaustive chromatographic means. Heterogeneity analysis (NLLS) was performed point-by-point for the six-component mixture, using all five of the modulation frequencies as well as different subsets of those five. The fractional contributions from the heterogeneity analysis were multiplied by the steady-state intensity of the chromatograms at corresponding points along the chromatogram. In this way the "resolved" component peaks could be "reconstructed" and compared to pure peaks due to the respective components. Figure 62 shows the results for the NLLS heterogeneity analysis using all five frequencies (4,10,15,25,35 MHz). The heterogeneity analysis was repeated using different combinations of the above frequencies in order to determine the effects of using fewer frequencies and particular groups of frequencies on the results. The results don't seem to degrade much, and are actually a little better when the 4 MHz data is dropped. This is because of the poor quality of the 4 MHz data for the short-lived components, since 4 MHz is optimal for a lifetime of approximately 40 ns. The results do degrade significantly when the data

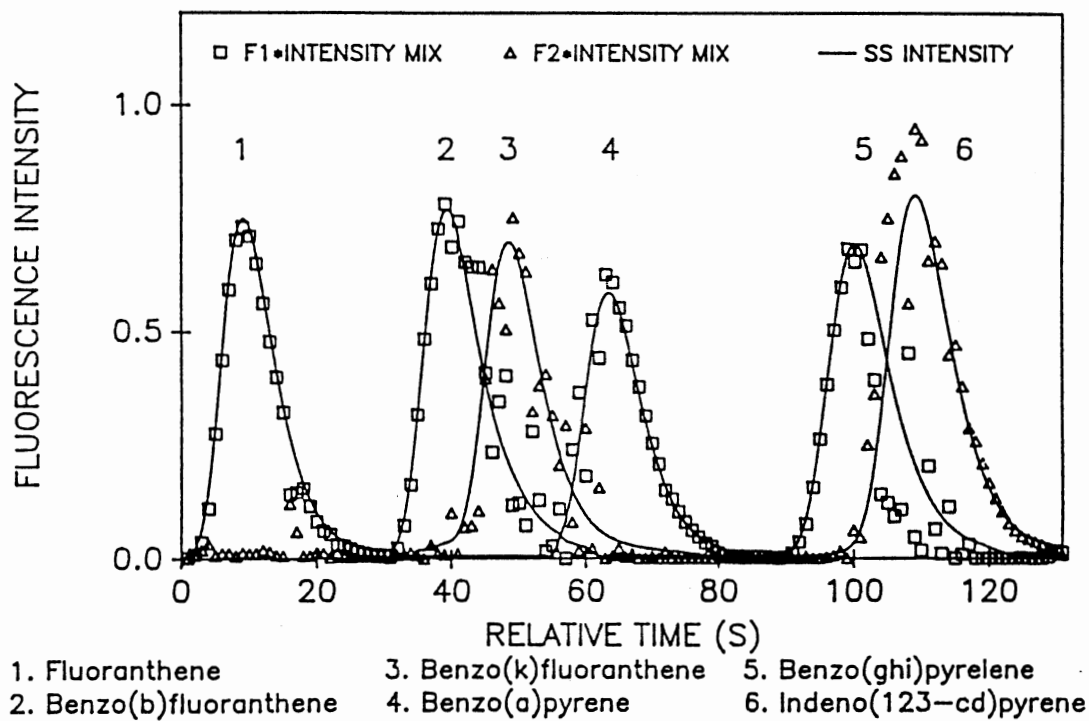


Figure 62. NLS Heterogeneity Analysis Results for Fractional Contributions Using 4, 10, 15, 25, and 35 MHz.

from 4 and 35 MHz are dropped (leaving 10, 15, and 25 MHz), and the major components are weighted more than they should be, as one might expect. The fractional intensities are good for the fluoranthene, showing that the heterogeneity analysis still finds only a single component when only one is present, despite attempting to fit the data to a two component system. The results are good for the B(b)F/B(k)F/B(a)P group, but are poor for the B(ghi)P/I(1,2,3-cd)P group.

Since very good fluorescence lifetime information is available from the on-line lifetimes at 10 MHz (Figure 61), the heterogeneity analysis was performed again but this time with fixed lifetimes. The NLLS heterogeneity analysis was then left only to calculate fractional contributions to the two given lifetime components. Figure 63 shows that significant improvement was obtained when the lifetimes were known and could be fixed in the heterogeneity analysis.

These experiments demonstrated the usefulness of the multifrequency phase-modulation fluorescence detection of PAHs separated by HPLC, especially in regions of chromatographic peak overlap. The fluorescence lifetimes were accurately determined, heterogeneous peaks were readily indicated and resolved, and quantitative information was obtained without complete chromatographic separation.

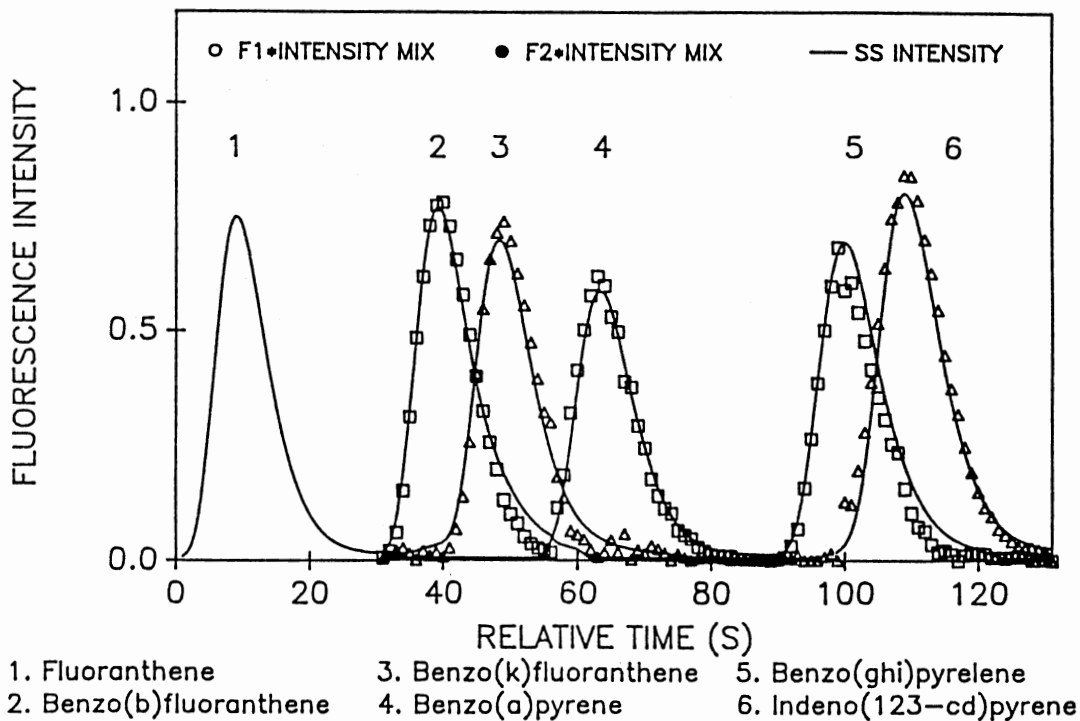


Figure 63. NLLS Heterogeneity Analysis Results for Fractional Contributions With Lifetimes Fixed Using the Same Frequencies as in Figure 62.

Phase-Modulation Fluorescence Lifetime
Chromatograms and Heterogeneity
Analysis For the Sixteen EPA
Priority Pollutant PAHs

The 16 PAHs on the EPA priority pollutant PAH list (5) were investigated along with benzo(e)pyrene (B(e)P). Good results were obtained for a set of six PAHs (discussed above) using excitation at 360 nm and emission using a 399 nm long-pass filter. For the following experiments the rest of the sixteen priority pollutant PAHs, as well as the six above, were investigated using a different set of excitation/emission wavelength conditions.

Experimental

Stock solution of PAHs along with samples were made up in 100% MeCN, with sample concentrations on the order of 1×10^{-6} M. The Waters HPLC system was used for separations, with the SLM 48000S spectrofluorometer used for fluorescence lifetime determinations. The 20 μ L black quartz flow cell (Hellma Cells) was used in the spectrofluorometer. All on-line fluorescence lifetimes were determined by reference intensity matching, a.c. correcting, and using 9-anthracenecarbonitrile (9-AC) as the reference fluorophore. All of these approaches were described in previous sections. Intensity matching calculations, lifetime calculations, and chromatogram

reconstructions were done using programs written by the author in Microsoft Quickbasic (see appendices).

Results

Spectral Considerations. For the six PAHs in the previous study, an excitation wavelength of 360 nm and emission through a 399 LP + 600 SP filter combination was used. The xenon arc lamp's emission spectrum is strong at 360 nm. However, as the wavelengths approach the UV region, the lamp output drops off dramatically, especially after passage through the modulation optics. This is illustrated in Figure 64, which shows the a.c. intensity, d.c. intensity, and modulation of the excitation light vs. wavelength.

Unfortunately, for some of the PAHs under investigation, the excitation spectra fall below 300 nm (see TABLE 12) and therefore they cannot be efficiently excited in the lifetime mode by the 450 watt lamp presently used on the instrument. However, 10 of the 16 compounds could be excited at 330 nm, and while the lamp output was fairly weak, there was sufficient power to study these compounds, along with B(e)P, using the on-line fluorescence lifetime chromatographic technique. The 11 compounds are shown in Table 21 in order of HPLC elution, along with their average lifetimes in 87% aqueous MeCN.

Chromatography. Figure 65 shows chromatograms of the mixture at 0.5 mL/min and 80% aqueous MeCN, using detection

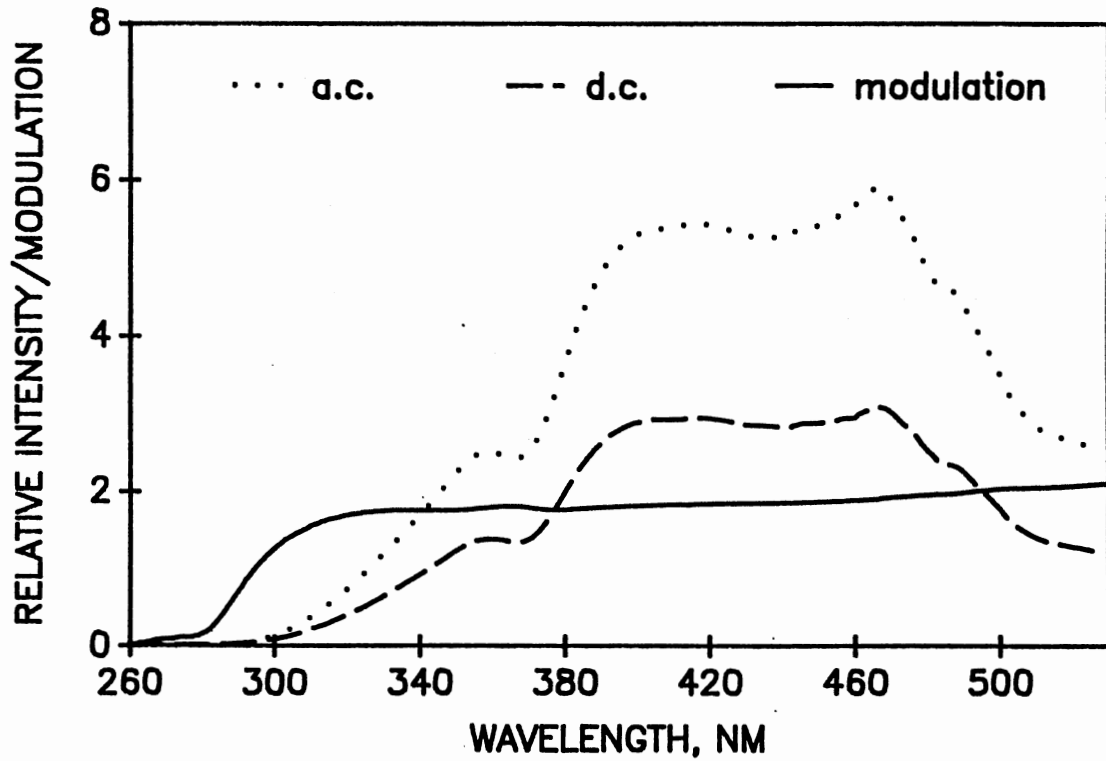


Figure 64. Intensity Output And Modulation of 450 Watt Xenon Arc Lamp vs. Wavelength.

TABLE 21
LIST OF PAHS USED IN ANALYSIS
IN ORDER OF HPLC ELUTION

#	Compound	Abbreviation	τ , ns
1	Anthracene		4.00
2	Fluoranthene		30.47
3	Benz (a) anthracene	B (a) A	15.77
4	Chrysene		12.87
5	Benzo (e) pyrene	B (e) P	16.90
6	Benzo (b) fluoranthene	B (b) F	27.28
7	Benzo (k) fluoranthene	B (k) F	7.82
8	Benzo (a) pyrene	B (a) P	14.95
9	Dibenzo (a, h) anthracene	D (a, h) A	13.89
10	Benzo (ghi) perylene	B (ghi) P	20.26
11	Indeno (1, 2, 3-cd) pyrene	I (123-cd) P	6.90

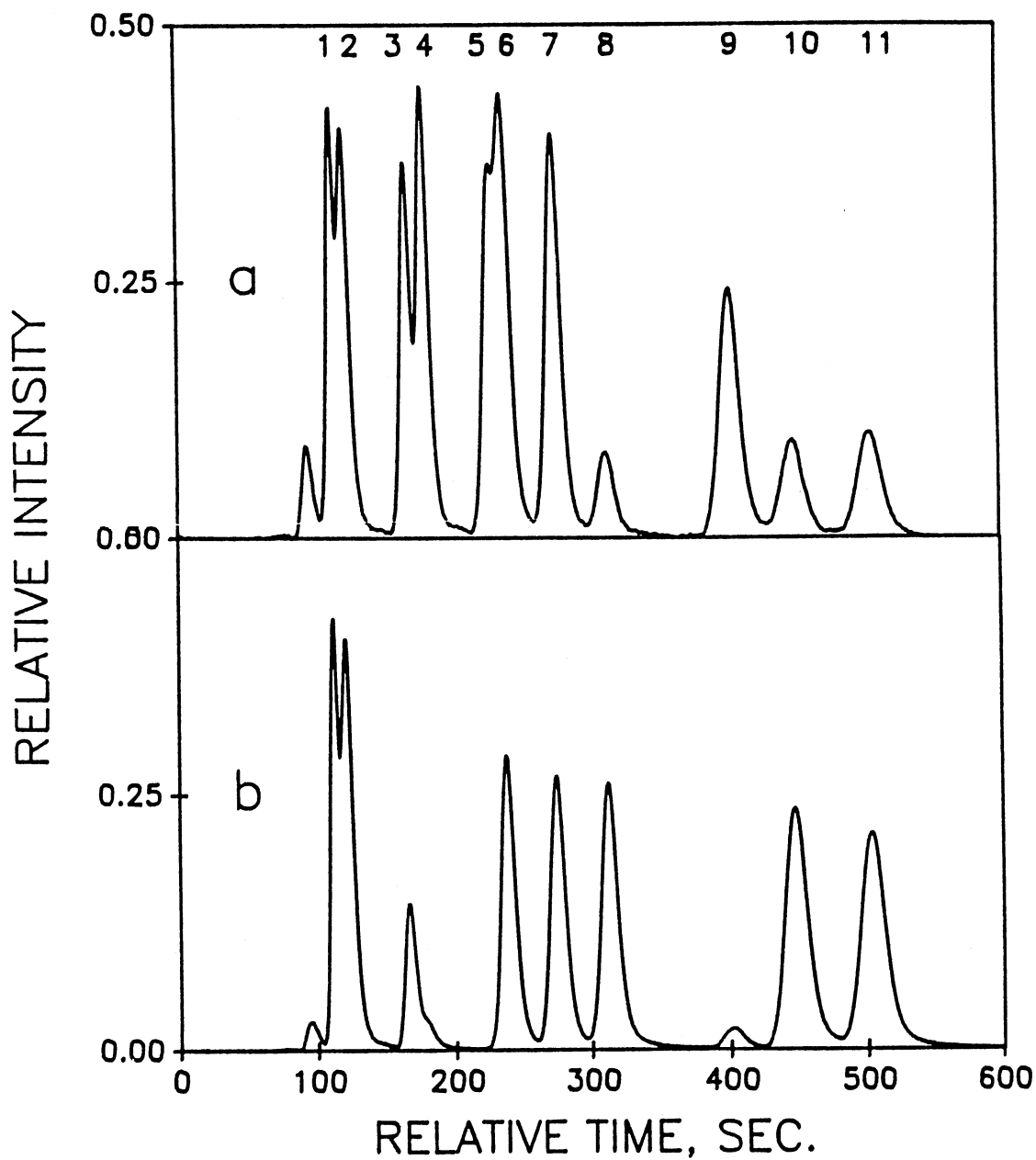


Figure 65. Chromatograms of Compounds Listed in Table 21 Using 0.5 mL/min, 80% Aqueous MeCN, and Fluorescence Detection With (a) Ex=330 nm, Em=345 nm LP + 600 nm SP Filters, (b) Ex=360 nm, Em=399 nm LP + 600 nm SP Filters.

at (a) $\text{ex}=330\text{ nm}$, $\text{em}=345\text{ nm LP} + 600\text{ nm SP filters}$, and (b) $\text{ex}=360\text{ nm}$, $\text{em}=399\text{ nm LP} + 600\text{ nm SP filters}$. The different response at the two ex/em wavelength pairs is evident, and the former was used in subsequent studies.

Flow Cell Luminescence. The black quartz fluorescence flow cell used in this research was specified as "fluorescence free" by the manufacturer, and was designed to be used for fluorescence detection without contributing to the observed signal from analytes in any way. However, when excited at 330 nm or below, there is significant emission from the flow cell. Figure 66 shows the excitation and emission spectra of the flow cell containing 100% MeCN. The emission occurs as a broad peak from 400 to 600 nm. As can also be seen in Figure 66, when the 345 nm LP and 600 nm SP filters are used, the first and second-order scatter peaks are masked as well as most of the Raman peak at about 370 nm, but the flow cell emission is transmitted. High PMT voltages were required to obtain these spectra, but significant signal is still observed at the voltages used for typical on-line work. The excitation spectrum (Figure 66) indicates that the excitation maximum is well below 300 nm, but extends out to about 350 nm. The same emission was observed using water, MeOH, MeCN, and with the flow cell cleaned and air dried.

When only steady-state detection is used, the constant emission from the flow cell can simply be "zeroed out" using PMT voltage offsets. Unfortunately, when lifetime

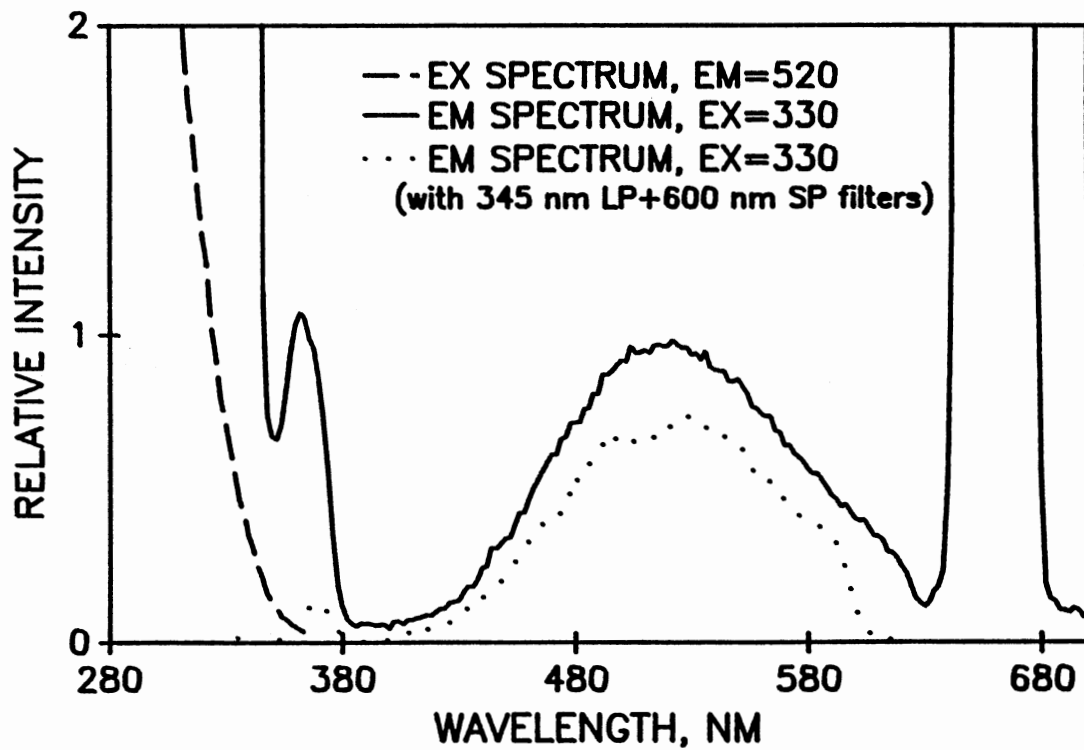


Figure 66. Excitation and Emission Spectra of Black Quartz Fluorescence Flow Cell.

measurements are made, any background signal can result in a phase-shift and demodulation of the excitation light. The d.c. signal may be zeroed out, but the a.c. information from the interferant is still contained in the signal from an analyte, thus causing lifetime determination errors.

An attempt was made to determine the lifetime of the luminescence from the flow cell. Although sufficient d.c. signal was observed, almost no a.c. signal was detected. Several modulation frequencies were used to try to find the optimum frequency to excitation modulation, but no a.c. signal was observed even at 1 MHz. This indicated that the emission was very long-lived ($\gg 160$ ns) since the optimum modulation frequency for a particular lifetime (τ) corresponds to $1/(2\pi\tau)$. This information and the large Stoke's shift seems to indicate the luminescence is due to phosphorescence, but this could not be verified with our instrumentation.

Since the emission from the flow cell contributed no significant a.c. signal, for these particular experiments it was possible to zero-out the d.c. signal and acquire the data for lifetimes of the analyte compounds in the usual way, without interference from the flow cell luminescence. Figure 67 shows the effect of the background emission from the flow cell on the lifetime chromatograms of B(k)F. It is, however, very important to be aware of this type of problem when taking lifetime measurements.

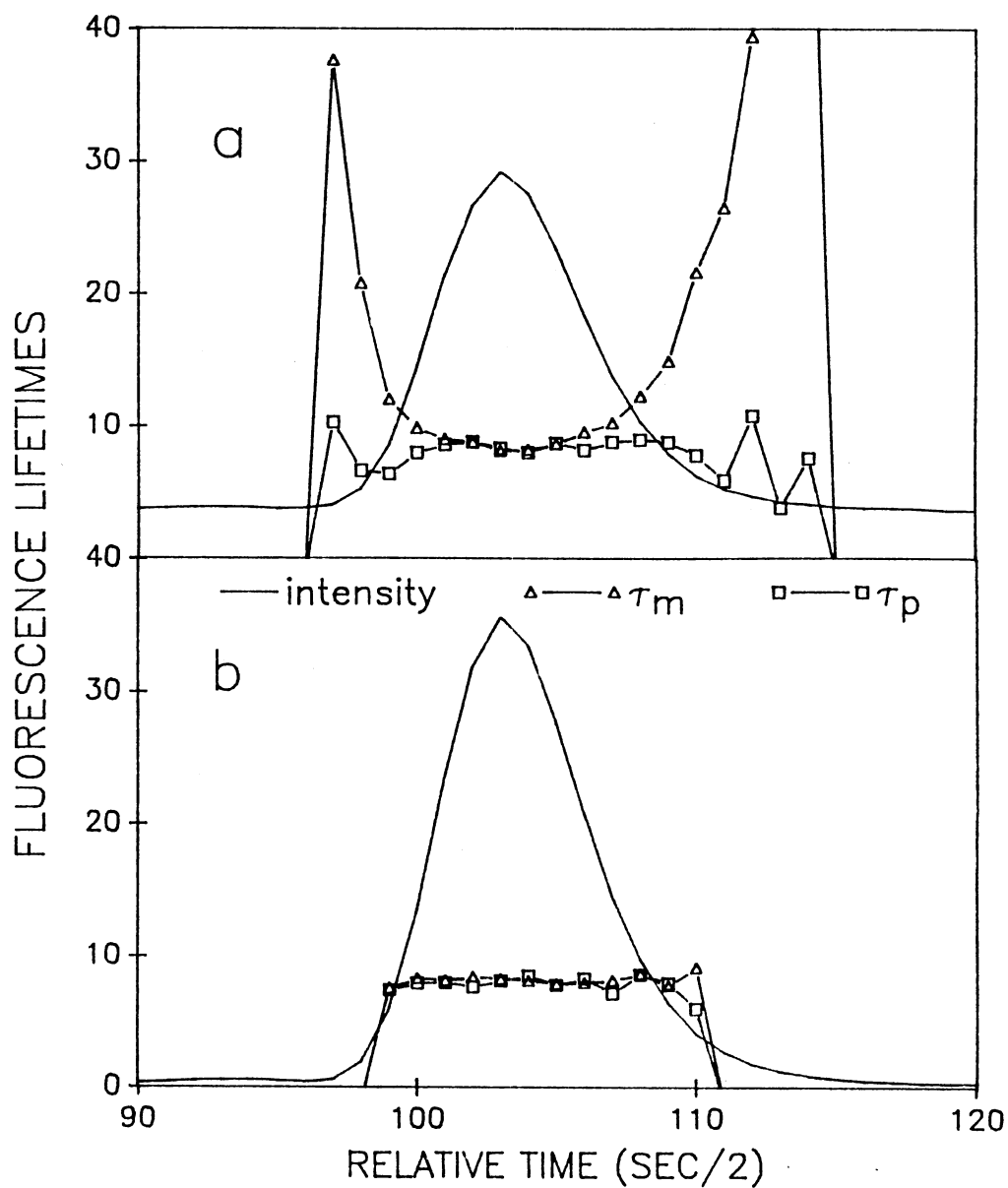


Figure 67. Effect of Flow Cell Luminescence on Lifetime Chromatograms of B(k)F. (a) Lifetimes Without and (b) With Offsetting Intensity Due to Flow Cell Emission.

Fluorescence Lifetime Chromatograms. Figure 68 shows the chromatogram of the 11-component mixture using 87% aqueous MeCN and a flow rate of 0.3 mL/min. Note that compounds 1,2 and 5,6 are highly overlapping, and compounds 3,4 are also unresolved under these conditions.

Fluorescence lifetime chromatograms were obtained for the 11-component mixture at 5, 10, 15, 25 and 40 MHz. Figure 69 shows the lifetime chromatogram for the mixture at 10 MHz. In looking at the complete chromatogram it is a little difficult to see how well the lifetimes pick up the heterogeneous regions in the chromatogram. Figure 70 shows the same data expanded over three different regions of the total chromatogram. The lifetimes for the first peak (Figure 70a) clearly indicate heterogeneity and initially indicate two components with lifetimes of 4-5 ns and 20-30 ns. For the second overlapped peak, this heterogeneity is not so obvious. The lifetimes indicate that the entire peak is composed of lifetimes of about 14-15 ns. This is a good example of the point at which the lifetime chromatogram can no longer be of great value as far as incorporating selectivity based on lifetime differences. This peak contains benz(a)anthracene (16 ns) and chrysene (13 ns). For the second expanded portion of the chromatogram (Figure 70b), the changing lifetimes across the first peak indicate heterogeneity and the observed lifetimes approach those of the two compounds present, B(e)P (17 ns) and B(b)F (27 ns). The remaining peaks on

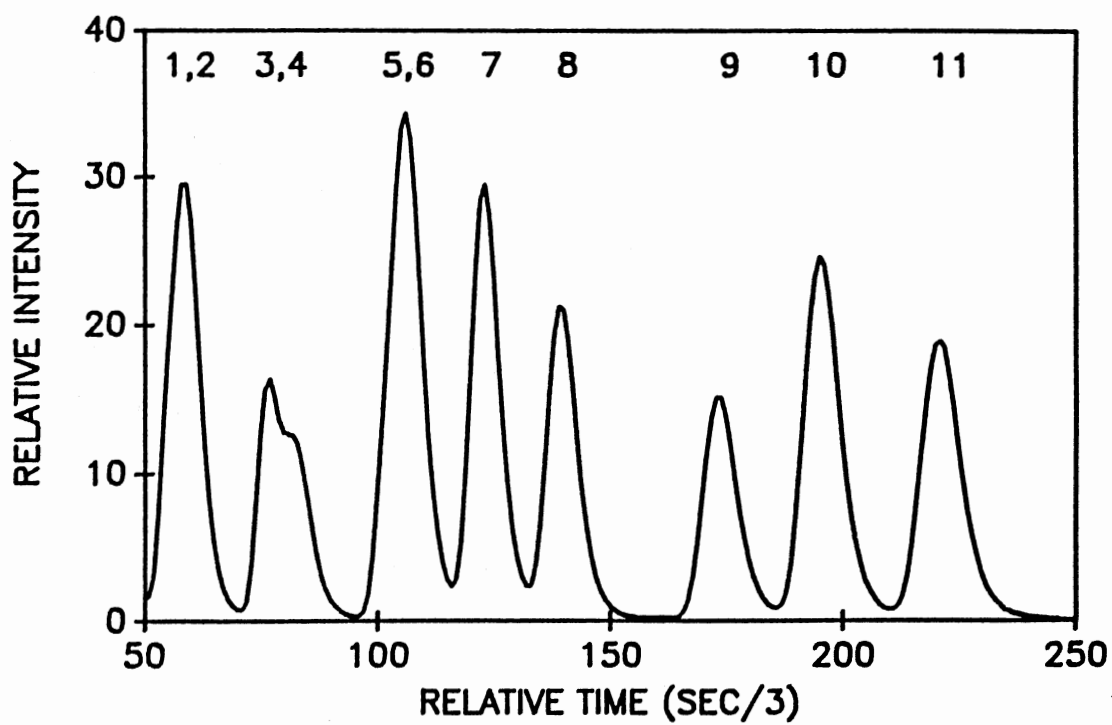


Figure 68. Chromatogram of 11 Compounds Using 0.3 mL/min and 87% Aqueous MeCN.

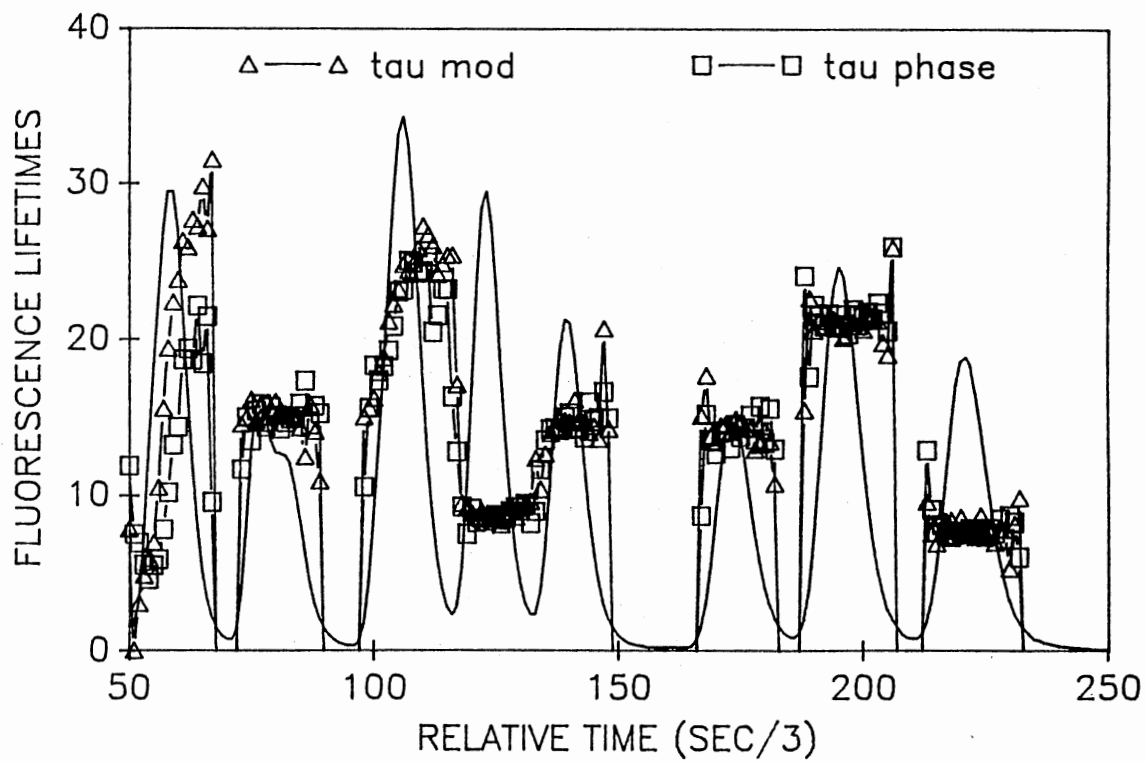


Figure 69. Lifetime Chromatogram For 11 Compounds at 10 MHz Modulation Frequency.

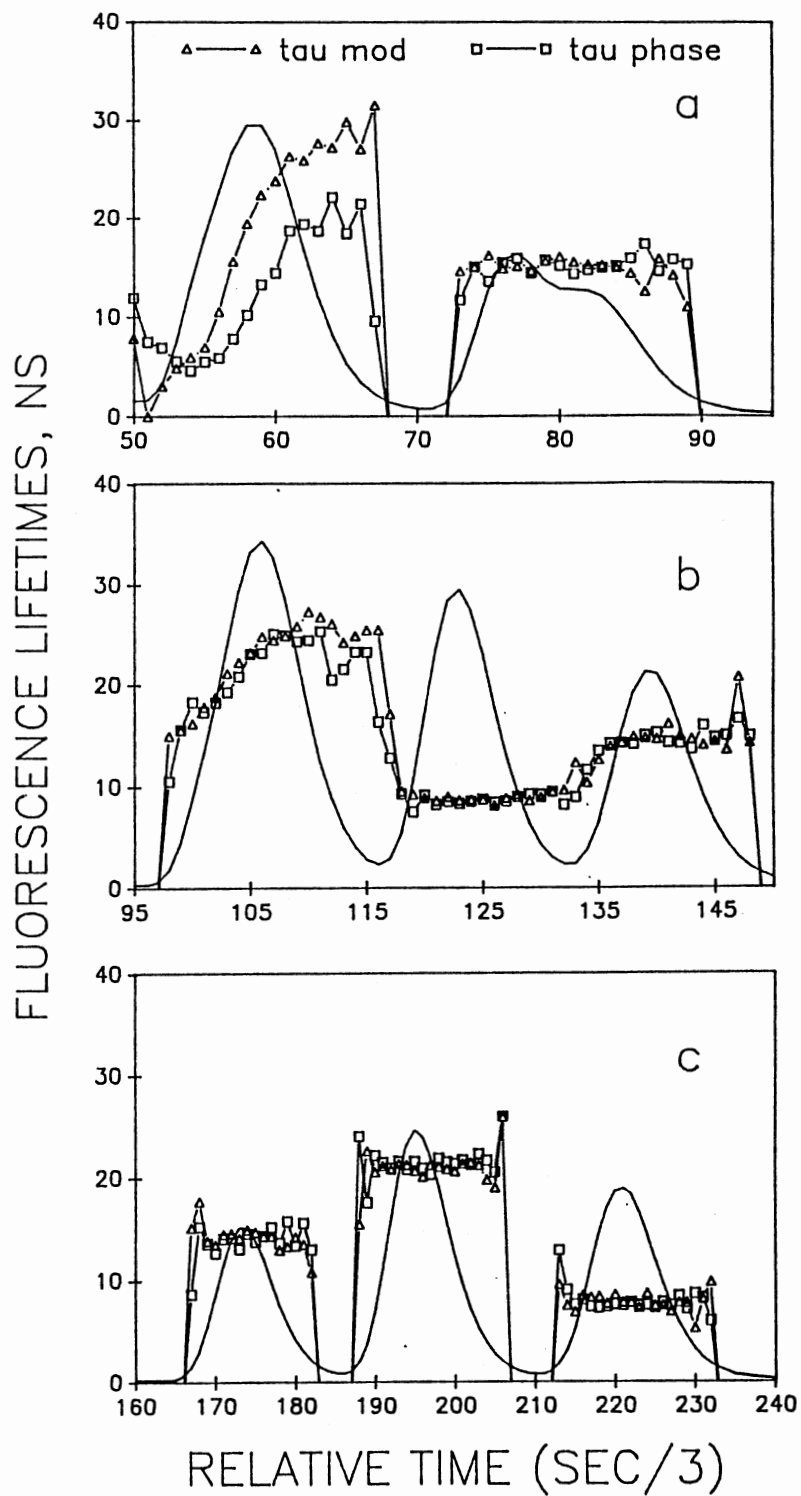


Figure 70. Data From Figure 69 Expanded in Time.

Figure 70b, as well as those on the last expanded portion (Figure 70c), correctly indicate pure compounds.

Heterogeneity analysis using the NLLS procedure available on the SLM software was performed using the data acquired at 5, 10, 15, 25, and 40 MHz for the unresolved peaks in the chromatogram. Figure 71a shows the reconstructed chromatograms obtained when both the lifetime and fractional contributions were allowed to float. As expected, for the center B(a)A/chrysene peaks, the heterogeneity analysis was unsuccessful due to the very similar lifetimes of the components. The results are poor for the B(e)P/B(b)F peak as well, and this is most likely due to the large intensity difference between components and the 10 ns lifetime difference. The success of the heterogeneity analysis is proportional to the lifetime difference between the compounds being resolved. For the first peak (anthracene / fluoranthene) the lifetime difference is about 26 ns. For the B(e)P/B(b)F the lifetime difference is about 10 ns, and the difference for the B(a)A/chrysene peak is 3 ns.

The errors in the heterogeneity analysis come from a combination of several factors listed here in approximate descending order of importance: (a) the lifetime difference between the compounds, (b) the quality (precision, accuracy) of the input data, (c) the relative maximum intensity contributions of the two components, and (d) the modulation frequencies used in the analysis. Figure 71b

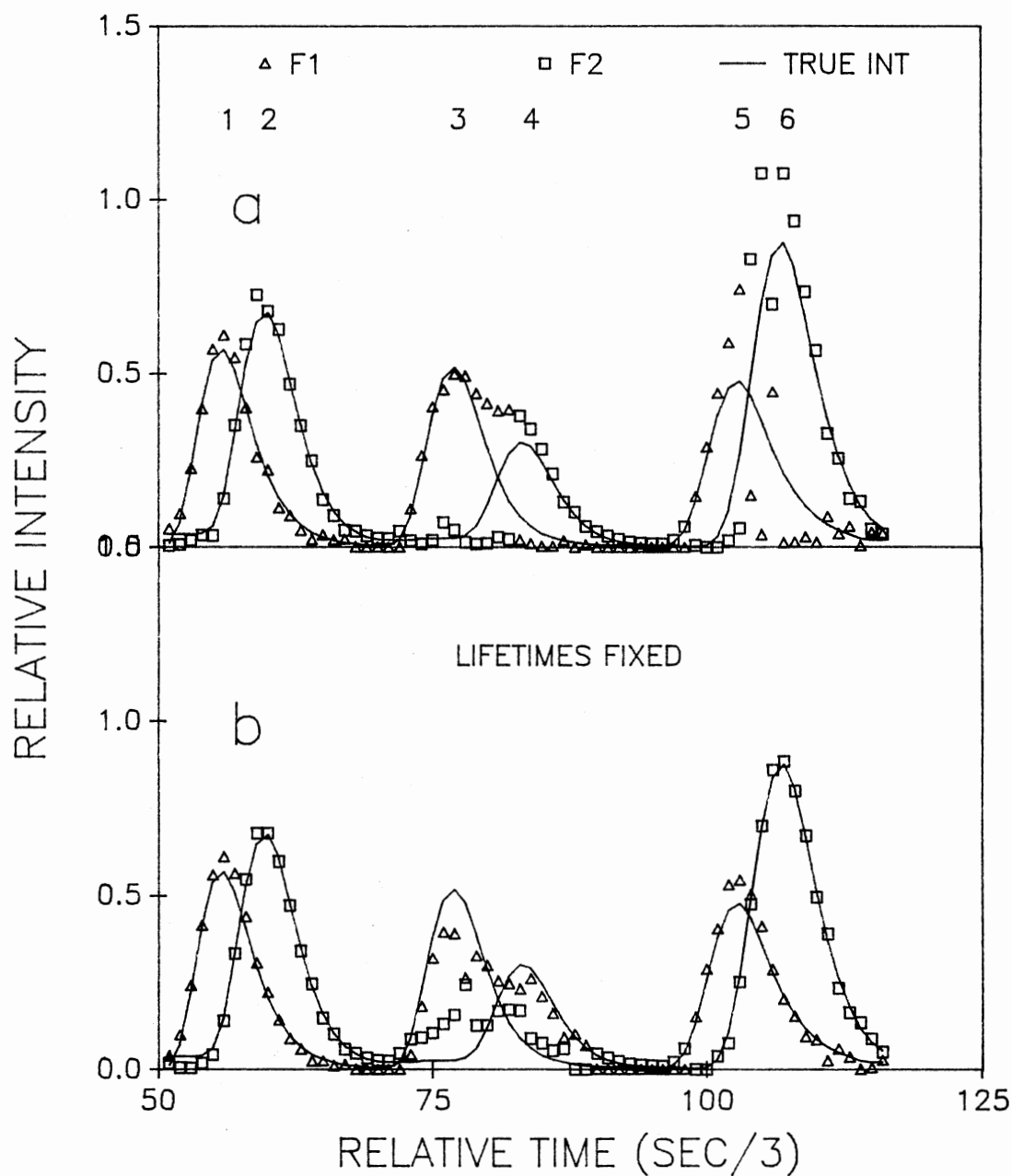


Figure 71. (a) Heterogeneity Analysis Results Using NLLS and Frequencies of 5, 10, 15, 25, and 40 MHz. (b) Same as in (a) but With Lifetimes Fixed.

shows that, when the lifetimes are fixed, the results improve substantially except for the center B(a)A/ chrysene peaks.

The above experiments were designed to investigate several important factors related to on-line determination of fluorescence lifetimes and reconstruction of resolved peaks through heterogeneity analysis. The luminescence from the flow cell, though it did not contribute significantly to the a.c. intensity, nevertheless contributed to the d.c. intensity and had to be compensated for in order to obtain useful lifetime data. The chromatographic and sample conditions used resulted in a chromatogram which contained (a) regions of complete, partial, and almost no resolution of components, (b) lifetime differences ranging from 3 to 26 ns for chromatographically unresolved components, and (c) maximum intensity differences of almost zero for the anthracene/fluoranthene pair to about 1:2 for the B(e)P/B(b)F pair.

Related Studies: On-Line HPLC / Phase-
Resolved Fluorescence Intensity
(PRFI) Detection of PAHs

Phase-resolved fluorescence spectroscopy (PRFS) was used as a detection technique for HPLC-separated PAHs. PRFS allows one to effectively "null-out" certain lifetime components in an unresolved chromatogram and monitor the

emission from the remaining components. Additionally, the phase-resolved fluorescence intensity can be measured as a function of time and frequency to selectively enhance or suppress components, thus allowing selectivity based on fluorescence lifetimes to be incorporated into the detection scheme.

Theory of PRFS

Phase-resolved fluorescence spectroscopy has been developed and used for various batch mode determinations by McGown and co-workers. This work has been reviewed elsewhere (86,87). PRFS uses the time-dependant, phase-modulation fluorescence technique to obtain a time-independent intensity signal. This is done by multiplying the a.c. portion of the fluorescence emission by a periodic function $P(t)$ where:

$$P(t) = 0 \quad \text{from } 0^\circ \text{ to the detector phase angle setting } \phi_D$$

$$P(t) = 1 \quad \text{from } \phi_D \text{ for } 1/2 \text{ cycle (} 180^\circ \text{)}$$

$$P(t) = 0 \quad \text{for the rest of the cycle (} \phi_D + 180^\circ \text{ to } 360^\circ \text{)}$$

The portion of the a.c. signal corresponding to $P(t) = 1$ is then integrated to give the time-independent signal. This is illustrated in Figure 72 with the ϕ_D aligned with various portions of an a.c. curve resulting in (a) maximum integrated intensity, (b) net zero intensity, and (c) an intensity level somewhere between the extreme conditions.

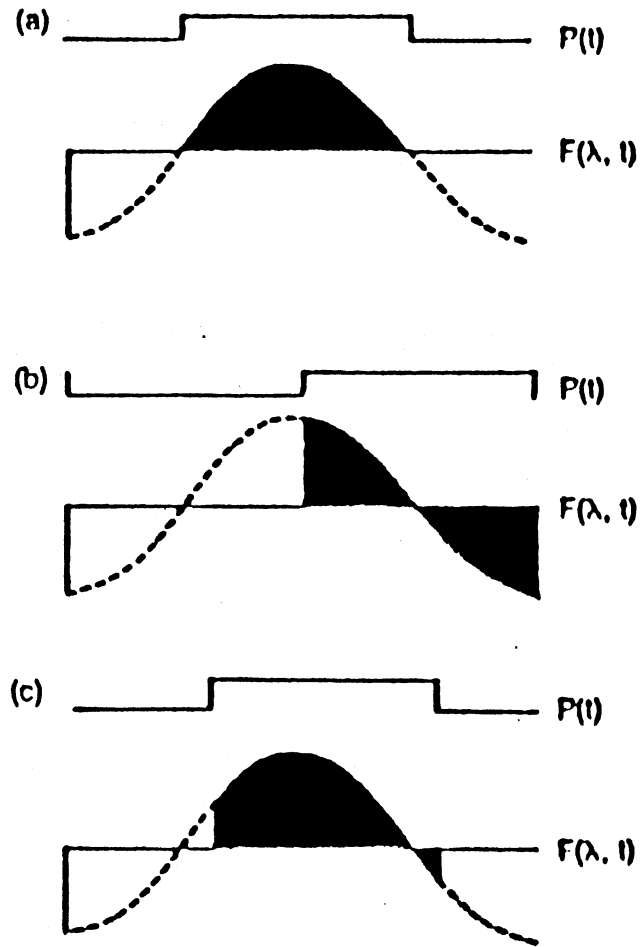


Figure 72. PRFI Resulting From Setting the Detector Phase (a) Exactly in Phase With a.c. Curve, (b) Exactly Out of Phase With a.c., and (c) at an Arbitrary Location on the a.c. Curve.

This time-independent phase-resolved fluorescence intensity is a function of the cosine of the difference between the phase angles of the fluorescence species ϕ and the detector ϕ_D :

$$\text{PRFI}(\phi) = A' m M \cos(\phi_D - \phi) \quad (25)$$

where A' is the d.c. component of the emission, m_{ex} is the excitation modulation, M is the demodulation, ϕ is the phase-shift, and ϕ_D is the detector phase angle. It is important to note that the total PRFI for a heterogeneous, non-interacting multicomponent system is simply the summation of the PRFI of the individual components at the particular set of instrumental parameter settings.

When using PRFS for chromatographic detection, at any particular point on the chromatogram, the d.c. portion (A') and the excitation modulation m_{ex} can be considered constant and equation 25 can be expressed as:

$$\text{PRFI} = K M \cos(\phi_D - \phi) \quad (26)$$

The demodulation and phase-shift can be expressed in terms of the angular modulation frequency ω , and lifetime τ :

$$M = ((\omega\tau)^2 + 1)^{-1/2} \quad (27)$$

$$\phi = \tan^{-1}(\omega\tau) \quad (28)$$

Inserting equations 27 and 28 into equation 26 gives:

$$\text{PRFI} = K \frac{\cos(\phi_D - \tan^{-1}(\omega\tau))}{((\omega\tau)^2 + 1)^{1/2}} \quad (29)$$

This illustrates the fact that the PRFI is a function of spectral parameters, modulation frequency, and detector phase angle:

$$\text{PRFI} = f(\lambda_{\text{ex}}, \lambda_{\text{em}}, \omega, \phi_D) \quad (30)$$

All of the above parameters can be utilized in PRFI detection on-line with HPLC.

Experimental

A mixture of six PAHs was used for these experiments, with concentrations on the order of 1×10^{-6} M. The Waters HPLC system was used with 100% MeCN and 0.5 mL/min flow rate. The SLM 48000S was used in the PRFS mode. Excitation was at 360 nm and emission was monitored through a 399 LP + 600 SP filter combination.

Results

PRFI Chromatograms vs. Frequency. The six-component PAH mixture is listed in TABLE 22 along with the fluorescence lifetimes and optimum modulation frequency for each lifetime. The detector phase $\alpha\gamma\lambda\epsilon\phi_D$ was set to null out scatter ($\tau=0$) by observing the scatter from the flow cell with the filters removed from the emission path and adjusting the detector phase angle to give zero intensity. The PRFI chromatograms were acquired at 2, 4, 6, 8, 10, 15, 20, 35, 50, and 80 MHz. The changes in the PRFI as the

TABLE 22
PEAK IDENTIFICATION FOR FIGURES 78 AND 79

Peak #	Compound	τ , ns	Optimum Modulation Frequency, MHz
1	Fluoranthene	29	5
2	B(b)F	25	6
3	B(k)F	7	23
4	B(a)P	11	15
5	B(ghi)P	15	11
6	I(1,2,3-cd)	7	23

modulation frequency is changed from 4 to 35 MHz are shown in Figure 73. Note that the long-lived components (1, 2, 5) are enhanced relative to the short-lived components (3, 4, 6) at 4 MHz, while the short-lived components are selectively enhanced as the frequency is increased to 35 MHz.

PRFI Chromatograms vs. Detector Phase Angle. An additional way of achieving selectivity using PRFS is to keep the frequency constant and vary the detector phase angle ϕ_D . Figure 74a shows the six-component mixture at a modulation frequency of 10 MHz with scattered light nulled. For the chromatogram shown in Figure 74b, ϕ_D was set to null out all components with a 7 ns lifetime (B(k)F, I(1,2,3-cd)P) which leaves only the long-lived components. Next, the 25 ns lifetime of B(b)F (peak 2) was nulled out, allowing peak 3 (B(k)F) to be monitored without interference from peak B(b)F (see Figure 74c). When the 25 ns contribution is nulled, the contribution of anthracene (29 ns) is also lost and the contribution of B(ghi)P (15 ns, peak 5) is attenuated. Thus, if a specific component is required to be monitored in the presence of another interferant, the contribution of the interferant can simply be "nulled out". This is true, of course, only if the lifetimes of the analyte and interfering species are different enough so that the analyte is not also nulled out. Though it was not a goal of this research to pursue this avenue in depth, one can certainly see the

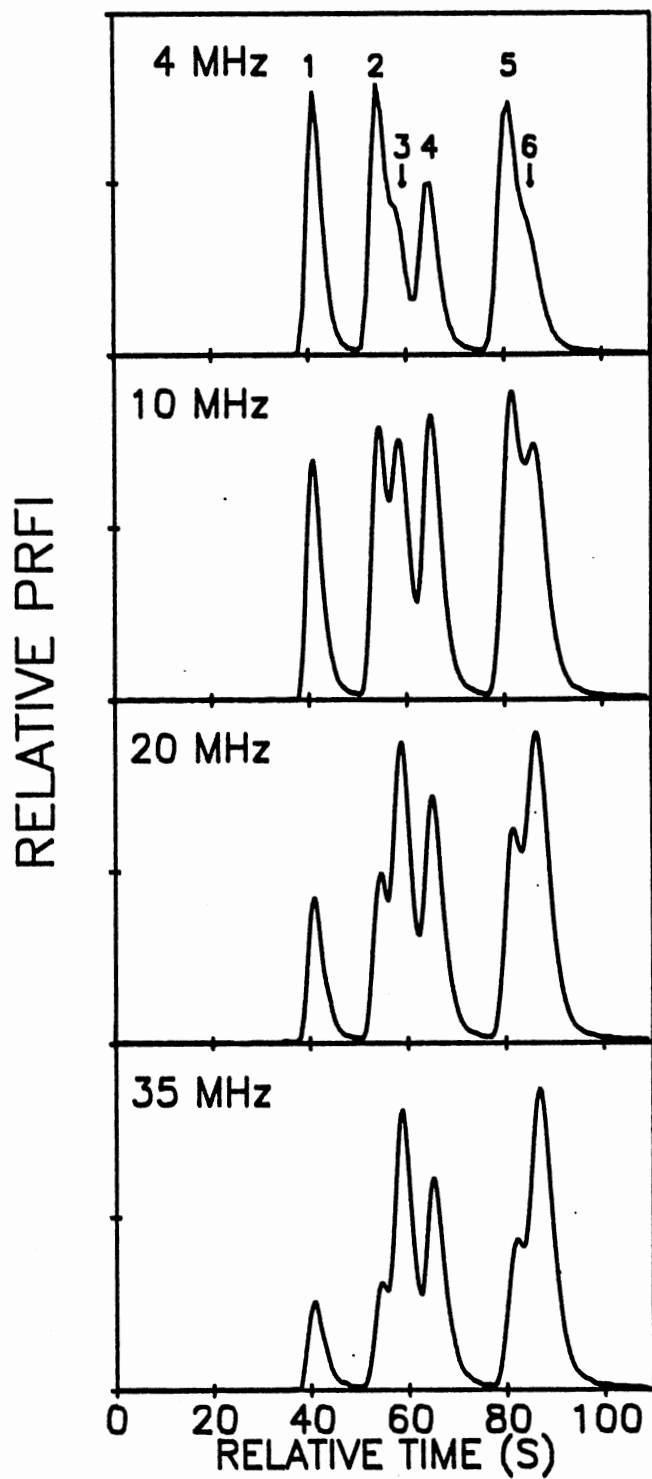


Figure 73. PRFI Chromatograms vs. Frequency With Detector Phase Set to Null Out Scattered Light.

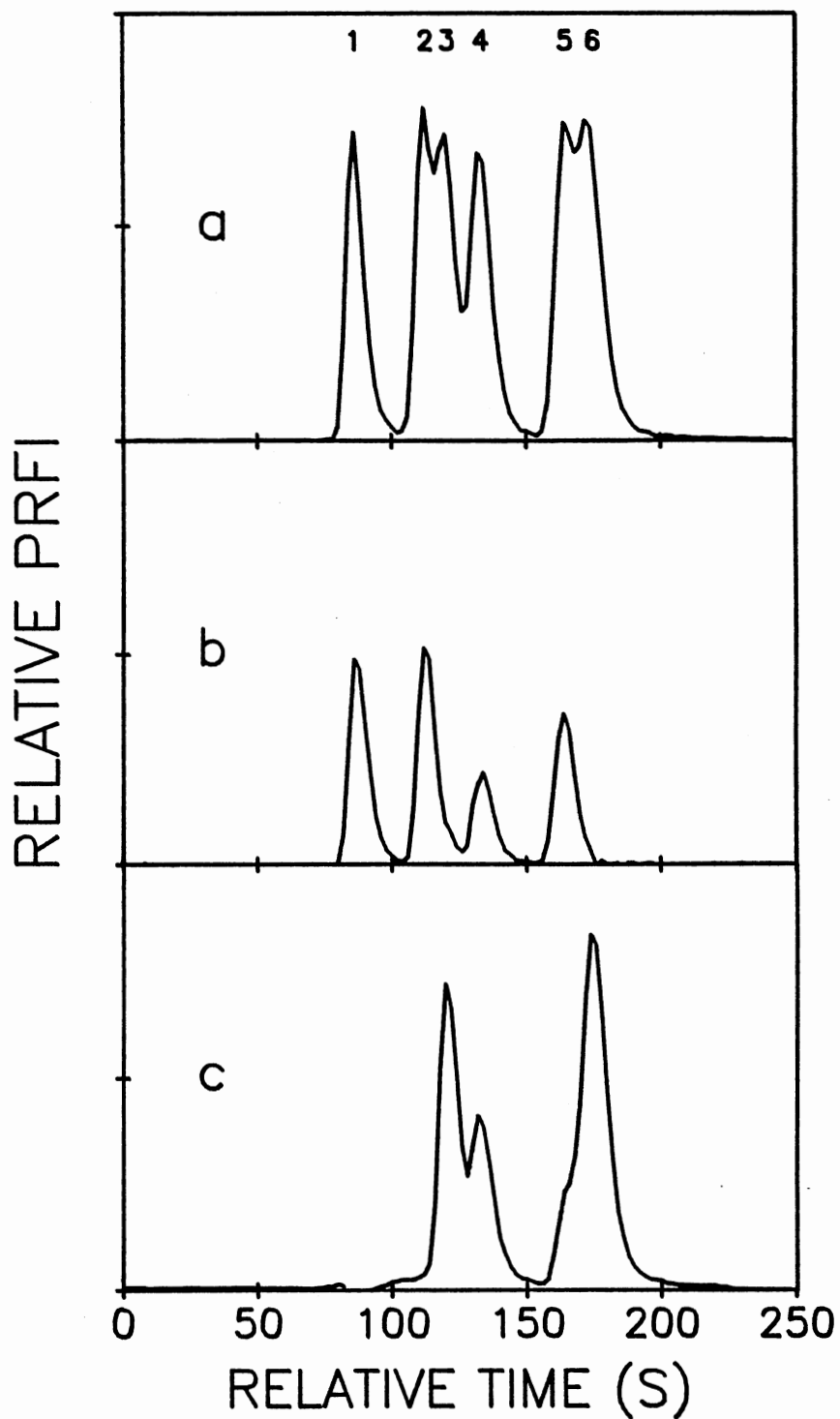


Figure 74. PRFI Chromatograms at 10 MHz With Detector Phase Set to Null Out (a) Scattered Light, (b) 7 ns Contribution, and (c) 25 ns Contribution.

possibilities for generating three-dimensional output of PRFI vs. time and either frequency or detector phase angle for complex sample analysis.

CHAPTER VI

CONCLUSION

The determination of phase and modulation fluorescence lifetimes on-line with HPLC was obviously more difficult than simply connecting the HPLC to the fluorescence flow cell and turning on the instruments. Through the research described in this dissertation the technique has been developed to the point that it is now possible, as long as one has a reasonable understanding of the procedure involved, for an inexperienced user to be collecting fluorescence lifetime chromatograms within a couple of days after introduction to the instrumentation.

The research which has been described in this dissertation has been conducted on two separate campuses, and with two significantly different spectrofluorometers. Many problems, often very elusive, affecting the lifetime determinations have been addressed, including: effects of scattered light, lifetime reference selection and intensity matching, mobile phase composition, flow rate, interfering emission, and instrumental artifacts. Several advances and simplifications have been achieved for data acquisition, calculations, transfer, storage, and output through software and hardware development. Also addressed were

various effects on the heterogeneity analysis for the different algorithms (Weber's, NLLS), fluorescence lifetime differences, relative intensity contributions, number and choice of modulation frequencies, and the fixing of the fluorescence lifetimes for fractional contribution determinations.

In summary, the research achieved the goals of (1) the determination of phase and modulation lifetimes on-line with HPLC, (2) indication of peak heterogeneity (unresolved peaks), and (3) quantitation of components in unresolved peaks using fluorescence lifetime selectivity without the need for chromatographic separation.

Future Directions

There are many interesting and very promising paths for the continuation of the techniques described on the previous pages. Obviously, analytical figures of merit will need to be determined in more detail such as detection limits for single components as well as the level at which one component can be determined in the presence of another. A detailed error analysis needs to be investigated, as well as possible matrix effects such as those which may occur in real samples. Although it was originally planned to carry this technique through to real environmental water samples, too many unforeseen problems blocked the progress and this definitely would be an interesting and challenging path for future research.

Several instrumental improvements will extend the usefulness of this technique. More intense excitation sources, such as a 1000 watt mercury-xenon lamp would increase the capabilities for excitation in the UV and improve overall performance. Also, the use of laser sources would increase performance through increased excitation intensity and the ability to focus more readily on the observation volume of the flow cell, although the choice of excitation wavelengths would be more limited.

Probably the most exciting and useful instrumental development which would be ideal for on-line detection is the multi-harmonic fourier fluorometer (MFF) recently introduced by SLM Instruments. According to SLM literature and conversations with SLM representatives, this instrument evidently will allow phase and modulation data from many (upwards of 250) frequencies to be acquired simultaneously. Thus, instead of having to make repeated injections for each frequency as is now required, data from all of the frequencies can be acquired in a single run. An additional feature of the new instrumentation is its ability to collect a multifrequency data set from 5 to 90 MHz in approximately 40 milliseconds (currently the smallest time-step increment is 1 second). This feature would allow much more data to be collected (and averaged) over a chromatographic peak, resulting in much improved precision over the current technique without requiring several repeated injections.

BIBLIOGRAPHY

1. Jacob, J.; Karcher, W.; Wagstaffe, P. *Fresenius' Z. Anal. Chem.* **1984**, *317*, 101-114.
2. Jacob, J.; Karcher, W.; Belliaro, J.; Wagstaffe, P. *Fresenius' Z. Anal. Chem.* **1986**, *322*, 1-10.
3. Das, B. In *Liquid Chromatography in Environmental Analysis*, Lawrence, J., Ed.; Humana: Clifton, N.J., 1984; pp 19-75.
4. World Health Organization, *International Standards For Drinking Water*, 3rd. ed., Geneva, 1971.
5. *Fed. Regist.* **1979**, *44*, 69464-69575.
6. Lee, M.; Novotny, M.; Bartle, K. *Analytical Chemistry of Polycyclic Aromatic Hydrocarbons*; Academic: New York, 1981.
7. Fetzer, J. In *Chemical Analysis of Polycyclic Aromatic Hydrocarbons*; Vo-Dinh, T., Ed.; John Wiley & Sons: New York, 1989; Chapter 3.
8. Snyder, L.; Dolan, J.; Gant, J. *J. Chromatogr.* **1979**, *165*, 3-30.
9. Ogan, K.; Katz, E.; Slavin, W. *Anal. Chem.* **1979**, *51*, 1315-1320.
10. Das, B.; Thomas, G. *Anal. Chem.* **1978**, *50*, 967-973.
11. Sorrell, R.; Reding, R. *J. Chromatogr.* **1979**, *185*, 655-670.
12. Symons, R.; Crick, I. *Anal. Chim. Acta* **1983**, *151*, 237-243.
13. Lankmayr, E.; Muller, K. *J. Chromatogr.* **1979**, *170*, 139-146.
14. Chmielowiec, J.; Sawatzky, H. *J. Chromatogr. Sci.* **1979**, *17*, 245-252.
15. Davis, J.; Giddings, J. *Anal. Chem.* **1983**, *55*, 418.

16. Ebel, S.; Mueck, W. *Chromatographia*, **1988**, *25*, 1075.
17. White, P. *Analyst* **1984**, *109*, 973-984.
18. Games, D.; Foster, M.; Meresz, O. *Anal. Proc.* **1984**, *21*, 174-177.
19. Christensen, R.; Hertz, H.; Meiselman, S.; White, E. *Anal. Chem.* **1981**, *53*, 171-174.
20. Hayes, M. *Anal. Chem.* **1983**, *55*, 1745-1752.
21. Quillian, M.; Gergely, R.; Tashiro, C.; Marr, J. In *Advances in Mass Spectrometry*; Todd, J., Ed.; Wiley and Sons: London, 1986, p 571.
22. Quillian, M.; Sim, P. *J. Chromatogr. Sci.* **1988**, *26*, 160-167.
23. May, W. et al. *J. Chromatogr. Sci.* **1975**, *13*, 535-540.
24. Saner, W.; Jadamec, J.; Sager, R. *Anal. Chem.* **1979**, *51*, 2180-2188.
25. Christensen, R.; May, W. *J. Liq. Chromatogr.* **1978**, *1*, 385.
26. Grushka, E.; Myers, M.; Giddings, J. *Anal. Chem.* **1970**, *42*, 21.
27. Grushka, E.; Monacelli, G. *Anal. Chem.* **1972**, *44*, 484.
28. Bylina, A. *J. Chromatogr.* **1973**, *83*, 357.
29. Ostojic, N. *Anal. Chem.* **1974**, *46*, 1653.
30. Webb, P.; Ball, D.; Thornton, T. *J. Chromatogr. Sci.* **1983**, *21*, 447.
31. Berg, R.; Ko, C.; Clemons, J.; McNair, H. *Anal. Chem.* **1975**, *47*, 2480.
32. Li, K.; Arrington, J. *Anal. Chem.* **1979**, *51*, 287.
33. Carter, G.; Schiesswohl, R.; Burke, H.; Yang, R. *J. Pharm. Sci.* **1982**, *71*, 317.
34. Milano, M.; Gruchka, E. *J. Chromatogr.* **1985**, *133*, 352.
35. Grant, A.; Bhattacharyya, P. *J. Chromatogr.* **1985**, *347*, 219.

36. Fell, A.; Scott, H.; Gill, R.; Moffat, A. J. *Chromatogr.* **1983**, 282, 123.
37. Warren, F.; Fidlingmeyer, B.; Delaney, M. *Anal. Chem.* **1987**, 59, 1897.
38. Cheng, H.; Gadde, R. *J. Chrom. Sci.* **1985**, 23, 227.
39. Drouen, A.; Billiet, H.; Galan, L. *Anal. Chem.* **1984**, 56, 971.
40. Fell, A.; Clark, B.; Scott, H. *J. Pharm. & Biomed. Anal.* **1983**, 1, 557.
41. Alfredson, T.; Sheehan, T. *J. Chrom. Sci.* **1986**, 24, 473.
42. Mueck, W. Ph.D. Thesis, Wurzburg 1987.
43. Miller, J.; George, S.; Willis, B. *Science* **1982**, 218, 241.
44. Beebe, K.; Kowalski, B. *Anal. Chem.* **1987**, 59, 1007A.
45. Sharaf, M.; Illman, D.; Kowalski, B. *Chemometrics; Chemical Analysis Series 82*; Wiley & Sons: New York, 1986.
46. McCue, M.; Malinowski, E. *J. Chrom. Sci.* **1983**, 21, 229.
47. McCue, M.; Malinowski, E. *Appl. Spectrosc.* **1983**, 37, 463.
48. Osten, D.; Kowalski, E. *Anal. Chem.* **1984**, 56, 991.
49. Vandeginste, B.; Essers, R.; Bosman, T.; Reijnen, J.; Kateman, G. *Anal. Chem.* **1985**, 57, 971.
50. Vandeginste, B. et al. *J. Chemometrics* **1987**, 1, 57.
51. Rossi, D.; Desilets, D.; Pardue, J. *Anal. Chim. Acta* **1984**, 161, 191-199.
52. Velapoldi, R.; White, P.; May, W. *Anal. Chem.* **1983**, 55, 1896-1901.
53. Xu, X.; Jin, Z. *J. Chromatogr.* **1984**, 317, 545-555.
54. Pellizzari, E.; Sparacino, C. *Anal. Chem.* **1973**, 45, 378.

55. Christian G.; Callis, J. ; Davidson, E. In *Modern Fluorescence Spectroscopy*; Wehry, E., Ed.; Plenum: New York, 1981; Vol. 3.
56. Jadamec, J.; Saner, W.; Talmi, Y. *Anal. Chem.* **1977**, *49*, 1316.
57. Fogarty, M.; Shelly, D.; Warner, I. *HRC & CC* **1981**, *4*, 561.
58. Shelly, D.; Fogarty, M.; Warner, I. *HRC & CC* **1981**, *4*, 616.
59. Lloyd, J. *Nature* **1971**, *231*, 64.
60. Vo-Dinh, T. In *Modern Fluorescence Spectroscopy*; Wehry, E., Ed.; Plenum: New York, 1981; Vol. 4, p 167.
61. Vo-Dinh, T. *Anal. Chem.* **1978**, *50*, 396.
62. Rubio, S.; Hens, G.; Valcarcel, M. *Talanta* **1986**, *33*, 633.
63. Spino, L.; Armstrong, D. *J. Chrom.* **1987**, *409*, 147.
64. Inman, E. Jr.; Winefordner, J. *Anal. Chem.* **1982**, *54*, 2018.
65. Inman, E. Jr.; Winefordner, J. *Anal. Chim. Acta* **1982**, *138*, 245.
66. Inman, E. Jr.; Winefordner, J. *Anal. Chim. Acta* **1982**, *141*, 241.
67. Kerkhoff, M.; Winefordner, J. *Anal. Chim. Acta* **1985**, *175*, 257-265.
68. Yeung, E.; Synovec, R. *Anal. Chem.* **1986**, *58*, 1237A-1256A.
69. Hercules, D. in *Fluorescence and Phosphorescence Analysis*; Hercules, D. Ed.; Wiley-Interscience: New York, 1966, p 12.
70. Sepaniak, M.; Kettler, C. in *Detectors for Liquid Chromatography*; Yeung, E., Ed.; Wiley & Sons: New York, 1986, pp 149-203.
71. Lakowicz, J. *Principles of Fluorescence Spectroscopy*; Plenum: New York, 1983; pp 65-71.
72. Demas, J. *Excited State Lifetime Measurements*; Academic: New York, 1983; pp 39-42.

73. Lakowicz, J. *Principles of Fluorescence Spectroscopy*; Plenum: New York, 1983; p 86.
74. Barrow, D.; Lentz, B. J. *Biochem. Biophys. Methods* **1983**, *7*, 217-234.
75. Spencer, R. Ph.D. Thesis, University of Illinois, Urbana, 1970.
76. Weber, G. J. *Phys. Chem.* **1981**, *85*, 949-953.
77. Jameson, D.; Weber, G. J. *Phys. Chem.* **1981**, *85*, 953-958.
78. Jameson, D.; Gratton, E. In *New Directions in Molecular Luminescence*, ASTM STP 822; Eastwood, D., Ed.; American Society for Testing and Materials: Philadelphia, 1983; p 67.
79. Dalbey, R.; Weiel, J.; Perkins, W.; Yount, R. J. *Biochem. Biophys. Methods* **1984**, *9*, 251-266.
80. Beechem, J.; Knutson, J.; Ross, J.; Turner, B.; Brand, L. *Biochemistry* **1983**, *22*, 6054-658.
81. Richardson, J.; Larson, K.; Haugen, G.; Johnson, D.; Clarkson, J. *Anal. Chim. Acta* **1980**, *116*, 407-411.
82. Imasaka, T.; Ishibashi, K.; Ishibashi, N. *Anal. Chim. Acta* **1982**, *142*, 1-12.
83. Furuta, N.; Otusuki, A.; *Anal. Chem.* **1983**, *55*, 2407-2413.
84. Desilets, D.; Coburn, J.; Lantrip, D.; Kissinger, P.; Lytle, F. *Anal. Chem.* **1986**, *58*, 1123-1128.
85. Desilets, D.; Kissinger, P.; Lytle, F. *Anal. Chem.* **1987**, *59*, 1830-1834.
86. McGown, L.; Bright, F. *Anal. Chem.* **1984**, *56*, 1400A.
87. McGown, L.; Millican, D. *Appl. Spectrosc.* **1988**, *42*, 1084.

APPENDIXES

APPENDIX A

COMPUTER PROGRAM WRITTEN IN MICROSOFT
QUICKBASIC TO CALCULATE INTENSITY
MATCHED LIFETIMES FOR CHROMATOGRAMS

```

'----- ChromCobb -----
'
'           Calculates Intensity matched lifetimes
'           and sets up data for heterogeneity
'           analysis for HPLC chromatograms.
'
'           W. Tyler Cobb
'           February 15, 1989
'-----
common shared howmany
common shared freq(1)
common shared i
cls
print
print "ChromCobb - calculates lifetimes for HPLC data"
print

'           ----- Main Program -----
dim freq(20)
dim DC(1000)
dim MODUL(1000)
dim PHASE(1000)
dim DEMOD(1000)
dim DPHASE(1000)
dim TMOD(1000)
dim TPHASE(1000)
dim RMOD(1000)
dim RPHASE(1000)
const PI=3.141593

print "What is the name (+ .ext) of the file
containing the"
input "intensity data?";intfil$
open intfil$ for input as 1
c=1
intmax=0
intmin=10
while not EOF(1)
input #1, DC(c)
if DC(c) > intmax then intmax=DC(c)
if DC(c) < intmin then intmin=DC(c)
c=c+1
wend
close 1
howmany=(c-1)
input "How many frequencies used?";freqnum

for i=1 to freqnum
print "What is frequency number";i;"in MHz?";
input freq(i)
next i

'           ..... Major Loop .....
for i=1 to freqnum

```

```

call GETDATA(MODUL(),PHASE())

input "Do you want to do reference intensity matching
(y/n)";B$
if B$="n" or B$="N" then goto Delta
call INTMATCH(DC(),MODUL(),PHASE(),DEMODO(),DPHASE()):
goto Taus
Delta: input "What is the reference modulation";REFMOD
input "What is the reference phase";REFPHASE
print "calculating demodulation and delta phase"
for j=1 to howmany
DEMODO(j)=MODUL(j)/REFMOD
DPHASE(j)=PHASE(j)-REFPHASE
next j
print "finished calculating demodulation and delta
phase"
Taus: call TAUCALC(DEMODO(),DPHASE(),TMOO(),TPHASE())
print "Do you want to calculate actual demodulation
and";
input " delta phase for heterogeneity analysis";s$
if s$="n" or s$="N" then goto onward
call HETANAL(TMOO(),TPHASE(),RMOO(),RPHASE())

onward: print "Do you want to set an intensity threshold:
by doing this",
print "at any intensity less than the set threshold
value the",
print "lifetimes will be set to -1 and thus lifetimes
calculated",
input "from areas with only background noise will not
appear";ts$
if ts$="y" or ts$="Y" then
print " The minimum intensity is";intmin
input "What is the threshold value";thresh
for k=1 to howmany
if DC(k) < thresh then
TMOO(k) = -1
TPHASE(k) = -1
end if
next k
end if

print "Do you want to multiply intensity data so it
will plot out";
input " well with the lifetime data (y/n)";m$
if m$="y" or m$="Y" then
print "The maximum intensity point is ";intmax
input "What is the constant amount to multiply the
intensity by";amnt
for k=1 to howmany
dc(k)=dc(k)*amnt
next k
end if

```

```

    print "Do you want a hardcopy of the intensity,"
    input "lifetimes, demodulation, and deltaphase
(y/n)";C$
    if C$="y" or C$="Y" then
    input "At which point would you like to begin
printing";begin
    input "At which point would you like to end printing
(0 for all)";final
    if final = 0 then final = howmany
    lprint "The data for ";freq(i);"MHz is as follows"
    lprint "number      intensity      Tau Mod      Tau Phase
demod      delta phase"
    for k=begin to final
    lprint using "###.";k,
    lprint using "#####.###";DC(k),
    lprint using "#####.##";TMOD(k),
    lprint using "#####.##";TPHASE(k),
    lprint using "#####.###";RMOD(k),
    lprint using "#####.##";RPHASE(k)
    next k
    end if
    input "Do you want to save the data to a file
(y/n)";D$
    if D$="y" or D$="Y" then
    input "At which point would you like to begin
printing";begin
    input "At which point would you like to end printing
(0 for all)";final
    if final = 0 then final = howmany
    print "What is the name for the output file for data
at";freq(i)
    input "MHz - add the .PRN to file name (<= 8
char)";OUT$
    open OUT$ for output as 1
    input "Do you want to print the descriptive header to
file";h$
    if h$="n" or h$="N" then goto SKIP
    print #1, "The data for ";freq(i);"MHz is as follows"
    print #1, "number      intensity      Tau Mod      Tau
Phase      demod      delta phase"
SKIP:      for j=begin to final
    print #1, using "###.";j,
    print #1, using "#####.###";DC(j),
    print #1, using "#####.##";TMOD(j),
    print #1, using "#####.##";TPHASE(j),
    print #1, using "#####.###";RMOD(j),
    print #1, using "#####.##";RPHASE(j)
    next j
    close 1
    end if
next i
end

```

```
' -----subroutine to get the data from disk files-----
--
```

```
sub GETDATA(MODUL(1),PHASE(1)) static
print "What is the name of the modulation file
for";freq(i);
input "MHz-don't forget the .PRN";mfile$
open mfile$ for input as 1
print "What is the name of the phase file
for";freq(i);
input "MHz- don't forget the .PRN";pfile$
open pfile$ for input as 2
print "loading modulation and phase data"
for j=1 to howmany
input #1, MODUL(j)
next j
for j=1 to howmany
input #2, PHASE(j)
next j
close 1
close 2
end sub
```

```
'subroutine to intensity match and calculate demod and
deltaphase
```

```
sub
INTMATCH(DC(1),MODUL(1),PHASE(1),DEMODO(1),DPHASE(1)) static
dim REFINT(1000)
dim REFMOD(1000)
dim REFPHASE(1000)
print "How many reference data points are there
at";freq(i);" MHz?";
input points
for k=1 to points
print "What is reference b/c for point";k;"?";
input REFINT(k)
print "What is reference modulation for
point";k;"?";
input REFMOD(k)
print "What is reference phase for point";k;"?";
input REFPHASE(k)
next k
Match: print "Matching intensities"
for j=1 to howmany
for k=1 to points
diff=DC(j)-REFINT(k)
check=(REFINT(k+1)-REFINT(k))/2
if diff < check then
last: DEMODO(j)=MODUL(j)/REFMOD(k)
DPHASE(j)=PHASE(j)-REFPHASE(k)
goto Again
end if
if k = points then goto last
```



```

        next k
Again:  next j
        print "finished intensity matching the data"
        end sub

'-----subroutine to calculate the lifetimes-----
-

        sub TAUCALC(DEMOD(1),DPHASE(1),TMOD(1),TPHASE(1))
static
        print "Calculating lifetimes"
        if i>1 then goto Calc
        input "What is the lifetime of the reference in
ns";REFTAU
Calc:   omega=2*PI*freq(i)*1e+6
        PSREF=ATN(omega*REFTAU*1e-9)
        REF = (omega^2)*((REFTAU*1e-9)^2)
        for j=1 to howmany
        DPHASE(j)=PI/180*DPHASE(j)
        TPHASE(j)=(1/omega)*TAN(DPHASE(j)+PSREF)
        TPHASE(j)=TPHASE(j)*1e+9
        part=((1+REF)/DEMOD(j)^2)-1
        if part < 0 then
        TMOD(j)=0
        else
        TMOD(j)=(1/omega)*SQR(part)
        end if
        TMOD(j)=TMOD(j)*1e+9
        next j
        end sub

'-----subroutine to calculate the actual demodulation
-----
'          and delta-phase values for heterogeneity
analysis

        sub HETANAL(TMOD(1),TPHASE(1),RMOD(1),RPHASE(1))
static
        print "Calculating actual demod and d-phase"
        omega=2*PI*freq(i)*1e+6
        for j=1 to howmany
        RPHASE(j)=ATN(TPHASE(j)*1e-9*omega)
        RPHASE(j)=(RPHASE(j)*180)/PI
        RMOD(j)=SQR(1/((omega*TMOD(j)*1e-9)^2 +1))
        next j
        end sub

```

APPENDIX B

COMPUTER PROGRAM WRITTEN IN MICROSOFT
QUICKBASIC TO CALCULATE FRACTIONAL
INTENSITIES FROM FRACTIONAL
CONTRIBUTIONS OBTAINED FROM
HETEROGENEITY ANALYSIS

```

'----- INTCALC -----
'
'           Calculates Fractional Intensities
'           from fractional contributions
'           from heterogeneity analysis for
'           HPLC chromatograms.
'
'           W. Tyler Cobb
'           March 25, 1989
'-----
      common shared howmany
      cls
      print
      print "FRACINT calculates fractional intensities for
HPLC data"
      print

'           ----- Main Program -----
      dim DC(1000)
      dim frac1(1000)
      dim frac2(1000)
      dim fracint1(1000)
      dim fracint2(1000)

      print "What is the name (+ .ext) of the file
containing the"
      input "intensity data?";intfil$
      open intfil$ for input as 1
      c=1
      intmax=0
      intmin=10
      while not EOF(1)
      input #1, DC(c)
      if DC(c) > intmax then intmax=DC(c)
      if DC(c) < intmin then intmin=DC(c)
      c=c+1
      wend
      close 1
      howmany=(c-1)

      another: input "At what number do you want to begin
calculations";start
      input "At what number do you want to end
calculations";finish
      for i=start to finish
      print "What is the Frac 1 for point";i;"?";
      input frac1(i)
      frac2(i)= 1-frac1(i)
      next i
      input "Do you want to save the fractional contribution
data";r$
      if r$="y" or r$="Y" then

```

```

        input "What is the filename for Frac data
(+.prn)";F1$
        open F1$ for output as 1
        for i=start to finish
            print #1, i,frac1(i),frac2(i)
        next i
        close 1
    end if
    input "Do you want a hardcopy of fractional
contribution data";s$
    if s$="y" or s$="Y" then
        lprint "The fractional contribution data is as
follows:"
        lprint
        lprint " #          frac1          frac2"
        for i=start to finish
            lprint i,frac1(i),frac2(i)
        next i
    end if

'      CALCULATING FRACTIONAL INTENSITIES

    for i=start to finish
        fracint1(i)=frac1(i)*DC(i)
        fracint2(i)=frac2(i)*DC(i)
    next i
    input "Do you want a hardcopy of fractional
intensities";t$
    if t$="y" or t$="Y" then
        lprint "The fractional intensities are as
follows:"
        lprint
        lprint " #          fracint1          fracint2"
        for i=start to finish
            lprint i, fracint1(i), fracint2(i)
        next i
    end if
    input "What is the filename for fractional
intensities(+.prn)";fracint$
    open fracint$ for output as 1
    for i=start to finish
        print #1, i, fracint1(i), fracint2(i)
    next i
    close 1

    input "Do you want to calculate another region";u$
    if u$="y" or u$="Y" then goto another
end

```

VITA

William Tyler Cobb

Candidate for the Degree of

Doctor of Philosophy

Thesis: ON-LINE HPLC / PHASE-MODULATION FLUORESCENCE
LIFETIME DETERMINATIONS FOR POLYCYCLIC AROMATIC
HYDROCARBONS

Major Field: Chemistry

Biographical:

Personal Data: Born in Minden, Louisiana, December 9,
1961, the son of William M. and Dolores E. Cobb.

Education: Graduated from McLoud High School, McLoud,
Oklahoma, in May 1980; received Bachelor of
Science Degree in Chemistry from Southeastern
Oklahoma State University in Durant, Oklahoma in
May, 1984; completed requirements for the Doctor
of Philosophy degree at Oklahoma State University
in December, 1989.

Professional Experience: Teaching Assistant,
Department of Chemistry, Oklahoma State
University, August, 1984, to May, 1985 and
January 1986 to May, 1986; Graduate Research
Assistant, Department of Chemistry, Oklahoma
State University, June, 1985 to December, 1985,
and June 1986 to July 1987; Graduate Research
Assistant, Department of Chemistry, Duke
University, August 1987 to July 1989.

Fellowships: Presidential Fellowship, Oklahoma State
University Center for Water Research, June, 1986
to July 1987.